Cape Peninsula
University of Technology

ENHANCED FREQUENCY REGULATION FUNCTIONALITY OF GRID-CONNECTED PV SYSTEM

by

OBU SAMSON SHOWERS

Thesis submitted in fulfilment of the requirements for the degree

Master of Engineering: Electrical Engineering

in the Faculty of Engineering

at the Cape Peninsula University of Technology

Supervisor: Dr AK Raji

Bellville Campus

December 2019

CPUT copyright information

DECLARATION

I, **Obu Samson Showers**, declare that the contents of this dissertation/thesis represent my own unaided work, and that the thesis has not previously been submitted for academic examination towards any qualification. Furthermore, it represents my own opinions and not necessarily those of the Cape Peninsula University of Technology.

Signed

Date

ABSTRACT

Electric utilities are confronted with challenges like rising fuel costs, aging equipment, increasing energy demand, frequency regulation and the difficulty to integrate renewable energy resources into the grid. The presence of photovoltaic (PV) penetration on the utility grid is also increasing significantly in recent years. With the recent rise in PV penetration and the advancement of the global PV industry, there is an urgent and a necessary need to introduce features in PV systems that will make them respond smartly. However, much of these can be addressed without negatively affecting the total performance and power quality of the grid.

Hence, engaging smart Grid technologies, and leveraging the benefits of the distributed nature of PV, new prospects to unearth value can be created. Through the implementation of progressive energy storage techniques, efficient two-way communications, a grid-tied PV system can create significant value, mostly through improved PV contribution in grid support functions like frequency regulation.

An enhanced frequency regulation functioning scheme for a grid-connected photovoltaic (PV) system is modelled in MATLAB/Simulink software environment. The system is designed to operate in grid ancillary services precisely, frequency regulation function. The model consists of a Photovoltaic (PV) plant with a battery connected to the grid through a three-phase inverter. A bi-directional DC-DC converter between the grid and the battery system is included. The model has a battery storage system that provide steady and regular active/reactive powers available while the grid transmit specific amounts of power needed for a specific duration. According to the design, either the grid or the PV system depending on the dominant energy situation charges the battery. The battery is designed to discharge only when the grid demands energy from the PV and if the PV system fails to meet the demanded active power or reactive power. The PV system and the battery storage is integrated with the grid with the aid of dc-ac inverter in such a manner that bi-directional flow of active and reactive power is achieved.

A 1 MW PV system is connected to the utility grid through a three-phase voltage source inverter system. The grid nominal frequency is set at 50 Hz under normal operation. However, the frequency decreased when the PV was not producing required power hence, the battery responded almost instantaneously and returned the frequency to the nominal frequency. The effectiveness of battery storage system for utility grid frequency regulation was substantiated from the simulation results attained.

Keywords: PV System, Frequency regulation, Grid connected, Battery, Power stability, MATLAB/Simulink

ACKNOWLEDGEMENTS

I wish to express my sincere thanks to Almighty God for granting me good and perfect health coupled with sanity of mind to complete my research successfully.

I would like to thank my supervisor (Dr AK Raji) for the continuous support, for his motivation, patience, guidance, and immense knowledge. His guidance has helped me from the beginning to the end of this research journey. I could not have imagined having a better supervisor and mentor. Your unwavering supervision ensured the success of this thesis.

I would also like to deeply thank all my siblings for the support and words of encouragement whenever required. Your show of love during this period cannot be overemphasized.

My genuine thanks also goes to all members of Faculty of Engineering, staffs at the centre for distributed power electronics system (CDPES) and friends for their immeasurable suggestions and contributions throughout this work.

I would also want to thank the Cape Peninsula University of technology for their financial assistance which was able to cover my tuition and other costs.

DEDICATION

This thesis is dedicated to my mother - Mrs Maria Obu Showers. Mum, you did not wait to say “congratulations” as always.

TABLE OF CONTENTS

LIST OF FIGURES

LIST OF TABLES

LIST OF ABBREVIATIONS

AC	Alternating Current
BESS	Battery energy storage systems
CAES	Compressed air energy storage
CPUT	Cape Peninsula University of Technology
CSI	Current source inverter
D	Duty cycle
DC	Direct Current
DER	Distributed energy resources
DG	Distributed generation
dq0	Direct–quadrature–zero
EMS	Energy management system
EPLL	Enhanced phase-locked loop
ESR	Equivalent series resistance
ESS	Energy storage system
EUBIA	European Biomass Industry Association
GCI	Grid-connected inverter
GHG	Greenhouse gas
GTO	Gate-turn-off thyristor
HVDC	High-voltage, direct current
IC	Incremental conductance
IEA	International energy association
IEEE	Institute of Electrical and Electronics Engineers
IGBT	Insulated gate bipolar transistor
IGCT	Integrated Gate-Commutated Thyristor
kW	Kilowatts
LCL	Inductor-capacitor-inductor
LV	Low-Voltage
MATLAB	Matrix laboratory
MG	Micro-grid
MPPT	Maximum power point tracker
MW	Megawatts
P	Active power
P&O	Perturbation and observation
Pbatt	Power out of the battery
PCC	Point of common coupling
PET	Power electronic transformer

PI	Proportional - integral
PID	Proportional-integral-derivative
PLL	Phase-locked loop
PMSG	Permanent-magnet synchronous generator
Ppv	Power output of the PV
PQ	Power quality
Pref	Reference power
PV	Photovoltaic
PWM	Pulse width modulation
Q	Reactive power
R/X	Line resistance to reactance ratio
RES	Renewable energy sources
SMES	Superconducting magnetic energy storage
SOC	State of charge
SPWM	Sinusoidal pulse width modulation
THD	Total harmonic distortion
TSO	Transmission System Operator
VCO	Voltage-controlled oscillator
VSI	Voltage source Inverter

RESEARCH OUTPUTS

1. Showers, O.S., & Raji, A.K., 2018, November. Enhanced Frequency Regulation Functionality of Grid-Connected Solar PV System. In *Cape Peninsula University of Technology (CPUT) Poster* presentation for *CPUT post graduate research conference*, *Cape Town* 2018.
2. Showers, O.S., & Raji, A.K., 2019, March. Frequency Regulation of Grid Connected Solar PV System Using Battery Storage System. *In Domestic Use of Energy (DUE), Conference, Cape Town* 2019.
3. Showers, O.S., & Raji, A.K., 2019, August. Benefits and Challenges of Energy Storage Technologies in High Penetration Renewable Energy Power Systems. *In IEEE PES/IAS Power Africa Conference, Abuja Nigeria* 2019.

LIST OF SYMBOLS

C_b	Base capacitance
C_f	Filter Capacitor
F_n	Nominal frequency
f_{sw}	Switching frequency
i_i	Inverter output current
i_g	Grid current
I_{rms}	Root mean square current
K_p	Proportional gain
K_i	Integral gains
L_i	Inverter-side inductor
L_g	Grid-side inductor
P_F	Power factor
P_n	Nominal power
R_i	Inverter-side inductor resistances
R_g	Grid-side inductor resistances
R_f	damping resistor
V_i	Inverter output voltage
Vc	Filter capacitor voltage
V_{dc}	Nominal direct current voltage
V_g	Grid voltage
ω	Angular speed
ω_n	Natural frequency in rad/secs
Z_b	Base-impedance
V_{rms}	Root mean square voltage
Z	Impedance
Z_L	Load impedance
Z_O	Output impedance
Z_{Line}	Line impedance

GLOSSARY OF TERMS

Distributed energy resources	Sources of electric power that are not directly connected With a bulk power transmission system; these include Both generation and energy storage technologies
Generator	An electric machine that converts mechanical energy to electrical energy
Inverter	A device or system that converts direct current to alternative current
Megawatts	A unit of power (rate of energy consumption) 1 megawatt is equal to 1 000 000 Watts
MATLAB	A multi-paradigm mathematical processing environment and fourth generation programming language
Model	A depiction of real world systems in a software Environment such as Simulink for improved understanding.
Simulink	An environment for block diagrams where multi-domain simulations and Model-Based Designs are carried out.
Distributed generation	The process of generating electricity using renewable energy resources – these resources generating the electricity are usually distributed over an area, like a photovoltaic farm. Electricity obtained by distributed generation is usually fed into a microgrid
Distribution network	A system of cables that deliver power to consumers at usage voltage levels
Electric power system	An assemblage of equipment and circuits for generating, transmitting and distributing electrical energy
Fossil Fuel	Fuel produced by remains of living organisms that built Up underground over geological periods; it mainly consists of carbon and hydrogen
Greenhouse emissions	Gas emitted into the atmosphere that absorbs infrared radiation, thus contributing to the greenhouse effect

Load	A device that consumes electrical power
Microgrid	A micro power system that comprises a cluster of loads, storage and multiple DG sources. A microgrid can usually function in autonomous mode, or it can be linked to the national electricity grid
Renewable energy resource	Natural sources of energy such as sunlight, wind, rain, tides and geothermal heat, which are naturally refilled
Smartgrid	The term given to the modernized electric grid that uses ICT and computational intelligence to improve the efficiency, reliability, economics and sustainability of electricity supply
Voltage profile	A plot of voltage differences of a given supply network over a period of time

CHAPTER 1: INTRODUCTION

1.1. Background

For more than two decades now, renewable energy resources as a source of power generation has been a major topic in technical literature for power generation. Major concern has been on the dwindling fossil fuel sources that has further increased research in the renewable energy sector (Du Plooy, 2016). Some of the characteristics that has supported this shift are the low maintenance, improved lifetime, non-polluting, and noise-free of renewable energy resources (Chao et al., 2013). This together with improvement in power electronics has contributed immensely to the extensive harvesting of renewable energy resources like wind and solar. Furthermore, National laws and policies of the department of power have amplified the implementation of renewable energy sources for power generation (Mazibuko, 2015).

According to (El Moursi et al., 2014), presently, there are wide-range of technical literatures available that supports the use of ancillary services in linking the breach between the grid and DG resources. However, (Yaramasu et al., 2015) further discusses the idea of “unbundled or ancillary “services in a more detailed manner. It also indicated that active and non-active power control has the capacity to increase grid friendliness by offering ancillary services like frequency regulation, supplemental reserve, spinning reserve, voltage control, peak shaving and backup supply.

The provision of increased energy density storage devices and improvement in semiconductors, have offered a new advantage to the use of ancillary services (Heydari et al., 2019). It has also been shown that either provision of ancillary services or strengthening the grid infrastructure can be employed to maintain reliable network operation (Kumar et al., 2016).

According to (Ibrahim & Raji, 2015), improved metering infrastructure and protected communication system, being the fundamental element of a Smart Grid infrastructure, can be used as the main support for the implementation of ancillary services. The challenges encountered by the steady-increase in electricity demand, degrading environmental impacts, and aging power infrastructure can be resolved significantly using smart grid. The new idea of power management systems together with two-way communication technology possess the capacity to create a reliable intelligent system (Joseph et al., 2017).

The intermittent nature of renewable energy resources presents some difficulty to their integration with the grid. Hence, reliability and power quality become essential elements to consider (Kumar et al., 2016). Omran (2010) in his study looked at the challenges and impact of DER on frequency regulation. They showed the necessity for different grid standards and development of mathematical representations for predicting the system behaviour in situations

of high penetration of intermittent energy resources. (Bevrani & Shokoohi, 2013) had in his study investigated the stochastic nature of renewable energy sources using an ANN-based method for predicting the ancillary services. This method is useful in forecasting non-spinning reserves, spinning reserves, and up-regulation and down-regulation requirements.
The aforementioned literature assessment obviously sets the foundation of this research regarding the significance of PV in current power market that is ultimately tilting towards the smart Grid. It hence encourages one to proffer solutions to the glaring issues regarding the integration of renewable energy resources at high penetration levels with the future grid.

1.1.1. Smart Grid

According to (Vijayapriya & Kothari, 2011), the smart grid concept is the integration of digital architecture to distribution and extended distance transmission grids to improve existing operations by reducing losses and building fresh markets for the generation of alternative energy. This is an intelligent automated system for monitoring the flow of electricity and ensuring a more improved distribution. Presently, protecting the environment has become a global concern; therefore, it is important to find cost-effective ways of decreasing power usage and increasing energy independence.

The present power grid system does not have the capacity to respond to power demand and supply while a smart grid has improved sensing and progressive communication and computing features. Individual components of the system are connected together with communication paths sensor nodes and combination of intelligent inverters to offer the capacity to inter-operate between them. Some of these are communication between distribution, transmission and substations such as commercial, residential and industrial sites (Petinrin & Shaaban, 2015). The smart grid improves the connectivity, automation and synchronisation between the suppliers, consumers and networks that implement a distant transmission or local distribution.

"Smart Grid is an electricity network that can intelligently integrate the actions of all users connected to it - generators, consumers and those that do both—in order to efficiently deliver sustainable, economic and secure electricity supplies" (Vijayapriya & Kothari, 2011). An example of smart grid system is presented in Figure 1.1. A Smart grid uses high technology equipment and services together with intelligent monitoring, control, communication, and self-healing technologies to accomplish the following:

- better simplify the connection and operation of generators of all sizes and technologies
- allow consumers to contribute significantly in improving the operation of the system
- afford consumers more information and choice of supply

- significantly reduce the environmental impact of the entire electricity supply system
- Provide improved levels of consistency and security of supply.

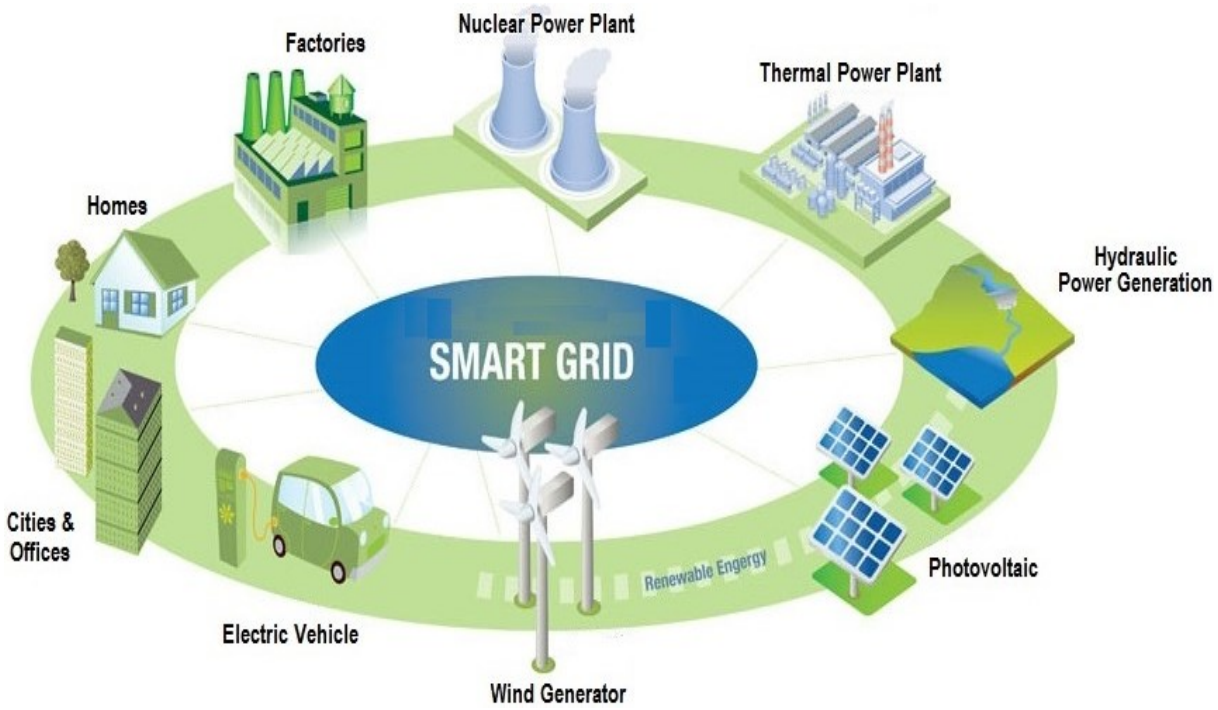

Figure 1-1: Smart grid concept (Electrical concept, 2016)

1.2. Statement of the research problem

Currently, electric utilities are confronted with challenges like rising fuel costs, aging equipment, increasing energy demand, frequency regulation and the difficulty to integrate renewable energy resources into the grid (Bhatt & Chowdhury, 2011). The presence of photovoltaic (PV) penetration on the utility grid is also increasing significantly in recent years. With the recent rise in PV penetration and the advancement of the global PV industry, there is an urgent and a necessary need to introduce features in PV systems that will make them respond smartly (Shah et al., 2015). However, much of these can be addressed without negatively affecting the total performance and power quality of the grid.

South Africa has a high potential for solar energy that will help mitigate the current high-energy demand, but this potential as an alternative source of energy appears to be underutilized (Mazibuko, 2015). Hence, engaging smart Grid technologies, and leveraging the benefits of the distributed nature of PV, new prospects to unearth value can be created. Through the implementation of progressive energy storage techniques, efficient two-way communications, a grid-tied PV system can create significant value, mostly through improved PV contribution in grid support functions like frequency regulation (Adhikari, 2013).

1.3. Significance of the Research

With the constant increase in electricity demand, fast dwindling of fossil fuel and the rising inclinations towards renewable energy resources, the integration of distributed energy resources (DERs) such as PV generation in the utility grid is acquiring huge popularity in recent years. However, the capacity of these integrated generators must be connected accurately in order to maximise the benefit of such integrated systems. Most distributed energy resources are linked to the utility grid with the aid of power electronics interface and have the capacity to generate both active and reactive power with adequate control of the inverter interface.

Recognising the operational difficulties associated with the installation of PV systems, especially power fluctuations, this study will contribute to the improvement of PV system integration to the grid by presenting methods of evaluating the performance of PV system and provide possible solutions to the operational challenges encountered. It will also expedite the increase in the penetration levels of PV systems in the electric network.

However, the anticipated model is an intelligent and efficient system that will generate a complete result capable of assisting the system operator to understand better the behaviour of Grid–connected PV system. Furthermore, the research will support and advocate the use of PV systems as an integral part of the energy mix policy of the national government thereby discouraging over reliance on fossil fuel economy and accepting cleaner sources of energy. Lastly, the results of this research will assist both utilities and PV system operators to select the most sustainable solution for levelling out the output power generated from PV systems.

1.4. Aims and Objectives of the research

These particular objectives will be employed to achieve the main aim of the research work:

- To model a system that will enhance frequency regulation of grid-connected PV system.
- To develop an advanced precise photovoltaic model that has the ability to simulate accurately Grid-connected PV system.
- To investigate the impact of frequency stability, reactive and active power control on Grid-connected PV system.
- To determine the effect of connecting the PV system to the grid taking into consideration the grid code.
- To develop a system that will increase the power quality of a Grid-connected PV system.
- To develop a bi-directional communication system between the grid and PV system
- To model a control mechanism that will advance compensation for power variations in microgrids.

- To carry out steady state and transient assessments on current power grid with several solar PV system ratings (100 KW to 1 MW)

1.5. Delineation of the research

In the thesis, due to the vastness of the research area, some limitations are drawn:

- The study used only grid-connected PV system
- Only the South African Grid code was employed
- The study focused only on frequency regulation

1.6. Thesis outline

Chapter 1 introduces the thesis presenting a small background of the Grid-connected PV system, smart grid, and statement of the research problem, the relevance and the contributions of the thesis.
Chapter 2 offers literature on the fundamental knowledge of renewable energy systems, solar power integration and frequency regulation in Grid-connected PV systems.
Chapter 3 presents a detailed literature review on previous works carried out in this field of knowledge.
Chapter 4 covers the design model of the Grid, PV system, battery, inverter, MPPT and the bi-directional DC-DC converter.
Chapter five presents the simulation results of the Grid- connected PV system designed for frequency regulation. Previous studies are summarized and the results of this research is evaluated accordingly.
Chapter 6 offers conclusions of this research, discusses the conclusion and makes some recommendations for further research.

CHAPTER 2: RENEWABLE ENERGY SOURCES

2.1. Introduction

This study was informed by the finite nature of fossil fuel and our over-reliance on it. Considering the amount of fossil fuel consumed globally, research has indicated that the world will be running out of oil and gas in approximately 50 years from now if our attitude towards the usage of this scare resource does not change. All though there has been recent discovery of oil and gas, it would still not meet global energy demands. Therefore, there must be a conscious effort to move away from oil and gas then embrace the renewable energy sources. In an attempt to make this switch, the photovoltaic (PV) has been identified as the most reliable and stable renewable energy sources in comparative terms (Marafia, 2001).

Government policies aimed at increasing the amount of renewable energy sources in the energy mix in recent years has actually resulted in a remarkable increase in distributed generators (DG) connected to the grid (Johnstone et al., 2010).

Renewable energy such as photovoltaic systems, Hydroelectric energy, Biomass and wind energy generates energy without the emission of greenhouse gases. In the past, these were previously referred to as small-scale electricity generation systems. Nonetheless, they are gravitating towards large-scale energy generation (Doukas et al., 2005; Marafia, 2001). With this development, the grid system needs additional systems to monitor the frequency, voltage and current of the grid (Trabelsi & Ben-Brahim, 2011). This has resulted into countries moving towards smart grid system to ensure stability of the entire system. The development of smart grid systems has also posed new challenges like grid stability and anti-islanding (Vijayapriya & Kothari, 2011).

This section discusses more on the background and literature on renewable energy sources, wind energy, biomass energy, hydro power, Solar energy, growth of photovoltaic technology, operating principle of PV effect, South Africa PV technology, electrical characteristics of PV, electrical characteristics of PV system, temperature and solar irradiance effect, types of PV system, stand-alone and grid-connected PV system.

2.2. Renewable Energy Sources

Renewable energy sources are energy sources that are renewed intermittently by natural courses and hence unlimited. Some examples of renewable energy sources are Hydro, solar, wind and biomass. These renewable energy sources are clean, does not generate greenhouse gases and therefore has minimal negative impact on the environment (Shamsipour & Shamsipour Dehkordi, 2015). However, contrary to fossil fuels, renewable energy resources

are more evenly distributed all over the world and offered at no cost. Table 2.1 indicates the annual energy consumption in South Africa and the World respectively.

Table 2-1: Total primary energy consumption in South Africa, 2016 (Department of Mineral Resources, n.d.)

Sources	South Africa (%)	World (%)
Oil	22	33
Natural gas	4	24
Coal	70	28
Nuclear energy	3	5
Renewable energies	<1	3
Hydroelectric	<1	7

Again, it can be seen from Figure 2.1 that the world still relies heavily on fossil fuel for energy generation and consumption. Only a little fraction, approximately 12% of the world's basic energy is supplied by renewable energy sources (Shamsipour & Shamsipour Dehkordi, 2015). Continuous growing energy demand and dwindling fossil fuel reserves has stirred collective interest in the use of renewable energy sources to meet global energy demands.

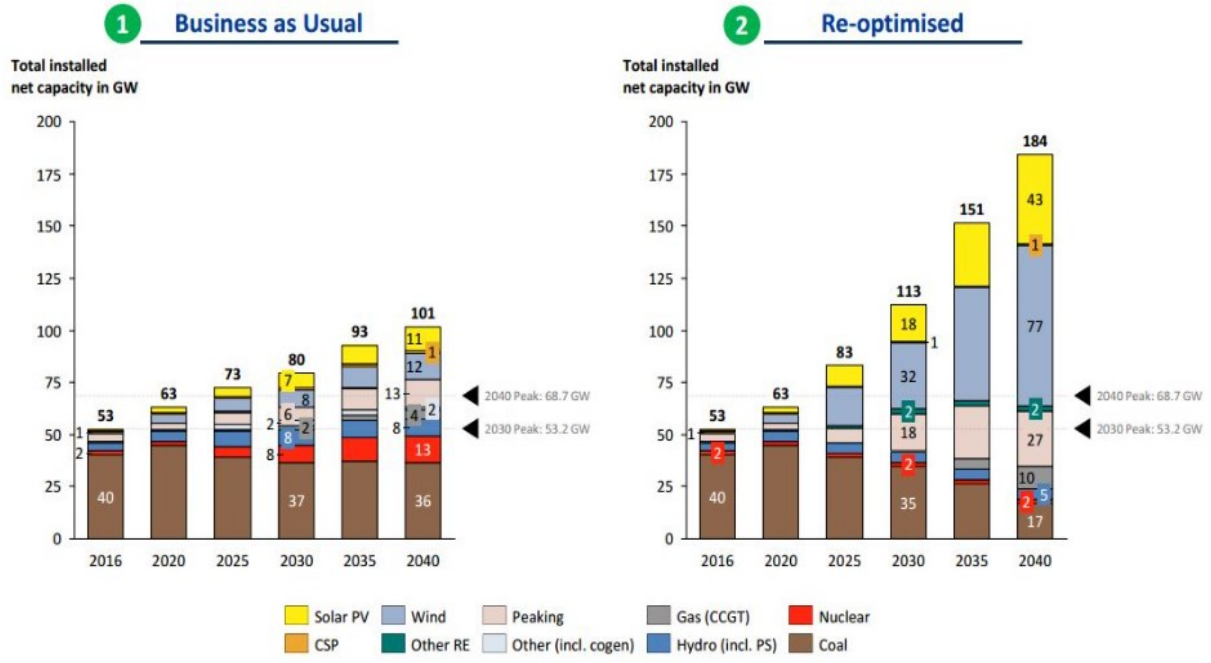

Figure 2-1: Capacity mix for 'Business as Usual' vs. 'Re-optimised' situation from 2016 to 2040, South Africa (Source: CSIR)

In the world of today, the use of electricity has become a fundamental need in our daily lives. The reliance on electricity has increased as the standard of living increases especially in developed societies. With over 60% of electric energy production generated by burning coal, oil and gas i.e., the use of fossil fuel resources. Fossil fuel as the basic source of electricity generation is not sustainable because of its non-renewability and finite nature. We can ignore the fact that fossil fuel will be extracted completely in the near future but that will be living in denial. The only question paramount is when this will definitely happen (Kofi-opata & Kofi-opata, 2013). Fossil fuel are unequally distributed on the surface of the earth. For instance, countries with high consumption rate have low reserves or not at all while countries with very high reserves consume very low. This situation has placed the developed countries with high fossil fuel consumption rate to depend heavily on imports from other countries (Alvarez et al., 2012).

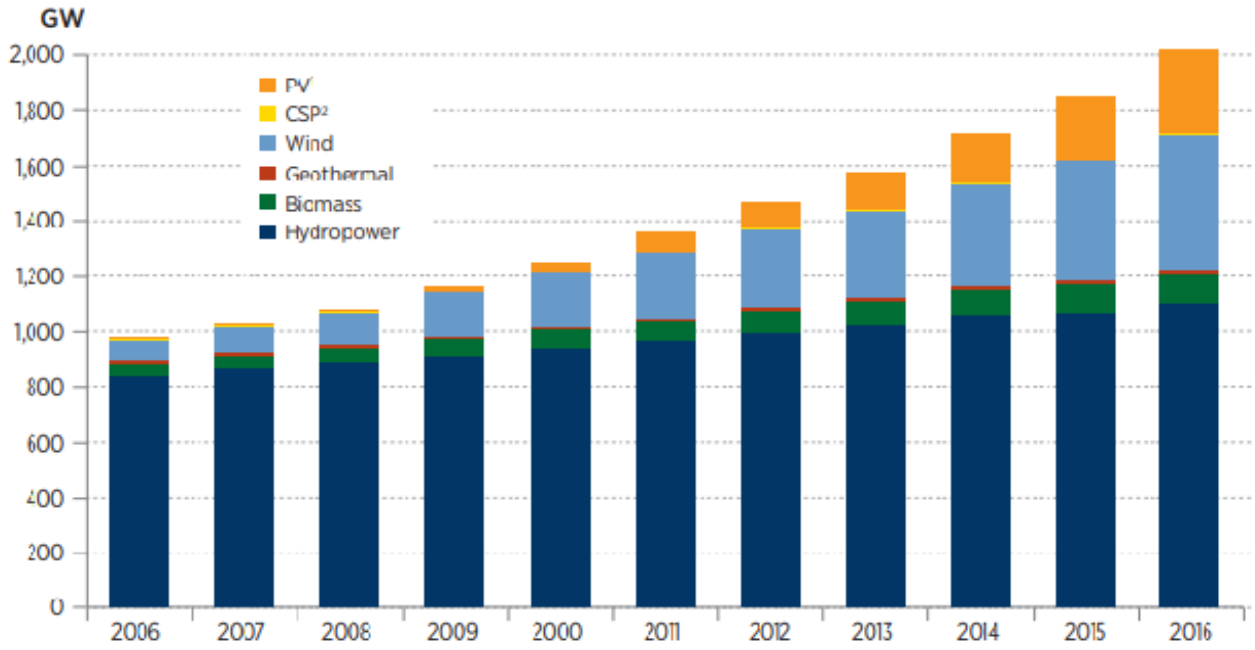

Figure 2-2: Global Renewable Electricity Capacity (Source: REN21)

Renewable energy sources (RES) as an alternative source of energy has the potential to meet the global energy demand if properly harnessed. Although, it is still a controversial topic for discussion in some sectors of society, it has been shown to be the solution to our future challenges. Most Renewable energy sources like solar, wind, hydro and biomass occurs as a result of the solar radiation that touches the earth (Alvarez et al., 2012). The only exception is that geothermal energy is possible through different processes within the earth, along with the ebb and flow energy, which does not originate from the sun rather generated by the gravitation of the moon and earth (Kofi-opata & Kofi-opata, 2013).

It has been shown that the solar energy reaching the Earth in an hour equals the total production of all primary sources in the whole planet for a year (Kim et al., 2016). In addition, the amount of incident solar radiation is enough to meet all our energy need and more.
Approximately 1.1 billion people in the world live without any form of electricity while many others experience repeated power outages (Doukas et al., 2005). Concerns related to global warming together with growing electricity demand and emergence of other technologies has encouraged research and interest in renewable energy technologies. Proper use of different renewable energy sources can create a pathway for sustainable growth. Hence, efficient design and planning for operating renewable energy sources is needed for sustainable growth of our society. The concern on global energy security, sustainable growth and climate change can be addressed by properly harvesting renewable energy sources. So, there is an urgent need to increase the development of renewable energy technologies. Hence, a brief explanation of different renewable energy sources together with their present status are presented below.

2.3. Wind energy

The development of wind energy is traced back to as early as 1888 in the US. This was largely prompted by the oil shortage and crisis of 1973 (Rahman et al., 2010). Installation of wind turbines saw a significant decline afterwards because of the drop in oil price. Currently, the interest in wind power has been revived due to developments in wind power technology, current oil crisis, and an attempt to mitigate greenhouse gas emissions from fossil-fuelled power plants. Wind power is gotten from solar energy because of the unequal spreading of temperatures in various parts of the earth. The corresponding movement of mass of air is the fundamental source of mechanical energy that energises wind turbines for water pumping, willing, domestic usage, electricity generation and other uses.

Because energy in wind grows as the cube of wind speed, even the smallest variation in wind speed will affect the output power generated from the wind turbine significantly. The impact of wind energy technology is minimal and the land occupied by the wind towers can be utilised for agriculture or provide locals an opportunity to earn more income. Developments in wind turbine technology have led to improvements in energy conversion techniques, reliability and rotor blade efficiency. Currently, the price of electricity generated from wind is competing favourably with coal-fired power plants and continues to drop (IEA, 2019). Recent developments have made the objective of supplying 12% of global electricity demand from wind by 2020 feasible (Fried, 2011). According to Figure 2.3, the total global wind generation capacity in 2017 is 539,123 MW with an annual growth rate of 15%. Wind energy as a source of power is attractive to different people for different reasons. In developed countries, wind power is attractive because of its outstanding environmental benefits and non-pollution of

greenhouse gases. While in developing countries, it is competitive because it is suitable for local production, operation and circumvention of the cost associated to long distance transmission lines (Fried, 2011).

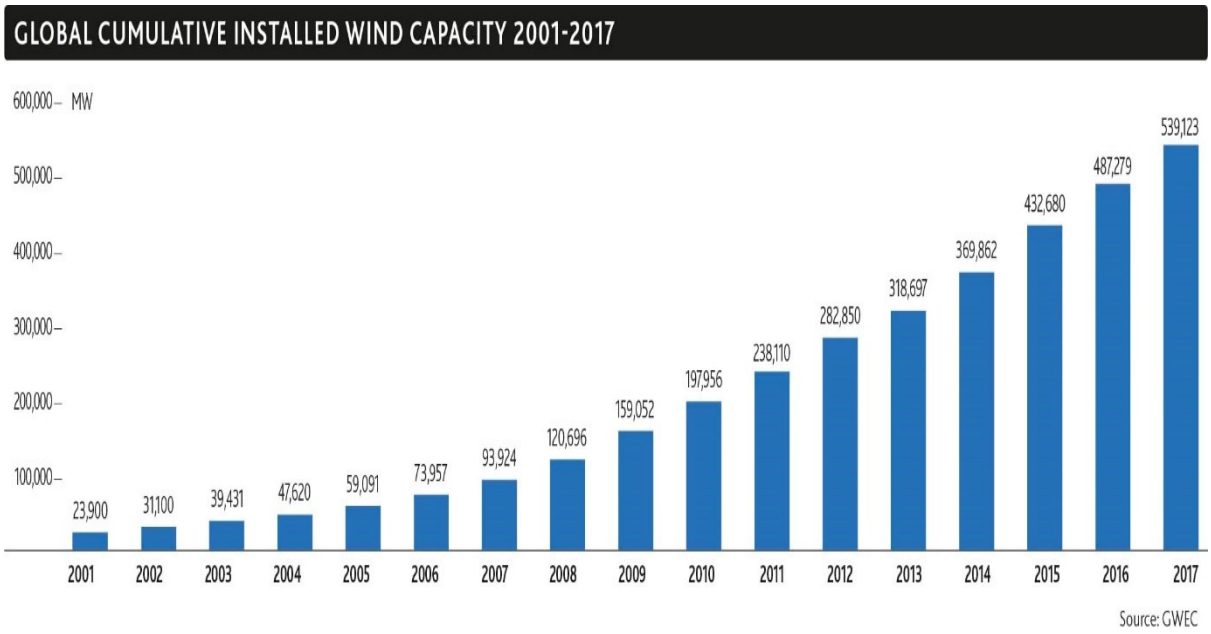

Figure 2-3: Global cumulative installed wind capacity from 2001-2017 (Source: GWEC)

2.4. Biomass Energy

Biomass energy or bio-energy as it is known by some is the energy gotten from living organisms or organic wastes gotten from humans, animals, plants and aquatic life. Some examples of biomass are sewage, grasses, trees, animal waste, wood chips, municipal wastes, agricultural wastes and garbage. Before the industrial revolution, biomass was the primary source of energy. Organic elements from domestic and industrial waste, agricultural wastes and landfills if applied efficiently has the capacity to reduce the emission of greenhouse gases globally.

A significant number of people in the developing countries rely mainly on freely collected conventional biomass like firewood, animal waste, domestic waste and forest residue. However, it is being used unsustainably with consumption more than replacement thereby creating deficit. Most of the local citizens in these developing countries use biomass mainly for cooking and heating purposes. The main advantage of this form of energy is its simplicity, availability, low cost and familiarity. The fundamental ways of utilizing biomass sources are gasification, biochemical conversion, direct combustion, chemical conversation or biological conversation (IEA, 2019). Most of the biomass is in the form of woody forest materials and

plants. Figure 2.4 shows the potential of biomass energy and current use in Africa, Asia, Europe, Former USSR, Latin-America, the Caribbean and North-America.

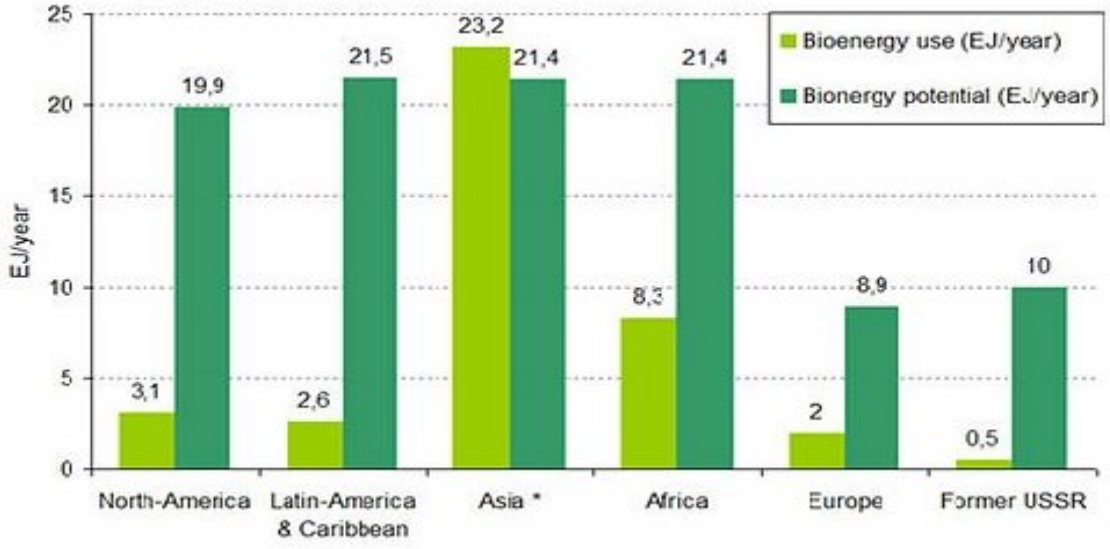

Figure 2-4: Biomass energy potential and present use in some regions (Source: EUBIA)

Currently, biomass resource potential is obviously underutilized. The potential is far more than its current use. Therefore, the potential can be used to produce electricity, heat, and fuels for the generation of electricity and transport. Biomass can be used for the production of biogas for cooking and lighting, biodiesel for transportation and bioethanol. Biomass energy has the potential to contribute meaningfully to carbon-restricted energy future and meet the future energy need (REN21 Steering committee, 2011). The spinoff of biogas production can be utilised as organic fertilizer and approximately, 44 million households globally use biogas for lighting and cooking daily (REN21 Steering committee, 2011).

2.5. Hydro Power

Hydropower technology is well established over time. This is renewable energy resource that emanates because of potential energy stored in water that moves from a region of higher potential to a region of lower potential with the help of gravity. However, hydro energy is been converted to electricity by water moving through turbines that rotates shafts that in turn drives electric generators (Mathema, 2008). The skills and technology required to implement the conversion is efficient and advanced. For some centuries, hydropower has been utilised to produce mechanical power, used for textile processing, industrial activities and grain milling.

Currently, the building of small hydropower plant technology has gained enormous popularity especially in the rural areas because most of the rural areas have rivers and little water heads

that has aided this development. Hydroelectric technology has been shown to be highly dependable with low operation and maintenance costs but demands high initial investment. This technology has a comparative operational life span of over a century (REN21 Steering committee, 2011). It provides approximately 16.5% of the global electricity and represents 71% of total electricity from renewable energy (REN21 Steering committee, 2011).

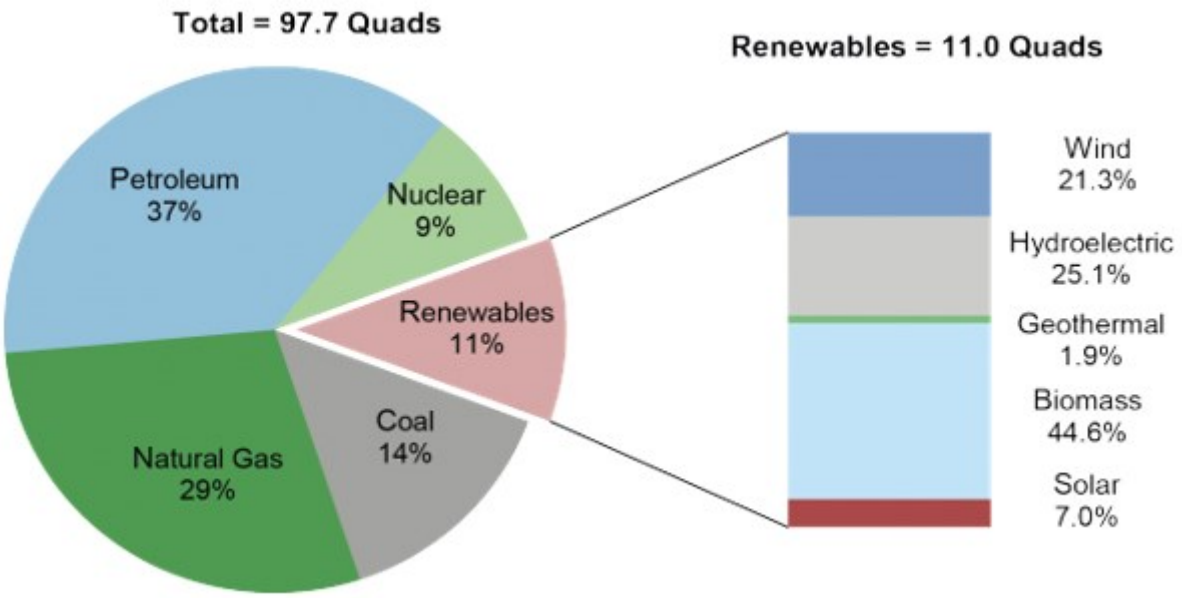

Figure 2-5: Percentage of Renewable energy in global electricity production in 2016 (Source: www.ren21.net)

Hydropower occupies a strategic position in the power management sector offering planners the opportunity to stabilise and regulate services my measuring peak load demands and assists in incorporating variable renewable energy in the energy mix as shown in Figure 2.5. There are various types of hydropower today but the three basic types are run-of-river hydroelectric plants, reservoir hydroelectric plants and pumped storage hydroelectric plants. However, due to the simplicity of technology of hydropower and cost of installation, rural communities have the capacity to build micro hydropower plants. This will also assist countries mitigate greenhouse gas emissions (Elbatran et al., 2015).

2.6. Geothermal

This is electricity produced by the use geothermal energy. The temperature below the earth surface are not the same in all locations and countries thereby making it difficult for some countries to operate this form of electricity production efficiently. Nevertheless, countries sited in geothermal hotspots possess a higher potential for high temperatures close to the earth surface causing a higher thermal output of heat transfer (Gerdi et al., 2013).

The heat energy underneath the earth surface certainly produces steam. This steam has the capacity to spin a turbine if linked to a generator thus generating electricity. However, because these natural steams are not common, the system employs a system that consists of liquid water converted to steam towards the earth surface (Sigfússon & Uihlein, 2015).
Globally, beginning from 2012 to 2015, 24 countries generated approximately 12.8 billion watts of electricity with a steady growth rate of 5% (Sigfússon & Uihlein, 2015).
The excess electricity produced by Geothermal system can be used to power our homes and useful for cogeneration. The primary advantage of geothermal energy over solar and wind is that it is steady and reliable. It can also provide base load power to the electrical grid thereby ensuring stability. Presently, the United States, Indonesia and Italy are amongst the highest producers of geothermal energy in the world. Geothermal energy makes up approximately 0.5% of the global primary energy supply due to lack of technology in most countries (Bertani, 2015).

2.7. Solar Energy

Direct solar energy is known to be essentially indefinite. If the entire energy released by the sun were converted to useful form in the earth, it would be able to meet the world's present energy demand and even more. Nonetheless, this is not visible due to cloud cover, amount of energy intercepted by the earth and rotation of the earth (Bracale et al., 2016).

This form of energy can be employed directly to provide domestic hot water and to heat or light buildings. It can also be used in pumping water, refrigerate foods and medicines, cooking and desalinate water. In addition, it can be converted to useful forms via different technologies; essentially photovoltaic (PV) and thermal. Solar thermal technologies convert solar energy to heat that can be used directly, stored in any storage system, or converted to mechanical or electrical energy by a suitable mechanism. While photovoltaic (PV) absorbs incident photons then converts the photon energy to either stored chemical energy or electricity (Rahim et al., 2015).
Concentrating solar power systems uses mirrors to concentrate the solar radiation so that it can be trapped as heat. This heat is further converted to electricity by a traditional thermal power plant or used to trigger chemical processes. This technology is at an advanced stage and understood to be appropriate for collective heat and power generation with significant potential in power system. The technology involves three approaches; trough, power tower and dish.
According to Figure 2.6 below, photovoltaic (PV) technology is developing speedily. This development is because of government's supportive policies, noticeable price reduction, technology advancement and material enhancements. PV is readily available, commercially available and is a dependable technology with a prospect of a long-term development in all the

continents of the world. However, some countries are more promising because of their high level of solar irradiation and available technology.

In 2016, the total Solar PV capacity reached nearly 300 GW and generated slightly above 310 TWh. This is about 26% more than 2015 and represents just above 1% of global power generated. Utility grids account for 55% of the total PV installed capacity, with the remaining in commercial, residential and off-grid systems. However, according to (IEA, 2019), Solar PV is projected to top renewable electricity capability growth.

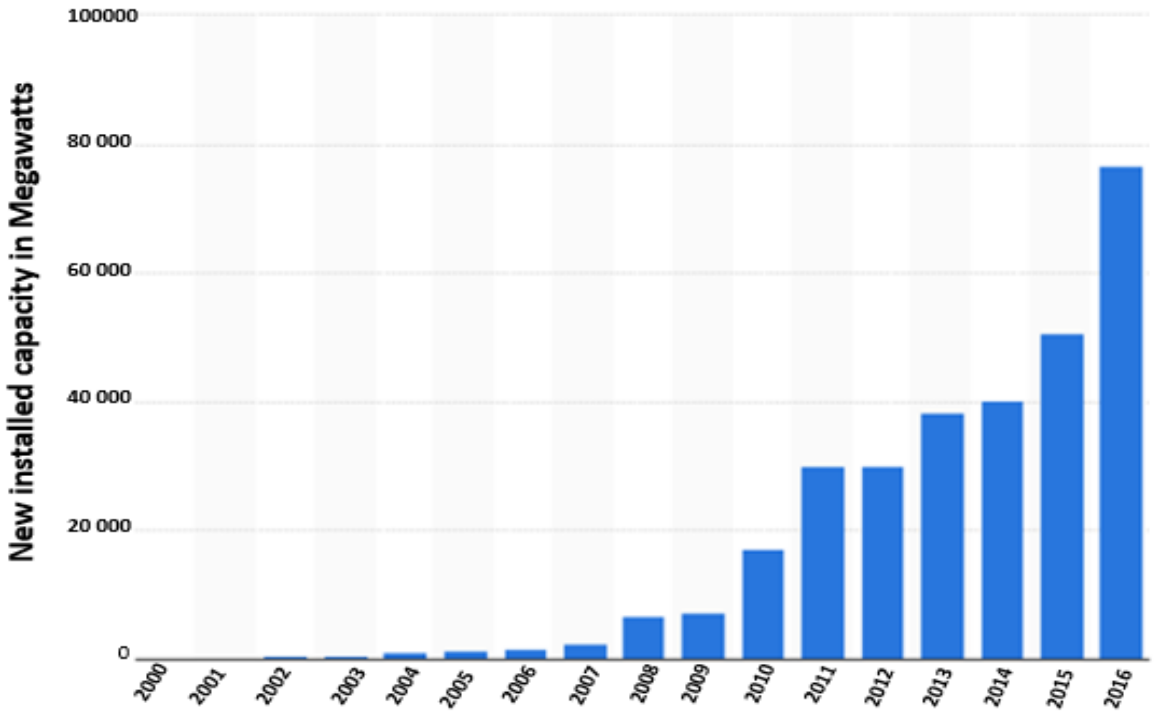

Figure 2-6: Global installed solar PV capacity from 2000 – 2016 (Source: REN21)

2.7.1. Growth of Photovoltaic technology

The concept and effect of PV was first discovered by Becquerel in an attempt to investigate the impact of light on electrolytic cells. Presently there are four major types of PV cells namely: thin film, Mono crystalline, Poly crystalline and transparent solar cells(Nelson, 2010).

A photovoltaic cell as a special semiconductor diode converts visible light into direct current. However, Some PV cells also have the capacity to convert infrared or ultraviolet radiation directly to DC electricity (Nelson, 2010). Photo means ‘light’ and voltaic means ‘voltage’. The sun hits the earth’s surface at a solar constant of approximately 1000 watts per square meter (1000W/square/m), but this figure varies according to geographical location and changing weather conditions. Series of research and technology advancement in the renewable energy

sector in recent years has made PV system a suitable alternative energy source to supplement the grid system (Ibrahim & Raji, 2015).

PV system as a system that converts sunlight into functional DC electricity consists of singular or multiple solar cells connected together to make up a panel. This system takes insolation directly from the sun and then converts to a functional DC signal hence sent to an input filter capacitor (Eltawil & Zhao, 2010). However, after the input filter capacitor, a DC to AC inverter is connected. This inverter converts the DC current from the DC point into a corresponding AC signal that is further synchronised with the grid. Minor loads like lighting systems, television, radio and DC motors could be supplied directly by the photovoltaic array or panel. Although, power conditioners are required for most PV usage for the electricity obtained from the photovoltaic device to be processed. The current and voltage is controlled by converters at the load side but they are not constant because of changes in the solar irradiation and temperature. Therefore, to track the maximum power point (MPP) of the device and to control the power flow in the grid system an MPPT is needed (Trabelsi & Ben-Brahim, 2011). According to (Nelson, 2010), to create PV modules, solar cells are combined into bigger units which are then connected in a parallel-series configuration to make up arrays of PV modules. The output voltage of the photovoltaic (solar cell) depends mainly on the photocurrent, which further depends on the amount of solar illumination during conduction. In order to realise a highly complete efficient PV system, the PV topologies must be cost effective, user-friendly and possess a high reliability. It is also very important to note that, to supply regular load demand to customers or supply electricity to the grid, the system will require power-conditioning systems like, DC-to-DC converters (Pappu, 2010).

However, photovoltaic panels are sources of power supply for situations were alternative sources of power supply or the grid is not available. Examples of some of these applications are water heaters, security systems, power institutions, small industries, households, customer equipment and telecommunication relay stations (Sidhu, 1999). Utility companies sets the standards that PV module connections must conform to before connected to the grid. Currently, the IEEE1547 is the established international standard that all grid-connected systems must conform to (Heydari et al., 2019). However, these standards will solve problems of detection of islanding operation, grounding, power quality, frequency regulation, and voltage stability (Bhatt & Chowdhury, 2011). So, in order to reduce power stability challenges, the generating systems must have a system management mechanism, the system must be robust, must maintain steady voltage profile and system restoration mechanism must also be included in the design. Nonetheless, Price reduction, improved efficiency of the PV panels, favourable government policies and increased environmental awareness has contributed immensely to the 60% annual growth the photovoltaic energy has experienced in the past five years (Alrahim Shannan et al., n.d.). With crystalline silicon as the leading PV material because of its high efficiency, lower cost and long service cycle (Zhong, 2017).

2.7.2. Operating principle of photovoltaic effect

The photovoltaic effect is the bases of the operating principle of the solar cell (Quaschning, 2005). The photovoltaic effect is the generation of potential difference at the P-N junction. When photons are absorbed by the material, electron-hole pairs are created. However, when these charge carriers enter the P-N junction, the electric field in the depletion layer will drive the holes into the P-type material and drive the electrons into the N-type material as indicated in Figure 2.7 (Messenger & Ventre, 2018). Whenever a material absorbs sunlight, the electrons in the material move to a higher energy level because of the acquisition of more energy. This is the energy difference between the first and last states represented as $\boldsymbol{h}^{+}$ which shows the internal field. This happens specifically when the energy of the photons creating the light is greater than the forbidden band gap of the semiconductor material (Nelson, 2010) material. Then the energised electrons quickly return to their original state. Photovoltaic device has in-built asymmetry made possible by doping (introduction of impurities) that pushes the energised electrons away before they can return to the original state and feed them to an external circuit. Hence, the additional energy of the energised electrons generates an electromotive force (EMF) or potential difference. According to (Mansouri, 2011), this is the force that drives the electrons through a load in the external circuit to perform electrical work.

(Quaschning, 2005), in his book represented photovoltaic effect as:

- Production of charge carriers as a result of absorption of photons in the material that creates a junction,
- Followed by the separation of the photon created charge carriers in the junction,
- Assembling of the photo-generated charge carriers at the terminals of the junction

Fundamentally, light strikes loose electrons of silicon atoms then these unrestrained electron acquires energy and gets pushed by the internal electric field to the end terminals allowing current flow. This is what is referred to as the photovoltaic effect and never run short of electrons as indicated in Figure 2.7 (Masters, 2005).

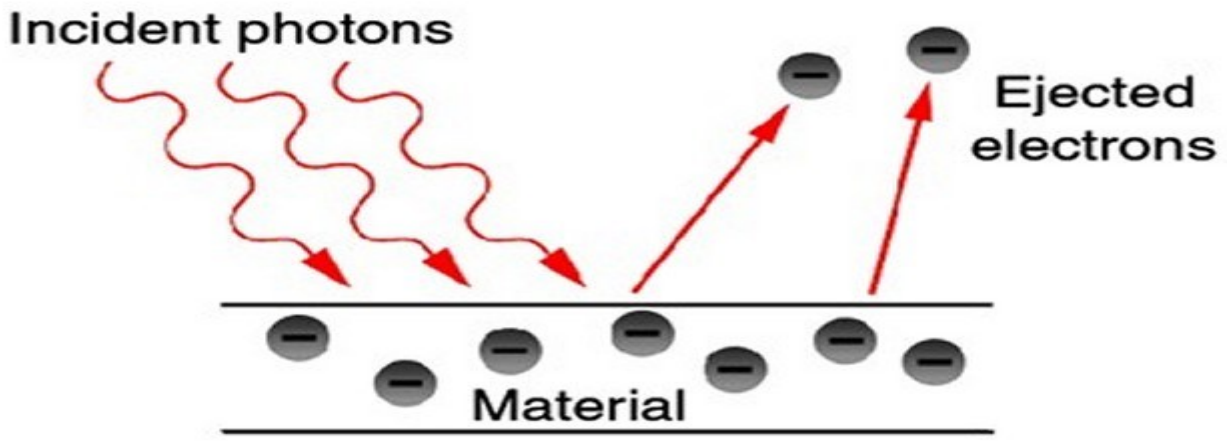

Figure 2-7: Photoelectric effect (Masters, 2005)

2.7.3. South Africa PV technology

According to the heat map shown in Figure 2.8, South Arica has a huge potential for solar energy considering her high irradiating intensity. Especially with the Karoo appearing to be the most suitable for PV systems with its constant high irradiation per square meter.

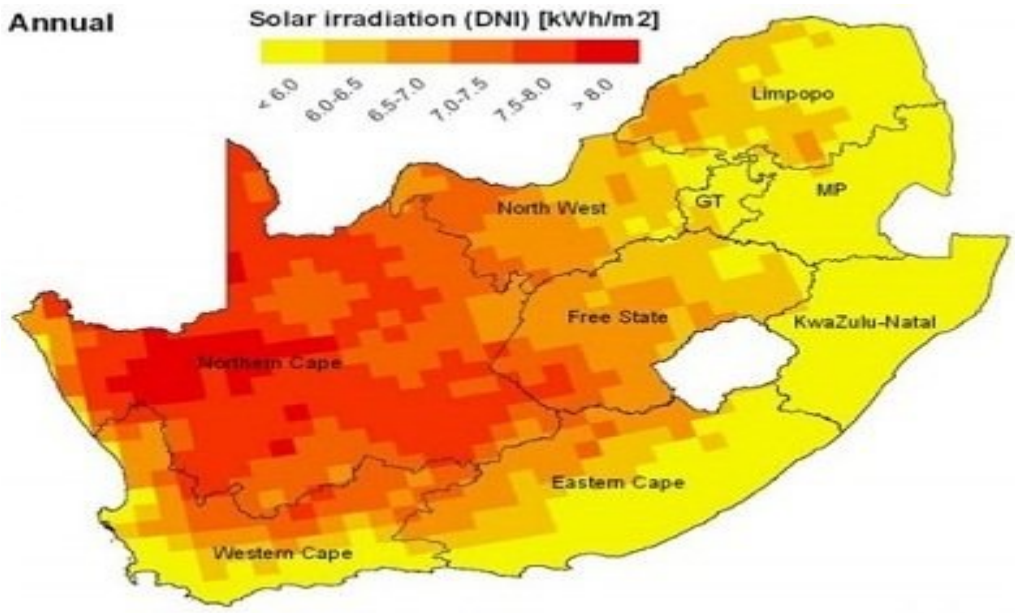

Figure 2-8: Global Horizontal Irradiation Data for South Africa showing average kWh/m^2 per year. (Source: SolarGIS)

South Africa is a growing economy and country where PV systems are readily available, easy to install and maintain. Although, the PV technology is common for residential and commercial renewable energy systems (RESs). The prevalent challenge present at this moment is that our peak demand is less than our reserved energy capacity. Eskom has also shown that sun can

only be used and optimised for PV production before the countries' acknowledged peak demand begins which is 17:00 – 19:00 during winter and 18:00 – 20:00 during summer seasons. The sun generates limitless power but simply efficient on approximately five hours daily (Department of energy Republic of South Africa, 2015). According to (Mazibuko, 2015), to avoid the problem of wastage, a system can be designed specifically to store the energy generated by the sun. Furthermore, Figure 2.9 has displayed the output power profiles of a typical residential load alongside a PV power generated:

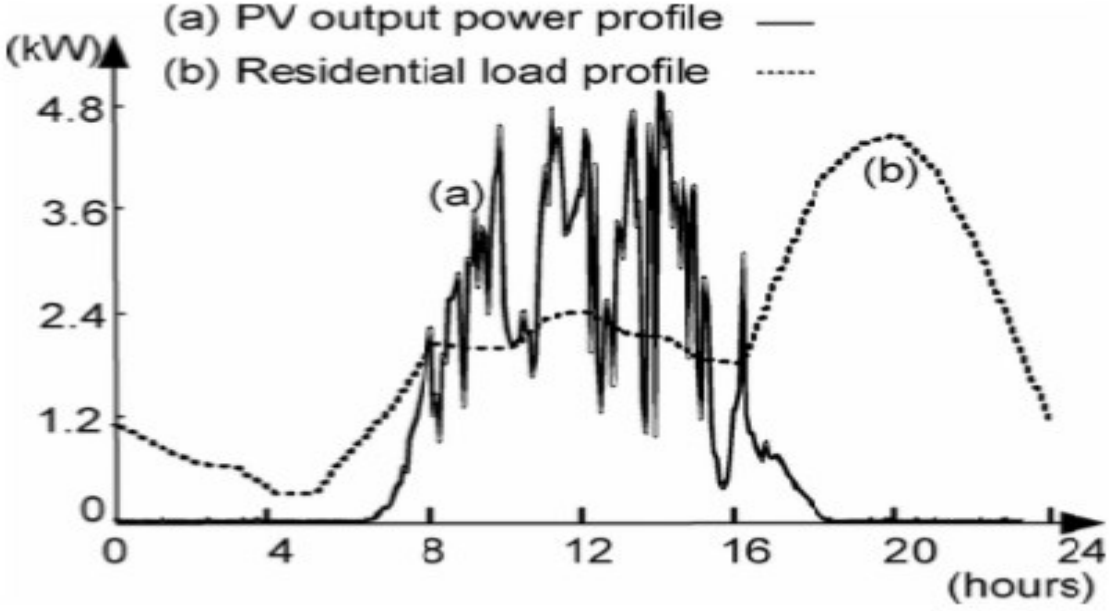

Figure 2-9: Electrical power output profile (Mazibuko, 2015)

Figure 2.9 indicates clearly that the PV output profile offers maximum power before the peak demand of the consumer begins and the residential peak load profile sits between 16:00H – 24:00H. This graph and study shows clearly the vital role that energy storage plays in the efficiency of renewable energy system.

2.7.4. Electrical characteristics of Photovoltaic

Photovoltaic models are characterised into different types with single diode model (SDM) as the simplest one. It is explained with the aid of a single diode which the improved Shockley diode equation includes the ideality factor (n) to describe the recombination mechanism that happens in the P-N junction, displayed as antiparallel diode to the current source (REN21, 2017). This model conceals the accuracy of the PV cell specifically at the maximum point because of its simplicity (REN21 Steering committee, 2011) as presented in Figure 2.10.

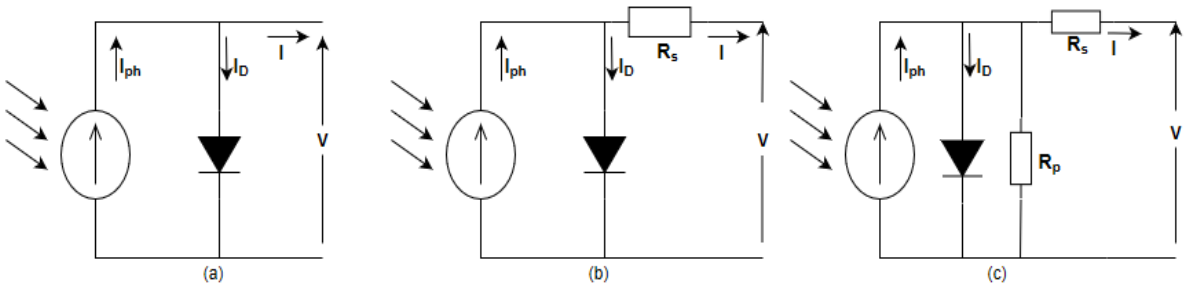

Figure 2-10: The equivalent circuit of a solar cell: a) ideal single diode model b) 4-p model c) 5-p model

The improved model with additional series resistor enhances the model to (4-p) but not applicable to this study. Equation 2.1 further shows the development of a single model to 5-p model. This model is common in research work because of its experimental accuracy (Messenger & Ventre, 2018).

$$I = I_{ph} - I_d - I_p = I_{ph} - I_o\left[e^{\left(\frac{V+IR_S}{nV_t}\right)} - 1\right] - \frac{V+IR_S}{R_p} \tag{2.1}$$

2.7.5. Electrical characteristic of PV system

Equation 2.1 shows the electrical characteristics of a solar cell and indicates the output current as a function of the cell voltage and the resistor in series ($\boldsymbol{R_s}$) represents the voltage drop at the P-N junctions. While for the recombination in space charge is diode reverse current and the parallel resistance ($\boldsymbol{R_p}$) represents the leakage currents at the cell edges (Messenger & Ventre, 2018).

The corresponding PV circuit of 5-p model explained in equation 2.1 is very challenging and has no clear defined solution for neither voltage nor current. Nonetheless, the I–V curve of the diode is by increasing the diode voltage on a spreadsheet until a corresponding current is achieved (Nelson, 2010). An example of a plot achieved by the above method is shown in Figure 2.11 (Richardson & Richardson, 2016) where the red curve indicates I-V curve while the blue curve is the product of the voltage and current (power) delivered by the PV cell.

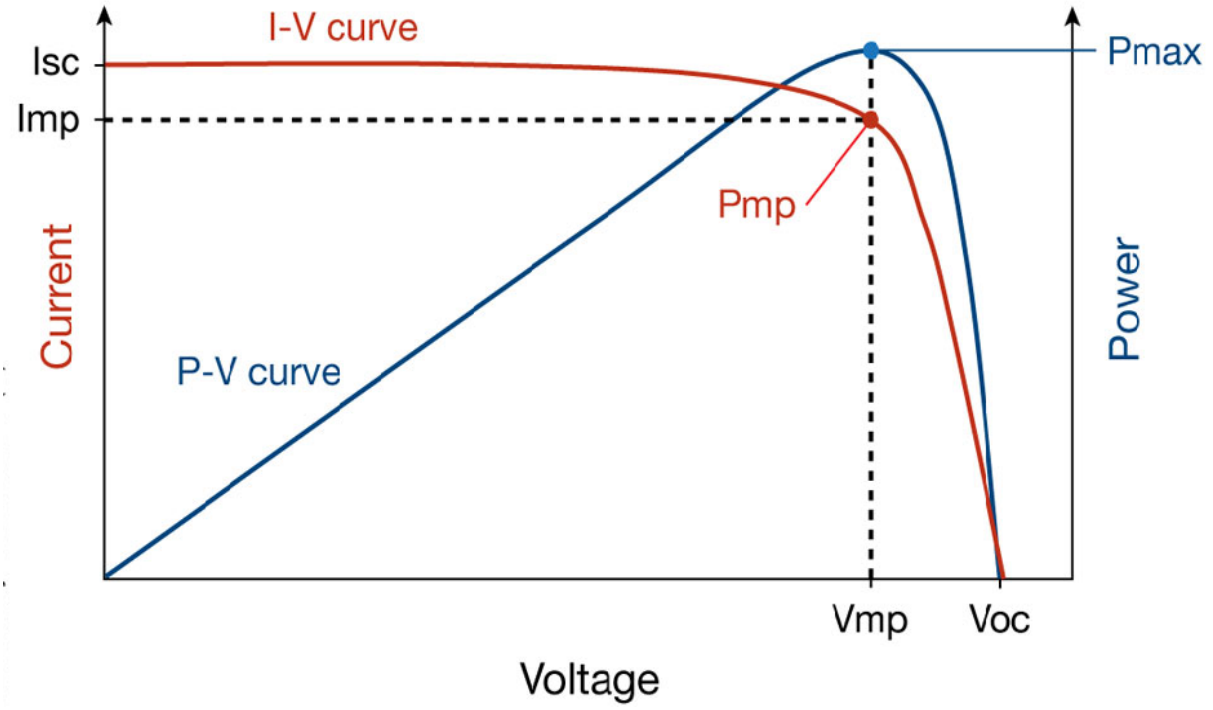

Figure 2-11: I-V curve (red) and P-V curve (blue)

There are three main points in Figure 2.11 above: the maximum power point ($\boldsymbol{P_{max}}$) which is a product of ($\boldsymbol{I_{mp}}.\boldsymbol{V_{mp}}$), Open voltage ($\boldsymbol{V_{oc}}$) and the short circuit current ($\boldsymbol{I_{sc}}$). These values are always provided by the manufacturer at standard test conditions (STC) (Alam & Alouani, 2010). The maximum power point is normally within the knee position of the I-V curve, the area where the product of the current and voltage gives the maximum power. This area is the most efficient point to operate a photovoltaic system given a particular weather conditions (temperature, irradiance, etc.) (Vijayapriya & Kothari, 2011). The open circuit voltage ($\boldsymbol{V_{oc}}$), is the maximum voltage that the Photovoltaic panel produces at no load (open circuit condition). This is a higher value than the maximum point voltage ($\boldsymbol{V_{mp}}$) which is related to the PV during operation. This value depends on the total number of PV panels when are connected in series (Adhikari, 2013).

Because a single cell produces approximately 0.5V, it would not be so beneficial for any application. Therefore, in order to boost the output voltage, the cells are connected in series and then later in parallel to increase the output current (Marafia, 2001). The fundamental building block of a PV array is the PV module, which comprises a number of cells connected in series. An example is the 36 cells connected to produce 12V at the output. Nevertheless, for grid connection, many solar cells are connected to meet the required voltage of the grid. Modules are connected in series therefore according to Kirchhoff's law, current in a series connection is the same but the voltage is added to produce the total voltage and it is given by the Equation 2.2 (Nelson, 2010).

$$V = \sum_{i=1}^{n} V_i \tag{2.2}$$

Where:

$$V = total\ voltage,\ V_i = Voltage\ across\ the\ first\ module,\ n = current\ at\ nth\ module$$

While for a parallel connection according to Kirchhoff's current law, current increases to achieve the required power output as described in equation 2.3 (Quaschning, 2005).

$$I = \sum_{i=1}^{n} I_i \tag{2.3}$$

Where:

$$I = total\ current,\ I_i = first\ module\ current\ ,\ n = current\ at\ nth\ module$$

The series and parallel connection builds up an array as shown in Figure 2.12 (d) (Ataei et al., 2015).

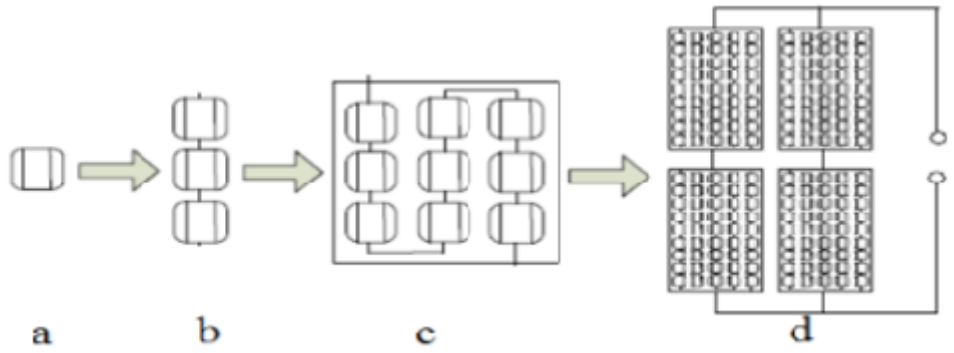

Figure 2-12: a) Photovoltaic cell b) cell series string c) Cell module d) PV array

Hence, for a PV module or PV array, a mathematical model can be realised where $\boldsymbol{N_s}$ the number of cells connected in series that multiplies the output voltage and $\boldsymbol{N_p}$ is the number of cells connected in parallel multiplied by the output current as indicated below: (Rahim et al., 2015).

$$I = N_p I_{ph} - N_p I_o \left[e^{\frac{1}{V_i}\left(\frac{V}{N_s} + \frac{I}{N_p} R_s\right)} - 1 \right] - \frac{N_p}{R_p}\left[\frac{V}{N_s} + \frac{I}{N_p} R_s\right] \tag{2.4}$$

The power delivered by photovoltaic can be calculated my multiplying $\boldsymbol{V_{dc}}$ by Equation 2.4 and realise;

$$P_{pv} = N_p I_{ph} V_{dc} - N_p I_o V_{dv} \left[exp\left(\frac{qV_{dc}}{nKT_{cell}}\right) - 1 \right] - \frac{N_p}{R_p}\left[\frac{V_{dc}}{N_s} + \frac{I_{ph}}{N_p} R_s\right] V_{dc} \quad (2.5)$$

Equation 2.5 indicates clearly that the power delivered by the photovoltaic depends on the voltage and current across solar cell circuit (Mandadapu et al., 2017).

2.7.5.1. Temperature and solar irradiance effect

From Figure 2.11 (I-V & P-V curves), it shows that the output characteristics of a solar cell is non-linear while the solar cell is significantly reliant on solar radiation, load condition and temperature (Mandadapu et al., 2017). Likewise, the current source depends on the solar irradiation and temperature as explained in Equation 2.6 that photo current is directly proportional to the radiation and linear temperature (Alam & Alouani, 2010).

$$I_{ph} = [I_{sc} + k_i(T - T_{STC})] \frac{\boldsymbol{E}}{\boldsymbol{E_{STC}}} \quad (2.6)$$

Where: $\boldsymbol{I_{ph}}$ = photo current

I_{SC} = Short circuit current

K_i = temperature coefficient of I_{SC}

T_{STC} = STC temperature at 25℃

T = Operational temperature

E = Operational irradiation

E_{STC} = STC irradiation (1000 w/$\boldsymbol{m^2}$)

Equation 2.7 is the open circuit voltage which explains that $\boldsymbol{V_{OC}}$ is a direct function of temperature (Richardson & Richardson, 2016).

$$V_{oc} = V_{oc-STC} + k_V(T - T_{STC}) \quad (2.7)$$

Where:

V_{OC}	=	Operational voltage
V_{OC-STC}	=	open circuit voltage
K_V	=	temperature coefficient for voltage
T	=	operational temperature
T_{STC}	=	STC temperature at 25℃

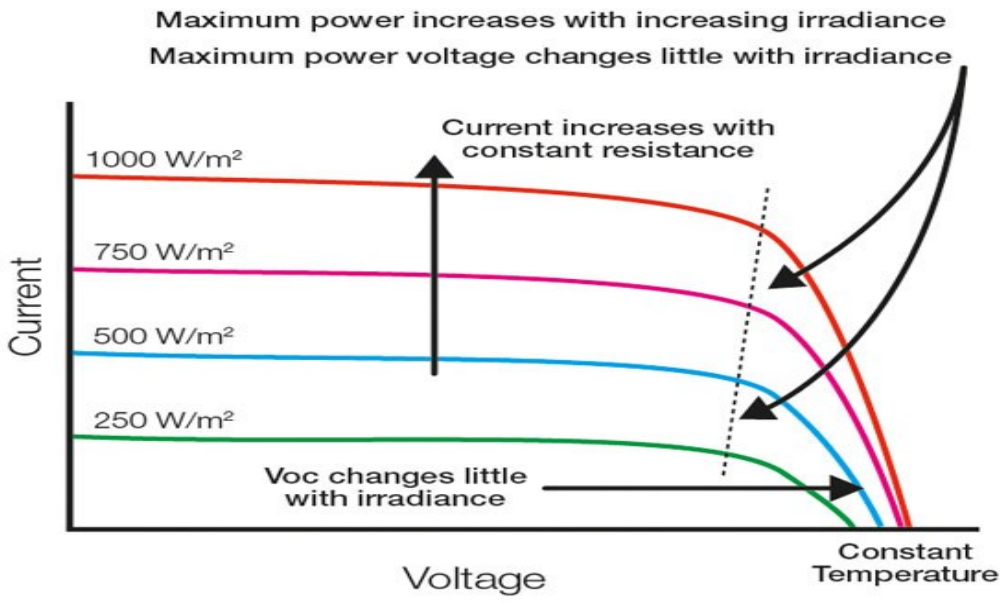

Figure 2-13: Temperature effect with constant irradiance on a PV system (Kim et al., 2016)

Figures 2.13 and 2.14 show the characteristics of a typical reaction of a photovoltaic system for a specific temperature and irradiance. The output voltage is significantly a function of temperature while current largely depends on the irradiance. The temperature and irradiance changes per minute in the atmosphere thereby affecting the maximum power point every minute (Adhikari, 2013). Therefore, the fluctuations will decrease the efficiency of the entire PV system. Hence, a technology is required to track the maximum power point of the system. However, to operate the entire system at maximum point and efficiently, the frequency must be stabilised (Rahman, 2017).

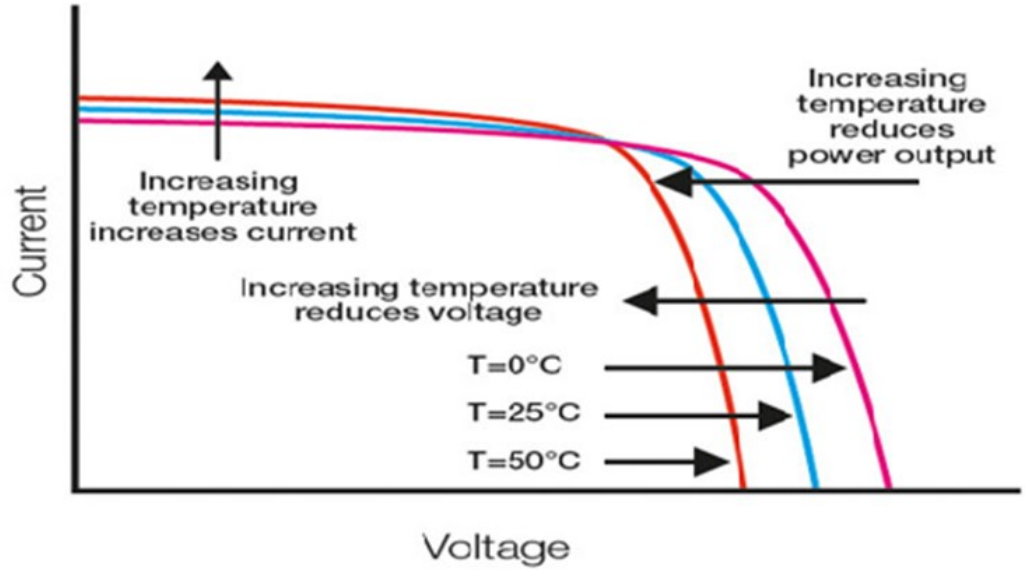

Figure 2-14: Effect of irradiance with constant temperature on a PV system (Kim et al., 2016)

2.7.6. Types of PV systems

A PV system in some instance is very easy to install and operate. One of such is a PV array connected directly to a load, such as powering a water pump motor or connected to the grid. However, depending on the PV system configuration, there are three major types of PV system in operation now: stand-alone, grid connected and hybrid PV systems. The principles and elements is the same for all three PV systems mentioned above. Each of the system can be improved or adjusted to meet a specific energy demand by changing the type and capacity of the fundamental elements in order to maintain frequency stability in the system (Mathema, 2008).

2.7.6.1. Stand-alone PV systems

The stand-alone or off-grid system can either be used for domestic or non-domestic purposes. This PV system, supply electrical power in areas where grid supplies is not cost effective or impossible. The stand-alone power system specifically designed to charge batteries that would ensure stable, steady and continuous supply of power. Stand–alone domestic supplies are of 3 KW or higher in size and has the capacity to provide electricity for cooking, refrigeration, lighting and other domestic use (Rahmann & Castillo, 2014). This system is good for most developing countries where the grid is non-existent or undeveloped particularly in the rural areas where the supply of any form of energy is economically difficult. Such areas will benefit immensely from photovoltaic off-grid system especially, areas with very high solar irradiation levels. However, to increase the output power of a stand-alone power system and to form a more reliable hybrid system, wind turbines, battery storage system and diesel generators are combined (Aghamohammadi & Abdolahinia, 2014). Although, in standalone systems, energy storage systems are used to store the power generated by the PV system. These storage systems are operated as input to the inverter which then converts the DC power into AC power before supplied to the immediate load.

2.7.6.2. Grid connected PV systems

In grid connected PV systems, energy storage system may be integrated or not depending on the choice of the operator or the prevailing design constraints. The DC power can be converted directly to AC power using an inverter then transferred to the grid. To accomplish the above, the inverter must be regulated in a pre-defined and systematic method using control loops to ensure that maximum power is achieved and transferred to the grid accordingly. The control loops must be either internal or external. But due to the harmonics content present in the output of the inverter as a result of the switching characteristics of the inverter, it cannot be connected directly to the grid. Therefore, a filter must be used to mitigate the effect of the harmonic. Presently, there are various standards introduced by IEEE, NEC, IEC and EN in Europe and

other parts of the world to ensure stable interconnection, operation and maintain power quality of utility grid globally (Bird et al., 2013).

CHAPTER 3: FREQUENCY REGULATION OF GRID-CONNECTED PV SYSTEM

3.1. Overview

This chapter presents literature relevant to grid-connected photovoltaic system in general and frequency regulation of grid-connected photovoltaic system in particular. It also presents an overview of the various components of a photovoltaic system with special focus on present research conducted in frequency stability of grid-connected photovoltaic system.

3.2. Power system frequency measurement techniques and developments

Power system frequency measurement is most critical in power grids compared to other ancillary services likes bus voltage measurement. The power grid frequency must be ensured to operate around the nominal grid frequency during normal operation (Heydari et al., 2019). Therefore, the grid frequency must be precise, fast and accurate. In the past years, different techniques have been implemented to measure the utility grid frequency possessing different levels of simplicity, precision and swiftness.

One of such fast and easy technique of measuring power system frequency implemented by the solid state relays is the identification of zero crossing of the voltage waveform. However, this method has indicated a major disadvantage regarding an inaccurate result when measuring grid frequency of the voltage signal with noise and distortion, hence, the presence of multiple zero crossings (Sidhu, 1999). To overcome this setback, several other methods have been introduced in recent past. Such as: Kalman filtering technique (Li et al., 2014), recursive phasor computation and Discrete Fourier transform (Ballance et al., 2003) and least error squares technique of approximating frequency (Rastegarnia et al., 2015; Durić et al., 1994). A digital signal processing (DSP) based method of measuring power system frequency was presented by (Ballance et al., 2003; Rastegarnia et al., 2015). This method was seen to be very accurate and fast with less setbacks. Balance et al., (2003), considered the digitised values of the voltage samples recorded at specific sampling intervals. The result obtained offered accurate and noise-free approximation close to nominal, nominal and off-nominal frequencies within time range of 25 milliseconds (ms). But, in an attempt to investigate the impact of time on frequency behaviour, Sidhu (1999), used iterative method in approximating power system frequency in the resolution range of 0.01-0.02 Hz in the time range of twenty milliseconds (20 ms). This method employed adequate design and fine-tuning of orthogonal filters integrated to block harmonic components of the measured voltage. Although, putting in recent perspective, Wilde area measurement systems (WAMS) executes phasor measurement units (PMUs) and frequency monitoring network (FNET) with the capacity to measure power system parameters conditions such as current, voltage, phasor angle and frequency over a wide spectrum (Mai et al., 2010; Tholomier et al., 2009; Tsai et al., 2006; Yari

et al., 2010; Zhong, 2017). The harmonization of the phase and power system frequency with regard to the variable oscillator, thus the measurement of these parameters for the real signal can be taken with the assistance of the Phase Locked Loop (PLL) (Lopes et al., 2006). A simple PLL consists of a loop filter, a Phase detector and a voltage regulated oscillator. The loop filter filters out the output from the phase detector; a phase detector compares the input signal against the output of the voltage regulated oscillator and the voltage regulated oscillator is basically and oscillator in which the output frequency variation is proportionate to the input signal.

3.3. Voltage and frequency control with distributed energy resources in microgrids

Subsequent to little disturbances such as change in load or significant disturbances like generator trips and faults, the frequency and voltage are likely to move away from the acceptable range of operation. But according to international standard, the voltage at the distribution stage should be maintained within 5% of the nominal value which is referred to as the “ANSI Range A” (Adhikari, 2013). In today’s power system, DERs are incorporated to control voltage dips created by the above mentioned disturbances. DERs have absolute responsibility to maintain the power system frequency in islanded microgrids where the central generators ensure the system frequency is maintained at the nominal frequency which is 50 Hz in this case. Hence, to ensure the stability of the voltage and frequency at the nominal values, inverters connected to DERs must have adequate control mechanism incorporated. Several studies have been carried out in the past decade to understand the voltage control techniques with DERs in grid-connected condition and both frequency and voltage regulation techniques in islanded microgrids.

In traditional synchronous generators, the governor drop control is used to control the frequency (Tsai et al., 2006). However, in micro-grid, the frequency and voltage can be controlled by performing the same conventional principle used in traditional droop control technique (Awad et al., 2008; Vásquez et al., 2008).

Vásquez et al., (2008), investigated and later suggested the active and reactive power control using adaptive droop controller. This study uses frequency locked loop according to second order generalized integrator (SOGI-FLL) to evaluate the current phasors and voltage with high level of accuracy. Against the traditional method of close connection between active power and power system frequency and reactive power and bus voltage, recent research has shown that in case of low voltage microgrid with the line resistance significantly higher than the line reactance hence, there is a close connection between voltage and real power also as the connection between frequency and reactive power (Laaksonen et al., 2005; Soultanis & Hatziargyriou, 2007).

Laaksonen et al., (2005), pointed out that a reference signal is required in a microgrid where the voltage and frequency references are somewhat difficult to obtain. This study achieved the required voltage reference signal from the main utility grid and an inverter is then assigned as the master component that will offer the required signal to the microgrid. While other inverters are designed to operate at constant active and reactive powers.

Delghavi & Yazdani (2009), proposed a mathematical model where the voltage and frequency control mechanism for islanded DER components are linked to the power system (grid) using a power electronic device as an interface. The mathematical model in this study is based on dq-frame current control system. It uses an inbuilt Phase Locked Loop (PLL) in the DER for connection to the grid voltage while a feed-forward signal is used to eradicate the connection between the q-axis and d-axis control loops. With the inverter connected system, the unbalances in the voltage waveform and power quality are considered very critical factors when carrying out the voltage and frequency control operations.

Şerban et al., (2007), proposed a controller based Dumped Load (DL) that has the capacity to control grid frequency by controlling the active power balance of the power system. The study used the same DL as a compensator of the unbalanced currents within the different phases. Hence, the study considered an induction machine and synchronous machine based DERs.

3.4. Power electronics (PE) interface for connection of DERs in power system

Distributed Energy Resources (DERs) are classified as renewable or non-renewable sources. Either of the above will definitely produce Direct Current (DC) or Alternating Current (AC) output voltage. But if it is DC supply, it must be converted to equivalent AC supply with acceptable frequency and voltage before it can be connected to the grid. This is only achieved and made possible by employing power electronics interface. The power electronics converters are capable of converting the generated DC voltage to an acceptable AC voltage or vice versa (Şerban et al., 2007; Delghavi & Yazdani, 2009). However, the DERs can be regulated to supply appropriate quantity of active and reactive powers to the power system with suitable controls of the inverter switching. Recent breakthroughs and technology advancement in power electronics converters has provided a convenient platform for the integration of DERs to the grid and also offered significant benefits (Kroposki et al., 2010; Majumder et al., 2011; Pan et al., 2012).

Some of the benefits provided by power electronics interfaces are reactive power and voltage support, interoperability with other DERs, power electronics standardization and modularity, power quality and improved DER fault current synchronization (Kroposki et al., 2010). According to (Majumder et al., 2011), having a proper communication between the various DERs and power electronics interfaces can be further enhanced for a better performance.

The performance physical characteristics of the power Electronics (PE) interfaces depends largely on the type of material used for the construction of switches of voltage source inverter and the topology of the VSIs (Pan et al., 2012). The switching losses present in power electronic converters can be minimised by improving the efficiency of individual components that makes up the PE converter. In this regard, and as compared to Silicon based MOSFET switches, Silicon carbide based switches provide less switching as well as conduction losses with the capacity of operating at higher levels of temperature. With these and other significant advantages shown by Silicon carbide over Silicon, Silicon carbide has demonstrated huge potential in the manufacture of switches used in power electronic interface for the integration of DERs. PE interfaces also have the ability to compensate for systems harmonics which is a major factor in power quality concerns in addition to offering ancillary services to power system or the grid (Savaghebi et al., 2011; Moreno et al., 2009).

3.5. Components of grid connected PV system

Grid-connected PV systems is progressively becoming the accepted standard as an integral component of smart buildings. These are connected to the grid through an inverter and do not require batteries because the grid has the capacity to receive the entire power generated by the PV generator. In some instances used as power stations (Shadmand & Balog, 2013). A grid-connected system is broadly divided into two main parts, which is the solar power conversion part and the interfacing section. The interfacing section is connected to the medium voltage transformer via a low voltage (LV) or high voltage (HV) transformer. The LV/HV transformer operates as an isolation transformer used for voltage regulation if necessary (Omran, 2010).

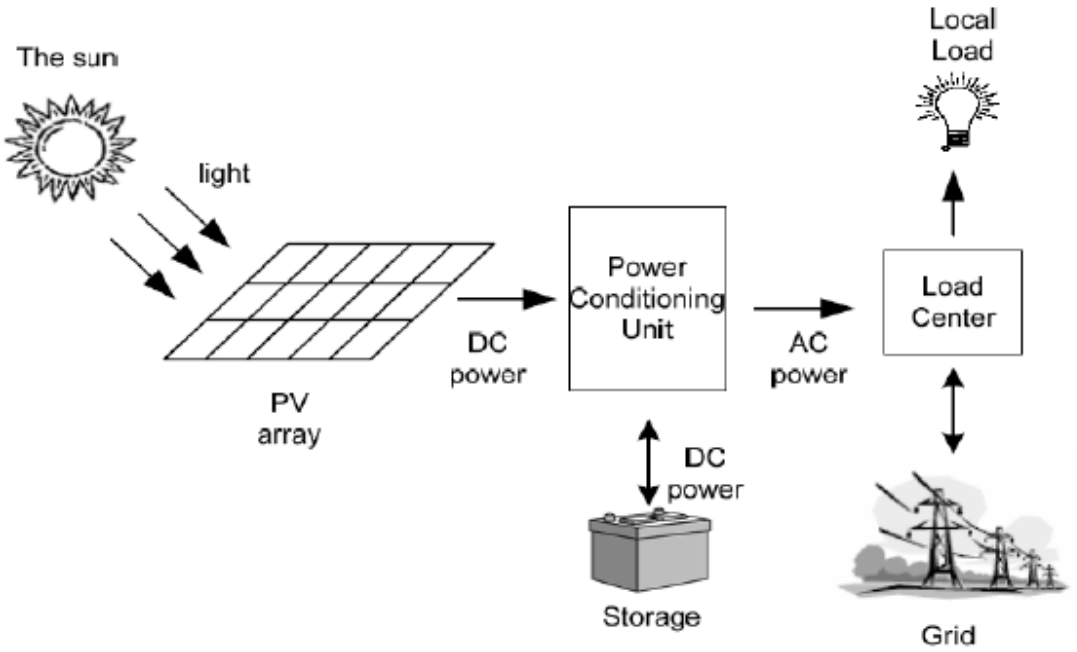

Figure 3-1: Components of a grid-connected PV system

3.5.1. The Sun

Irradiance is the immediate solar power absorbed on a particular surface area of the earth and measured in W/m². The total irradiance that touches the horizontal part of the earth is a combination of two obvious components (Kim et al., 2016). These two components are:

- Direct irradiance: This irradiance reaches the horizontal part of the earth without interference by the atmosphere.
- Diffuse irradiance: These reaches the horizontal part of the earth after dispersed by clouds.

There is the third component known as the Albedo. This is used in slanted surfaces and it is the measure of solar irradiance reproduced by the earth's surface (Kim et al., 2016).
Usually in weather stations, one would station pyranometer at specific positions to measure the global solar irradiance of that particular location. Contrary to the pyranometer, Pyrheliometer is an instrument used to measure the direct solar irradiance received by a material perpendicular to the sunrays. One can calculate the direct solar irradiance value accurately. The pyranometer and Pyrheliometer is shown in Figure 3.2.

Figure 3-2: Pyranometer (left), Pyrheliometer (right)

The solar radiation occurrence on a specific location in the earth significantly differs from place to place due to clouds, water vapours, pollution, atmospheric effects, season of the year, time of the day, and the latitude of the location. Which means that, the direct power received from the solar radiation on the earth differs from place to place and from time to time.

Solar irradiance is generally used to estimate the output of a PV system during a specific time of the day. To design a PV system, the average solar irradiance over a specific period is used. The combination of solar irradiance over a period in a specific location is expressed in kWh/m². This value (solar irradiation) is used as a yardstick to evaluate the potential of solar electricity

capacity of different regions. To ensure that maximum direct solar irradiance is achieved, solar arrays are mounted at an angle that will ensure maximum power production. However, the solar irradiance provided by the weather station is different from the value generated by the tilted surface of the PV array. Different models that will ensure maximum solar production are available nowadays. The exactitude of any model depends heavily on the atmospheric conditions of the location in question (Kim et al., 2016). According to (Jain et al., 2017), installing solar panels at the best angle and maximum point can improve the annual solar electricity production by 9-26%.

Most areas in South Africa have an average of slightly above 2500 hours of sunshine annually with an average solar radiation level of between 4.5 and 6.5 kWh/m² daily. South Africa in particular and Africa in general, experience sunshine all year round. With South Africa having an annual 24-hour global solar radiation average of approximately 220 W/m² compared to 150 W/m² for some areas of the USA, and 100 W/m² for Europe and the UK. This places South Africa at the place of advantage in terms of local resource availability (Mazibuko, 2015).

3.5.2. PV Array

A PV array is a complete power-generating unit that comprises a number of PV modules and panels connected in series and parallel respectively. The power output of these PV modules and arrays are categorised based on the maximum power output under standard conditions. The number of PV connected to the grid has increased in recent years because of development of technology and government policies. Grid-connected PV systems comprises PV arrays that are linked to the grid and generates most of the power required during the day while still connected to the electric utility at night.

However, the PV array in some instances especially during the summer months produce more electricity that the immediate load can consume and as such fed into the grid or stored in a battery (Awad et al., 2008). In grid connected PV system, electricity moves to and from the electric utility grid according to the availability of sunlight and the prevailing electrical demand at that moment. The excess electricity produced by the PV array is fed into the grid while the grid also charges the battery when the PV array produces less power (Pegels, 2010). Grid connected PV systems are relatively simple to operate, maintain also offers reduced electricity bill relative to conventional fossil fuel. Although, several number of solar panels must be installed to generate the required amount of power at any particular instance.

3.5.3. Energy Storage System

Presently, energy storage systems in PV systems has taken a centre stage with more emphasis placed on how the energy can be stored. This is because of the intermittent power produced by PV system. The installation of effective and efficient storage system can improve

the total power output of the PV system. It can also supply critical loads during power outages, provide reactive power support, bridge power fluctuations, shift the peak generation time, and regulate grid frequency. The industry is flooded with different energy storage system now (Heydari et al., 2019). Some examples are: compressed air storage system, Pumped Water Energy Storage, Superconductive Magnetic Energy Storage (SMES), Super-Capacitors, Flywheels, and batteries. However, these storage systems differ in their mode of operation, the tasks they can accomplish, and physical appearance. Therefore, selecting the appropriate storage device for a specific function is crucial and central. Furthermore, economic value and durability are some other factors that must be considered when choosing a storage system because most of these devices are expensive.

3.5.4. Power Conditioning System

Power conditioning systems (PCSs) are systems used to regulate the DC output power produced by the PV arrays. The output power from the PV is converted into a perfect AC power before fed into the electric grid. Power processing in PV system can be achieved in single-stage and two-stage systems. An inverter performs the control task in single-stage system. While in a two-stage system, a DC-DC converter performs the control task before the DC-AC inverter. This means that the control task is split between the two converters. However, two-stage system offers more control options than single-stage system but with added cost and decrease in the dependability of the system (Jaramillo-Lopez et al., 2013).

Power conditioning systems are designed to perform the following tasks:

i. Regulate current

Power conditioning systems (PCSs) designed to regulate the AC current injected into the electric grid in order to operate at the same frequency with the grid. Furthermore, to have same phase shift with the voltage at the point of linkage within the allowable boundaries. Likewise, the harmonic ingredients must be regulated to operate within the boundaries indicated in the standard. So much research has been done in this area trying to apply improved control mechanisms to regulate injected power and power factor at the point of grid interface (Heydari et al., 2019). However, current regulator used in MATLAB/Simulink environment is better explained and presented in appendix 4.

ii. Maximum power point tracking

The primary responsibility of power conditioning systems (PCSs) is to regulate the output current and voltage of the PV array to operate at maximum potential power at a specific temperature and irradiance. Presently, there are different technologies available that can achieve this purpose with the Incremental Conductance and Perturb-and-Observe

technologies appearing to be the most acceptable ones (Del Pero et al., 2016). In an effort to express this phenomenon (Esram & Chapman, 2007; Del Pero et al., 2016) investigated and compared nineteen different maximum power point tracking (MPPT) methods that will be the yardstick to choose a suitable method for a specific boundary. However, partial shading of PV array is regarded as one of the major obstacles encountered by MPPT methods. Currently, there are several research in this field at the moment that are focused on investigating more efficient and effective MPPT methods and power conditioning method (PCM) topologies that can accomplish this task (Esram & Chapman, 2007)

iii. Voltage amplification

Normally, the output voltage level of the PV system is low and as such need to be boosted in order to equal the electric grid voltage and to reduce power losses in the entire system. A multilevel inverter or DC-DC converter can achieve this task (Shadmand & Balog, 2013). The three-level inverter can also be used to achieve this purpose because it offers a reasonable trade-off between output and cost in high-power and high voltage systems (Şerban et al., 2007).

iv. Islanding detection and protection

Islanding in this context is a situation where a part of the electric utility system that contains distributed resources and loads continue to be energized even when it is insulated from the rest of the electric utility system (IEEE, 2011)Majority of the standards stipulates that power-conditioning systems (PCSs) should stop supplying more power into the electric grid under a particular irregular situation together with those leading to islanding (IEEE Standard Association, 2014). Islanding detection methods is grouped into three broad classes (IEEE, 2011)

The first is Communication method system that is based on relating signals between the PV system and the electric grid in an attempt to detect islanding situation. Secondly is the Passive method that relies on monitoring a particular component and equating it with a specified established value and thirdly, is the Active method that is based on introducing an irregular situation on the electric grid like injecting harmonic current with a particular value at the point of interconnection to the electric grid. However, most of the research is centred on evaluating and comparing various islanding methods and creating new methods with reduced non-detection areas (Jaramillo-Lopez et al., 2013).

v. Added functions

The PCSs can be designed to accomplish supplementary responsibilities like reactive power control, power factor correction, harmonic filtering and to function with an energy storage unit

or a dispensable energy source like diesel generator as a steady power supply (Vásquez et al., 2008)

3.6. Connection Topologies of PV Systems

PV-inverter system topologies are broadly categorized into four main groups namely: Centralized topology, Modular Topology, String topology and multi-string topology.

i. Centralized Topology

This is one of the most widely employed topologies in recent past. The PV modules in a centralized inverter topology are separated into series to circumvent voltage amplification. The series connected PV modules are further arranged in parallel by string diode to produce high power output. Centralized topology is best suitable in situations where there are many PV arrays available and where there is high power demand. It is also very simple to maintain and less expensive compared to other topologies. However, the major disadvantage of this topology is the fact that, if there is failure in the inverter it will definitely result in total failure of the entire PV system. This singular reason makes this topology unreliable. Furthermore, there is a substantial power loss when there is power mismatch because of centralized maximum power point tracking, PV module mismatch losses and rigid design, and string diode losses (Weckend et al., 2016).

ii. Modular topology

This is a current topology where the inverter is implanted in individual PV modules. The primary purpose of this type of inverter is to boost the low output voltage of the PV to a suitable level for the grid. This topology experiences reduced power loss because of shading, improved monitoring of module failure, and PV array flexibility design. However, the inverter cannot easily be replaced in case of damage, it has a short life span, and increased cost of production because it is mounted in an open air along with the PV module (Omran, 2010).

iii. String Topology

In string topology, individual strings are linked to a particular inverter thereby improving the reliability of the system. Furthermore, individual string operates at maximum power point thus reducing losses due to partial shading. The system is consistent and highly flexible in operation. It does not require additional voltage amplification because each string is committed to a specific inverter (Heydari et al., 2019). This type of inverter system finds its use in homes and commercial environments because it is applicable to both single phase and three phase systems. In string topology, the entire performance of the system can be examined at individual string level. String topology unlike the central topology has no loss of energy because of

shading and no string diode losses. However, the major setbacks of this topology is high cost due to installation of several inverters and can only be used for low power rating of 3-5 KW per string (Alepuz et al., 2006).

iv. Multi-String topology

In multi-string topology, each string is connected to a specific DC-DC converter to track the maximum power point and to amplify the voltage. However, all the individual DC-DC converters are then connected to a single inverter through a DC bus. Which means that each string can be controlled independently thus increasing the reliability and efficiency of the system. It also increases the power output of the system because of the individual tracking of the maximum power point. The topology is highly flexible by design as new strings with converters can be added on existing system. However, the obvious shortcoming of this topology is the high cost compared to centralized topology and added losses in the DC-DC converter (Yang & Blaabjerg, 2015).

3.7. Effects of PV Systems on the Grid

The primary reason why PV systems are installed and linked to the electric grid is to improve the overall performance of the electric network through the reduction of power losses and enhancing the voltage profile of the entire system. However, this has not always turned out to be the situation especially at high penetration. At high penetration of PV system, the electric network experiences voltage and power instability problems, underloading and overloading of feeders, weakening of protective devices, and harmonic distortion (Omran, 2010).

Researchers and electric utility companies are currently investigating the potential impacts of high penetration of PV system on the grid. This is considered very necessary and important because proper assessment of these potential impacts as well as offering realistic solutions for the operational challenges due to high PV penetration is seen as a main contribution that will encourage extensive use of PV systems.

3.8. Challenges associated with Grid-connected PV system

PV systems has presented substantial benefits to electric utilities alongside some operational glitches. Most of these problems are because of the fluctuations of power output from the PV system that is caused by the variations in the solar irradiance due to cloud movement. Such solar irradiance variation presents many operational glitches and makes the power output prediction of the PV system a difficult undertaking (Bjørk & Nielsen, 2015).

The negative influence of Grid-connected PV system on the effective operation of the electric utility did not attract necessary attention until recently when the level of PV penetration became

significant (Mathema, 2008). This section is categorised under three distinct sub-headings: a. Impact on distribution networks, b) Impact of PV systems on the generation part, and c) Impact on transmission and sub-transmission systems. Nonetheless, it is vital to offer a brief overview of some of the sources of power instability in these systems before exploring the potential negative effects of high PV penetration.

3.8.1. Intermittent power output of the PV system

There are several documented causes of intermittent PV system power output. However, irregular solar irradiance caused by the passage of clouds through the PV array is considered as the major cause. According to (Alam & Alouani, 2010), there are ten noticeable cloud formations, with cumulus clouds and squall lines as the most responsible clouds for variations in the power output of a PV system. One of the advantages of the squall lines is that it is predictable, which means that the duration that the PV system would be generating zero can be forecasted and necessary provisions made accordingly. This is however, the worst-case scenario of a PV system (Samrat et al., 2014). Cumulus clouds on the other hand leads to reduced loss of power from the PV system thereby resulting into intermittent power supply. The time interval of fluctuation depends largely on the size and kind of clouds, the area covered, PV system topology and the wind speed (Alam & Alouani, 2010). At maximum irradiance level, which is mostly at noon, is where the PV system experiences the most significant fluctuations in the PV power output. This period corresponds with the off-peak loading period of the electric utility network and as a result the PV system operating level is at the peak (greatest). Nonetheless, the magnitude of the PV power output variability on the electric utility is guided by the penetration level, location of the PV system, PV system topology, kind of clouds, topology of the electric utility network, and the size of PV system.

3.8.2. Solar irradiance information needed to evaluate the effect of PV systems

The time interval of the solar irradiance data needed to evaluate the changeability of the power output of the PV system must be consistent and precise because it is an important requirement for detailed result.

However, the solar irradiance data required for accurate evaluation can be divided into two separate constituent (Govender & Sivakumar, 2019): a) stochastic constituent that includes the variability of the deterministic constituent which is informed by the daily weather, and b) deterministic constituent informed by the daily, weekly, monthly and annual climate of a specific geographic location. The hourly solar irradiance data or the deterministic constituent can be employed in situations where the anticipated power output of a PV system is to be projected over a specific period (Govender & Sivakumar, 2019). It is equally crucial to understand the operation of the PV system alongside how the PV system affects the electric utility network. In order to understand this, the time resolution of the solar irradiance data must be investigated

to include mid-hourly fluctuations of the solar irradiance (Ibrahim & Anani, 2017). Furthermore, solar irradiance data with improved time resolution like 11-minutes can provide better projection accuracy because the auto-correlation coefficients will present increased positive results as opposed to those gotten for 1-hour resolution. A summary of the how the PV system affects the electric grid is separated into generation side, transmission side and distribution side and presented in Figure 3.3.

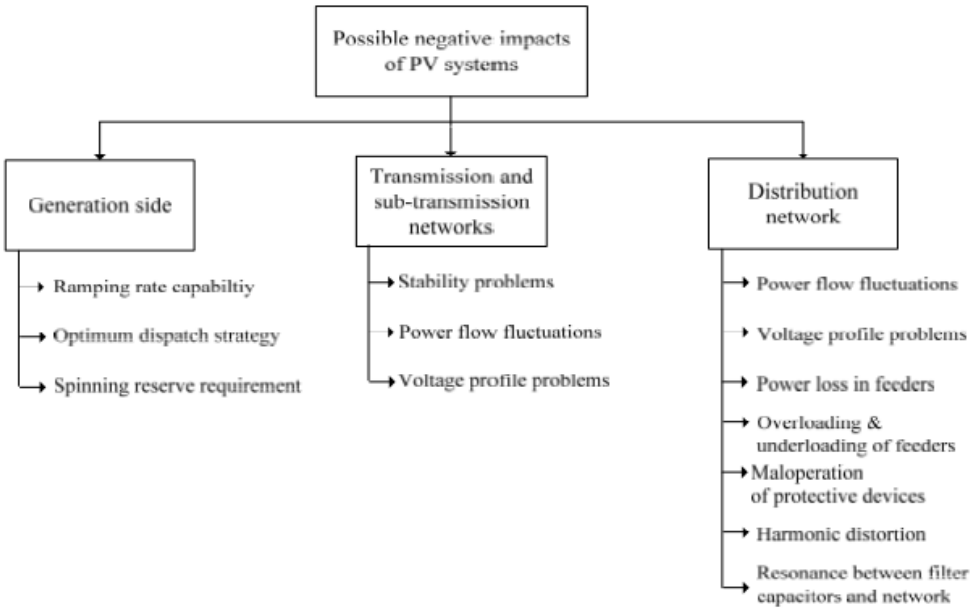

Figure 3-3: Effects of PV systems on the electric grid

3.8.3. The effect of PV systems on power generation

Significant power output fluctuations of PV system have the potential to disrupt power generation in electric utility grid. This is because the electric utilities must keep up to these power fluctuations and compensate for the inconsistency accordingly. Therefore, the generating parts of the electric utility that are designed to function when the PV systems are generating must have ramping rate abilities that are designed and installed to handle these PV power output fluctuations in the system. Furthermore, it is challenging and difficult to forecast the power output of the PV system because of the significant power output fluctuations present in the system when planning the power generating parts in the system. Several researches have been conducted in this area in an attempt to address this problem and provide effective solutions that can assist electric utility companies (Ari & Baghzouz, 2011). Some examples are the studies presented by (Tan et al., 2017; Freitas et al., 2018) where they both considered the impact of increasing PV penetration on the electric network. The main findings according to (Freitas et al., 2018), indicates that the peak power technique has restricted success if PV systems are to be considered. Furthermore, high PV penetration leads to a locally less effective grid, thus a solar PV factor in required to handle future arrangement of PV systems in city

centres. While (Tan et al., 2017) concludes that, ramping rate ability of the electric utility is central in the control of PV system penetration. However, both studies investigated the impact without offering significant information on the frequency and periods when these happens.

In conclusion, the generation part of the electric utility is prone to disturbance by high PV penetration if the level of penetration is equal to the size of the generating systems. Nevertheless, because of high cost of PV systems, these sizes are not to be installed any time soon. Hence, the impact of PV system on the generating part is not urgent at the moment.

3.8.4. The effect of PV system on power transmission networks

Power output fluctuations experienced by PV systems can create significant complications along the transmission lines if the power output of the PV system is big enough to influence the electric network. These glitches are attributable to the power output variability of the entire system, which may result to undesirable voltage variations, power reversal, power swings along transmission lines and under/over loading in certain lines (Tan, 2004). According to (Richardson & Richardson, 2016), the impact of big PV system on the voltage levels and the reliability of transmission lines after it has undergone fault conditions is significant. The study indicated that changing traditional generating units with huge PV systems influences the voltage levels of the entire electric network significantly during normal working conditions. However, during fault conditions, the rotating parts of the traditional generators in a network may operate at increased scales because of the PV systems present.

3.8.5. The effect of PV system on distribution network

Electric utility companies and researchers are presently studying the influence of large PV systems on distribution networks. This is because the siting and size of connected PV system affects the electric network significantly. PV systems and distributed generators present similar operational problems that offer stable active power like fuel cells and conventional diesel generators. These glitches are experienced mostly due to the addition of generators at the consumer end in a feeder designed for a single directional power flow. Some of which are reverse power flow, underloading or overloading of specific feeders, voltage control problems and faulty protective relays. Furthermore, some other problems are as result of interfacing electronics which introduce harmonic distortion, parallel and series resonances only if many inverters are mounted in a particular area. Besides, the intermittent power output of large PV systems contributes to the problems encountered by utilities companies and has the capacity to weaken the power quality of the entire electric network (Richardson & Richardson, 2016).

In recent years the amount of small solar PV systems mounted on rooftops has increased significantly. This increase has created notable problems on the distribution network hence government and researchers are busy trying to proffer adequate solution. This increase is as

a result of various government incentives and programmes offered to residential customers together with technological advancement by researchers. These Solar PV systems are in the range of 1 to 50 KW in most cases (Bracale et al., 2016).

According to (Vokas & Machias, 1995; Verhoeven, 1998; Oliva & Balda, 2003), the problem of harmonic content distortion in also encountered when using small PV systems. But all the scenarios investigated showed harmonic distortions much more less than the indicated standards. This is attributed to the significant technological advancement achieved in inverter design in recent years. Although, in LC or LCL-filters, the capacitor or capacitors of the connecting inverters might create resonance with the utility network in areas where there is a significant number of PV systems installed (Enslin & Heskes, 2004; Kotsopoulos et al., 2005). The impact of mounting PV systems of 1 to 50 KW on the local profile of various distribution network topologies was investigated in (Paatero & Lund, 2007). The results obtained showed that the allowable voltage limits were surpassed in situations when the capacity of each PV system was 200% of the total load of that particular locality. Although, the study made some unrealistic assumption that PV systems were installed at each node in the distribution network. But the reliable result of a practical situation was presented in (Oliva & Balda, 2003) that showed the presence of accurate transients in the voltage of a medium voltage in the distribution feeder equivalent to the frequency of variations of the power output present in PV systems of the aforementioned capacity (1 to 50 KW) mounted on rooftops.

Some studies have shown that when PV systems are connected in a distribution network, it reduces the lifespan of the transformer tap changers because of the increased operation. While other studies investigated the influence small PV systems have on the voltage profile of a low distribution network (Canova et al., 2009). But none of these studies considered the changes in the solar irradiance.

Generally, small PV systems mounted on building rooftops might not exact significant problems on the distribution network. This is majorly due to the capacity of these systems as it requires a high concentration in a particular location in order to have any significant impact on the operation of the network. Presently, to have large concentration of PV systems installed in a particular area is not common and as such not likely to happen because PV systems are normally distributed over a large area. Such dispersion decreases the impact of variations because the total irradiance profile over the entire area is smoother than the individual system (Omran, 2010).

Only few studies have investigated the impact of installing large number of PV systems in a specific area on the distribution network. One of such study was conducted by (Ari & Baghzouz, 2011) which showed that the wrong choice of locating a large PV system has the capacity to impact the stability of the network negatively. Such problem is intensified if the generation of

the PV system corresponds to the peak loading of the electric network as this might overload already heavily loaded network. Although, the total operational performance of the network, comprising power losses and voltage profile were not investigated because of the scope of the study. Hence, large centralised PV systems have become the primary interest in understanding the impacts of PV systems on the frequency of distribution networks.
But after considering and analysing the consequences, it is imperative to investigate the variations in the output power of the PV system because it creates typical challenges for the system. In addition, to achieve reliable results, it is vital to study the performance of the network for a longer period of time in order to investigate various likely configurations of production emanating from a PV system and loading situations of that particular feeder under investigation (Alam & Alouani, 2010). Therefore, to investigate these configurations, it is important to employ a technique with the capacity to manipulate existing data effectively to offer accurate calculations on the performance of the network.

3.9. Frequency Regulation in large interconnected systems

This section presents available knowledge of frequency regulation in large interconnected systems. The principles of frequency control in power systems are presented in details alongside the components capable of frequency control. It also highlights the difference between theory of frequency control and frequency control practices.

3.9.1. General points on Load Frequency Control (LFC)

The control of frequency is generally known as load frequency control (LFC) (Golpîra & Bevrani, 2019). This is a practice that tries to maintain automatically or manually the balance between active power generated and consumed. Actually, if the active power generated is greater than the active power consumed, then the frequency will increase but when the active power generated is less than consumed then the frequency will decrease. Hence, the difference between the active power generated and consumed has the capacity to affect the frequency significantly if the difference is higher than allowable standard. Load frequency control basically is a method of preventing automatic activation of under frequency load shedding and ensuring the frequency within allowable frequency spectrum. Although, the frequency spectrum differs from one system to another.

In grid connected PV system, frequency control is achieved using these complementary control systems, primary control, secondary control and tertiary control systems. The secondary control system is also referred to as Automatic Generation Control (AGC). The three abovementioned control systems are mainly an attempt to regulate the MW output of generators using automatic, manual, local and integrated methods. Presently, there are other means of controlling frequency of interconnected system such as using energy storage

systems. This method is gaining popularity due to economic factors and inability of some generators. Tertiary control is manual while primary and secondary control systems are automatic. Primary control is a local control that maintains appropriate frequency movements. It includes a proportionate action as regards the frequency. But secondary and tertiary control systems are integrated and used to restore the frequency to its reference point after experiencing changes in frequency (Gul et al., 2016). Secondary control is typically used in interconnected systems and also used for automatic reinstatement of the power exchanged between the various parts of an interconnected system to their specific values. The main purpose of tertiary control is to restore the contributions of primary control and secondary control to allowable values. Individual contributions of various controls are measured in MW, which represents the total amount of consumed reserve. These reserves are equal to the total amounts of spare power remaining in generation units already underway to perform specific controls. However, these reserves are normally restricted due to economic factors because not all generation units offer reserves for frequency control. Furthermore, the response time of the reserve is also restricted as a result of restricted capacities of individual resources. Hence, it is very vital to set the frequency control requirements to a level that will ensure that the amount of reserves provided are adequate for effective operation of primary and secondary control. In addition, the requirements must also make sure that the resources offering the necessary amount of reserves are capable of offering the essential response when needed and on time. The contribution of primary, secondary and tertiary controls are not always measured when performing dynamic simulations. Actually, some can be avoided depending on the period of the studies phenomenon (Bevrani & Shokoohi, 2013).

3.10. Theory, characteristics and dynamic behaviour of frequency control

The dynamic behaviour of frequency is a function of various factors. Some of which are:

- The load frequency sensitivity
- The system inertia
- The characteristics of the differences: sizes, types (i.e. steps, such as loss of units, and ramps such as changes in the production programmes)
- The magnitude of the system
- The impact of the units to the primary control, the secondary control and the tertiary control

From the characteristics mentioned above, not all of them can be determined with accuracy in large interconnected systems because of the difficulty it entails in modelling power systems. One of such characteristics is the system inertia and the load frequency sensitivity. Hence, parameter identification method is used to obtain the values of such parameters (Gul et al., 2016). The system inertia and the impact of the load on the frequency are vital in explaining the natural characteristics of the frequency subsequent to imbalance in the system.

3.10.1. The load frequency sensitivity (D)

In a situation when there is a discrepancy between the available power generated and the power demand, it is possible to return the frequency to the normal value by either changing the active power generated (MW) or the power demand by customer depending on the prevailing condition. Hence, the load frequency sensitivity can be restored naturally. For instance, when the frequency drops, motors run slower, thereby using a smaller amount of power. The contribution of loads in restoring the frequency can be seen as either damping of loads or self-regulation of loads. Generally, the value of the damping load is a decrease of 1% - 2 % of the load for every 1% change in frequency (Magdy et al., 2017). According to (Tsai et al., 2006), load frequency sensitivity and the natural behaviour of a system frequency can be achieved using Equation 3.1.

$$J\Omega\frac{d\Omega}{dt} = M\frac{df}{dt} = dP = P_{Generator} - P_{Load} - D \times \Delta f \quad (3.1)$$

Where:

- *f is the system frequency [Hz]*
- *J is the total moment of inertia of all the generators and motors connected to the grid [kg.m^2]*
- *M is the equivalent moment of inertia of all the generators and motors connected to the grid [MW.s. Hz^{-1}]*
- *Ω is the electrical operating speed of the synchronous generators [rad. s^{-1}]*
- *$P_{Generation}$ is the power produced by the whole system generation [MW]*
- *P_{Load} is the power consumed by the entire system load [MW]*
- *D is the load frequency sensitivity of the system [MW/Hz]*

3.10.2. The system inertia

Whenever a system experiences an imbalance, there is a phenomenon associated to the inertia of the generating units, (i.e. the rotating masses linked to the grid) that constraints the rate of the frequency deviations. Using Equation 3.2, the inertia (J) for a generator can be determined.

$$J = \frac{2HS}{\Omega^2} \quad (3.2)$$

Where:

- *J is the moment of inertia [kg.m^2]*
- *H is the inertia constant [MW.s/MVA]*

- *S is the rated apparent power [VA]*
- *Ω is the nominal angular frequency [rad.s^{-1}]*

Typical values of inertia constant (H) is presented in table 3.1

Table 3-1: Typical values of inertia constant (H) (Gul et al., 2016)

Type of generation unit	Value of H
Thermal unit	
(a) 3600[4] r/min (2 pole)	2.5 – 6.0
(b) 1800[5] r/min (4 pole)	4.0 – 10.0
Hydraulic unit	2.0 – 4.0

The values of system inertia of different types of generation units such as big vertical hydroelectric generators and big steam turbines with focus on the generator ratings expressed in megavolts (MVA) was presented by (Misak & Prokop, 2017). The amount of the total inertia of the grid is expressed in the behaviour of the frequency which can be explained using the swing Equation 3.3 and 3.4 as shown.

$$J\frac{d\Omega}{dt} = T_m - T_e \tag{3.3}$$

$$with\ \Omega = 2\pi f \tag{3.4}$$

Where:

- *F = frequency [Hz]*
- *J = moment of inertia [kg.m^2]*
- *T_m = mechanical torque [N.m]*
- *T_e = electrical torque [N.m]*

A bigger inertia hence decreases the original rate of change of the frequency. Normally, the mechanical torque is the power generated and the electrical torque is the power consumed in the system. Thus, the system inertia of a power system is normally presented using the moment of inertia (M) and expressed in equation 3.5:

$$M = \frac{2HS}{f} \approx \frac{2HS}{f_0} = \frac{2H_{eq}P_{Generation}}{f_0} \tag{3.5}$$

Where:

- *M = equivalent moment of inertia of total generators and motors connected to the grid [MW.s. Hz^{-1}]*
- *S = total apparent power produced by the entire system [MVA]*
- *f = system frequency [Hz]*
- *f_0 = reference frequency [Hz]*
- *$P_{Generation}$ = total power produced by the entire system [MW]*
- *H = system inertia constant [s]*
- *H_{eq} = equivalent system inertia constant [MW. s/MVA]*

Therefore, the behaviour of the frequency gotten using the swing equation can be further expressed in equation 3.6:

$$J\Omega\frac{d\Omega}{dt} = M\frac{df}{dt} = dP = P_{Generation} - P_{Load} \rightarrow \frac{df}{dt} = \frac{f}{2HS}\Delta P \approx \frac{f_0}{2HS}\Delta P\frac{df}{dt} \approx \frac{1}{M}\Delta P \qquad (3.6)$$

3.10.3. The characteristics of the imbalances (i.e. sizes and types)

The fluctuations of frequency occur due to the imbalance between the power produced and power consumed in a power system. These happens as a result of one or more of the following factors:

- Load forecast errors
- Imbalances that produce deterministic frequency deviations during peak hours
- Unexpected loss of production, loads or HVDC link interconnector
- Random imbalances created by unwanted noise in the production and consumption of power

The various imbalances can be generally grouped according to their possibility of occurrence and their extents. Imbalances can be further classified as step or ramp. The type of imbalance determines the duration of the activity as well as the provisions of primary control, secondary control and tertiary control. A ramp imbalance which is not very common is caused by a continuous mismatch between the power generated and consumed over a number of minutes. A step imbalance on the other hand can be caused by unexpected loss of a power unit or a load. One of such instance of ramp imbalance can be a slow mismatch between the power produced by solar PV system and predicted period due to unforecasted change in weather condition. Figure 3.4 shows a ramp and step imbalances for values less than zero ($\Delta \boldsymbol{P} < \boldsymbol{0}$).

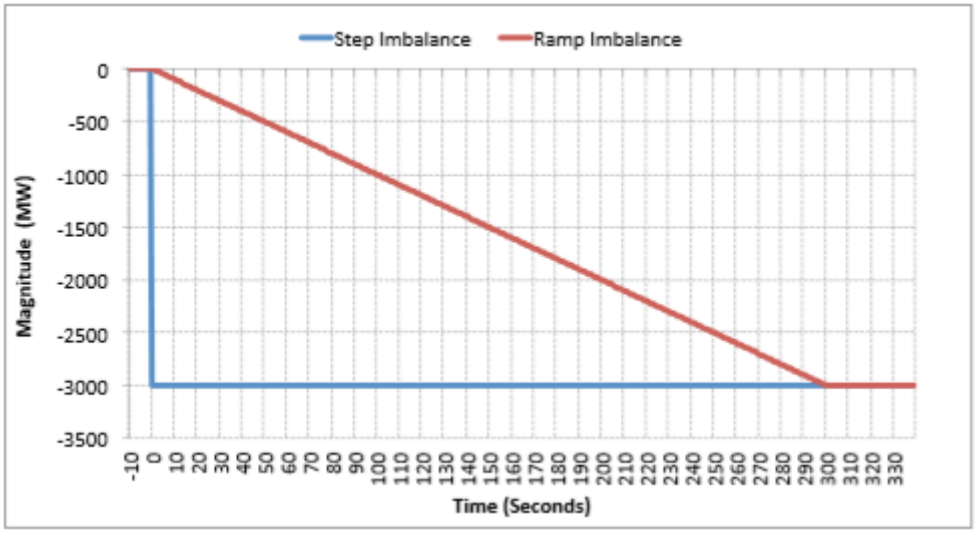

Figure 3-4: Difference between a ramp imbalance and step imbalance

From Figure 3.4, a ramp imbalance is characterised by the extent and period $\Delta \boldsymbol{t}$, while a step imbalance is defined by its magnitude $\Delta \boldsymbol{P}$. The period $\Delta \boldsymbol{t}$ permits an individual to calculate the value of the ramp as, $\Delta \boldsymbol{P}/\Delta \boldsymbol{t}$. For instance, the size of the imbalances $\Delta \boldsymbol{P}$ shown in Figure 3.4 is equivalent to $-\mathbf{3}$ GW while the period $\Delta \boldsymbol{t}$ is equivalent to 300 seconds. Therefore, the ramp is given as, $\Delta \boldsymbol{P}/\Delta \boldsymbol{t}$ = -10 MW per second.

3.10.4. The size of the system

The size of the system in most instances is not considered when investigating the frequency control while it affects the frequency dynamics and requirements. This is because the load frequency sensitivity and system inertia are affected by the size of the system and value of the load, the frequency would either be improved or it would get worst as a result of the variation in the load only. Normally, it is not appropriate to consider an imbalance equivalent to a percentage of the load while investigating frequency control in power system and performing dynamic simulation analysis. Actually, combining two systems of different magnitudes and characterised with very similar characteristics A (presented in percentage of the load second/hertz) and B (presented in percentage of the load/hertz), an imbalance equal to the percentage of the load will pull equal natural system frequency characteristics in both systems. Although, investigating the magnitude of the imbalance expressed in megawatts, it might appear correct and adequate in one system but not adequate in another system (Diouf, 2013).

Generally, it is important to measure the sensitivity of the performance regulation with all the necessary characteristics because frequency dynamics depend on a variety of characteristics in order to evaluate the efficiency of frequency regulation in large grid connected PV systems. Therefore, it is vital to simulate different activities that are chosen appropriately and to consider

various situations, such as different magnitude of loads, variations in the system inertia and variations in the load frequency sensitivity (Farmer, 2018).

For instance, according to (Farmer, 2018) in Guadeloupe (an overseas constituency of France in the Caribbean), the shutdown of the largest power unit which is the reference incident and equal to a loss of 25 MW represents between 10% to 16% of the total load. But in European synchronous system, the shutting down of the largest unit, the reference incident equivalent to 1500 MW and 3000 MW respectively represent only 1% and 2% of the total load respectively. Thus, the amounts of primary reserve needed in these two different locations are comparable according to the individual sizes of their reference incidents. According to these two different reference incidents, Guadeloupe it takes 1 to 2 seconds for the frequency to reach the first step of under frequency load shedding while it will take more than 10 seconds before it reaches the first step of under frequency load shedding in the European synchronous system (Farmer, 2018). Therefore, according to the frequency needed for the operating of electrical equipment of the two systems are similar and the comparative sizes of the reference incident in each system is different, hence, the necessities for primary regulation will also be different proportional to the size of the system. The above example has shown that the requirements for frequency regulation for small systems is different from that of large systems and as such must be considered individually. Therefore, the load and size in power system must be studied in detail in order to properly understand grid frequency regulation and control because the sizes of imbalances that occur in power system are comparatively different. Hence, making the inertia of the system, the load frequency sensitivity and the size of the load major factors to consider.

3.10.5. The impact of the units on primary, secondary and tertiary controls

Frequency is one of the most significant parameters in power system operation stability. It is of vital importance to ensure that the frequency of the system is kept within an acceptable range under any disturbances. System frequency is controlled by primary and secondary frequency controls. Primary frequency control (PFC) controls the system frequency in a dynamic process; meanwhile secondary frequency control maintains the system frequency as close as its steady state value by regulating the loads of generating units contributing in frequency control. If the function of PFC is not totally utilized, large frequency deviations may occur and this may cause serious consequences in the power systems (Zhou et al., 2014). The timing for primary control, secondary control and tertiary control is shown in Figure 3.5 below.

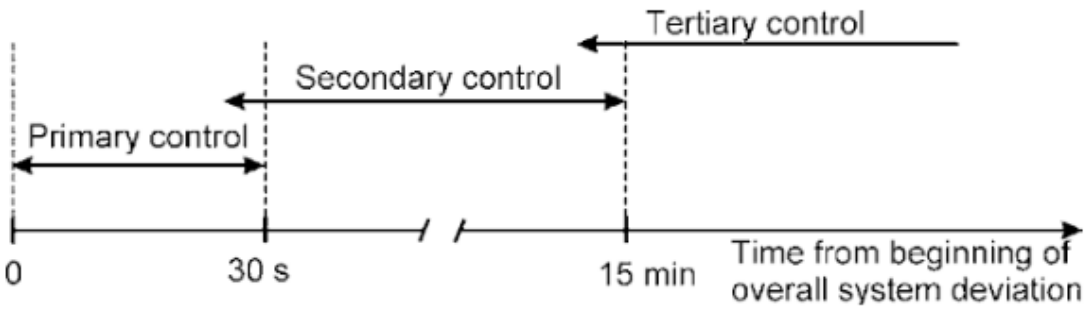

Figure 3-5: Timing of Primary, Secondary and Tertiary control ranges in Power System (Farmer, 2018)

3.10.5.1. Primary Control

The impact of the primary control is generally represented with the coefficient K, which is also referred to as the frequency response of the resources offering primary control and is expressed in MW/Hz. Actually, the impact of the load frequency sensitivity D is not considered sufficient to offer safe acceptable frequency variations in power systems to prevent the automatic disconnection of loads or generators during a condition of significant imbalances. Hence, primary control which includes automatic, bidirectional action of few generators is operated by Transmission System Operators (TSOs). This is to prevent the automatic disconnection of individual loads or generators in specific conditions and retaining allowable frequency fluctuations. Therefore, the primary control entails shifting the MW output of the power sources depending on the frequency. Indeed, the primary control is exactly the contribution of selected generators which is inversely proportional to the system frequency changes as shown in equation 3.7 (Zhou et al., 2014).

$$P_{primary} = -K\Delta f \tag{3.7}$$

However, including the impact of the load frequency sensitivity and the primary control action to equation 3.1, then the behaviour of the frequency can be expressed as:

$$M\frac{df}{dt} = P_{Generator} - P_{Load} - D\Delta f - K\Delta f \tag{3.8}$$

3.10.5.2. Secondary Control

Secondary control has proved to be more suitable for interconnected power systems but can also be used in specific isolated power systems. When used in interconnected systems, the

main purpose is to ensure automatically the tie-line power "$P_{tie\text{-}line}$" that flows across the various areas that make up the interconnected system (Diouf, 2013).

Hence, the primary purpose of this particular control is to remove the quasi steady state aberration caused by the primary control and also to return the scheduled power trade-off between various areas. Congestion might occur if and if not handled properly lead to entire system collapse if the scheduled power trade-offs between the areas are not restored. Although, in isolated power systems, the secondary control is restrained to offset the quasi steady state deviations of the frequency automatically. While in interconnected system, the secondary control also referred to as Automatic Generation Control (AGC) is based on the evaluation of the Area Control Error (ACE) expressed in [MW] as shown in equation 3.9.

$$ACE = \lambda\Delta P - \Delta P_{tie-line\ out\rightarrow in} \tag{3.9}$$

Where:

- $\lambda = Network\ Frequency\ Bias\ of\ the\ system\ [MW/Hz]$
- $\Delta f = frequency\ deviation\ [Hz]$
- $\Delta P_{tie-line\ out\rightarrow in} = power\ interchange\ deviation\ [MW]$

The control error (ACE) is the total approximation of the current imbalance of a control area. The evaluation of the ACE operation is based on the evaluation of the impacts of primary control added to the impacts of the load frequency sensitivity and unscheduled tie lines power flows. Actually, if the initial values are equal in magnitude and size, then the ACE is equal to zero. When this happens, then there is no imbalance in that particular area and the triggered primary reserve will be implemented in another area to recompense the imbalance in that area. However, the Load frequency sensitivity is expressed as: $(\mathbf{K} + \mathbf{D}) \times \Delta\mathbf{f}$ while the unscheduled tie lines power flows as: $\Delta\mathbf{P}_{\mathbf{tie-line\ out-in}}$

Hence, to restrict the operation of the secondary control of an area in only recompensing the imbalances of that area, the value must be exactly equivalent to the totality "K + D" of that area and this is to acknowledge the Darrieus equation (Rahman et al., 2010). This outcome can be expressed as:

$$\Delta P = \Delta P_1 = P_{Generation} - P_{Load}\ and\ \Delta P_2 = 0 \tag{3.10a}$$

$$\Delta P = (K + D)\Delta f = (K_1 + D_1)\Delta f + (K_2 + D_2)\Delta f \tag{3.10b}$$

$$\Delta P_{tie-line\ 2\rightarrow 1} = -(K_2 + D_2)\Delta f \tag{3.10c}$$

$$\lambda_1 = K_1 + D_1 \quad (3.10d)$$

$$\lambda_2 = K_2 + D_2 \quad (3.10e)$$

Therefore:

$$ACE_1 = \lambda_1 \Delta f - \Delta P_{tie-line\ 2\to1} = \lambda_1 \Delta f + (K_2 + D_2)\Delta f = \Delta P \quad (3.10f)$$
$$\Rightarrow ACE_1 = \Delta P$$

$$ACE_2 = \lambda_2 \Delta f - \Delta P_{tie-line\ 1\to2} = \lambda_2 \Delta f - (K_2 + D_2)\Delta f = 0 \quad (3.10g)$$
$$\Rightarrow ACE_2 = 0$$

Where:

- Δf = *system frequency deviation [Hz]*
- $P_{Generation}$ = *total power produced by the entire system [MW]*
- P_{Load} = *total power consumed by the entire system [MW]*
- ΔP = *difference between* $P_{Generation}$ *and* P_{Load}
- $P_i P_{io}$ = *measured and scheduled npower exchange, with other balancing areas [MW]*
- $\Delta P_{tie-line\ out\to in}$ = *difference between* $P_i\ and\ P_{io,}$ *the power interchange deviation, the importation exactly [MW]*
- $\Delta P_{tie-line\ 2\to1}$ =*the difference between* $P_i\ and\ P_{io}$ *inside the area [MW]*
- $D_{,}\ D_i$ = *contributions of the self-regulating effect of loads of the system and the balancing area I [MW/Hz]*
- $K_{,}\ K_i$ = *the contribution of generators offering primary control in the system and balancing area i respectively [MW/Hz]*
- λ_1 = *the network frequency Bias of the system and exactly the approximation of the value of Ki [MW/Hz]*

Although, in actual power system $\boldsymbol{\lambda_1}$ does not equal the sum "$K_i + D_i$" of the area at all times because of the following factors, which are the practical significance of frequency regulation in power systems:

- In some instances, the assistances of the generators K_i to primary control can be achieved with comparatively high accuracy. For instance, when TSOs are responsible

for primary control is a service, then the value of the contribution of generators offering primary control in the system "K" in each unit is determined by the producers to the TSO and in addition monitored. Hence, by adding these values, the value of the balancing area "K_i" can be reconstructed.

- The load frequency sensitivity "$\boldsymbol{D_i}$" has a low level of accuracy because it is not evaluated in real time. This value is significantly affected and influenced by the type pf load and the loads connected to the grid. Hence, computing this value is very challenging and complex in most operations. Therefore, to achieve the value of the ACE in power systems, an informed approximation of the value of $\boldsymbol{D_i}$ is done in order to evaluate $\boldsymbol{\lambda_i}$.

In addition, the immediate value of $\boldsymbol{K_i} \times \Delta \boldsymbol{f}$ is not continuously equivalent to the impact of the primary control because the impact of the primary control is not immediate. It may also be caused by the simple fact that the insensitivity in some instances are not included in the resources that offer primary control which is not always considered in the ACE calculation. The action of the primary control is centralised and faster than the action of the secondary control. The action of the secondary control entails projecting a single signal or in some instances, multiple signals to different power supply units (Generating units) to counterbalance the ACE. The secondary control loop is generally modelled with the aid of PI controllers. The impact of the secondary control can be stated as (Diouf, 2013):

$$P_{secondary} = -\sum_{Area\ i}\left(\alpha_i ACE_i + \frac{1}{T_i}\int_{t>0} ACE_i dt\right) \tag{3.11}$$

Where:

- $\boldsymbol{\alpha_i}$ = *equivalent value for the PI controller*
- $\boldsymbol{T_i}$ = *time constant of the PI controller*

Hence, the frequency characteristics of an interconnected system with secondary control implemented in the different areas can be expressed as:

$$M\frac{df}{dt} = P_{Generation} - P_{Load} - D\Delta f - K\Delta f - \sum_{Area\ i}\left(\alpha_i ACE_i + \frac{1}{T_i}\int_{t>0} ACE_i dt\right) \tag{3.12}$$

Although, this relationship in not practical and does not always produce significant accurate explanation of the characteristics of frequency in power systems. Actually, the reactions of the resources used in frequency control are not immediate. Their responses are in most instances restricted by the degree of reserves used and by the capacities of the resources used. However, for secondary control, there are evaluations and calculations that are made including delays because of several signals integrated to implement this type of control. But these

characteristics are not incorporated in the above relation and they affect the value of the frequency. Hence, (Diouf, 2013) provides a better understanding when both the primary control and secondary control are expressed differently with their separate influence on the frequency included as expressed in equation 3.13:

$$M\frac{df}{dt} = P_{Generation} - P_{Load} - D\Delta f - P_{Primary} - P_{Secondary} \quad (3.13)$$

Therefore, to properly explain frequency behaviour of power systems, one must take into consideration the above mentioned characteristics for effective dynamic simulation (Diouf, 2013). Previously, most simulations results based their model and findings on the relationship given in Equation 19. Estimated frequency aberration and the estimated impact of the different controls during an unexpected loss of a generation unit is shown in Figure 3.6. This is the outcome of a simulation of a step imbalance after repeatedly integrating the impacts of the system inertia ($\boldsymbol{ie\ M = \approx 0}$) , the load frequency sensitivity ($\boldsymbol{ie\ D\ \approx 0}$), the primary control and lastly the secondary control.

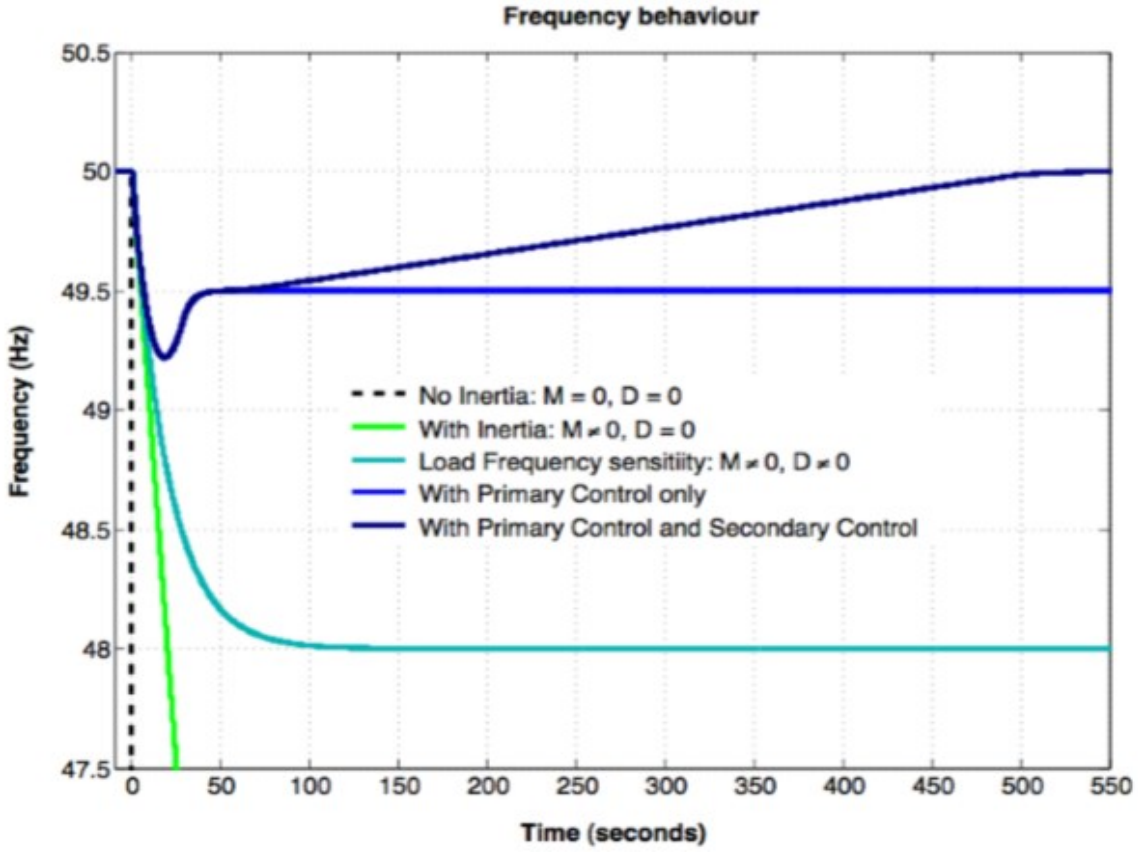

Figure 3-6: Characteristics of the frequency when a step imbalance happens (loss of generation unit) (Diouf, 2013)

The impact of load frequency sensitivity, the primary control and secondary control during condition of imbalance was shown in Figure 3.6. It illustrates two scenarios: a case with secondary control and another without secondary control (no AGC). It was observed that implementation of the primary control and the load frequency sensitivity D, influences the restriction of frequency variations due to the implementation of secondary control and the dynamic implementation of the secondary control are instantaneous. Hence, power systems must always ensure the steady availability of primary reserves to control the frequency in case of imbalance. This will provide for load frequency sensitivity D and ensure that the load produced is equal to the power consumed at all times. In the course of implementing primary control, the frequency charateristics may appear different from the one presented in Figure 3.6. Actually, even with primary control frequency moight look the same compared to frequency behaviour after introducing load frequency sensitivity D. It is exclusively in this condition that frequency undershoot is not significant (Ela et al., 2014). This can be explained using the reasons below:

- Drained primary reserve
- Large system inertia
- Significant impact of the load frequency sensitivity against primary control
- Comparatively small imbalance compared to the size of the system

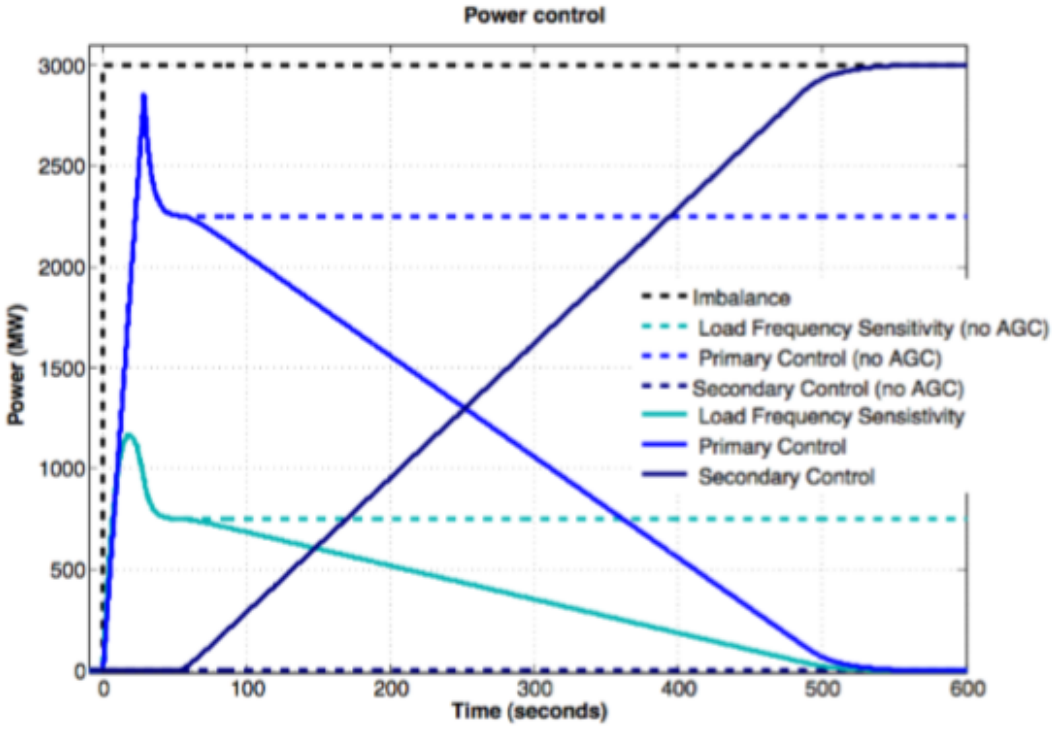

Figure 3-7: Contributions to retain the frequency when step imbalance happens (loss of production unit), frequency characteristics shown in Figure 3.6 (Diouf, 2013)

The major difference between the contribution of both the primary control and secondary control is their response time (ie. activation time). But, from Figure 3.9, it can be stated that the primary control and secondary control influence the restriction of frequency deviations in a power system. The frequency deviation is caused by the delay in the response time of the secondary control. Therefore, the quality of frequency in power systems can be improved by implementing any thre of these methods:

- effect secondary control in power system if it is not effected
- Increase the activation time of the secondary control if effected
- Increase frequency response K

Nonetheless, increasing the activation time of the secondary control is not on its own alone enough because the dynamic of the ramp imbalance can be greater than the dynamic of the activation of the secondary reserve (Ela et al., 2014). In conclusion, primary control is necessary and important in reducing frequency variations during imbalance in a power system, but does not have the capacity to return the frequency to its original value. But, secondary control returns the frequency to its original value but also affects the reduction of the frequency variations during ramp imbalance. Hence, frequency response K and primary control are very important and required for frequency excursions caused by step imbalance while secondary control is required to maintain the system frequency.

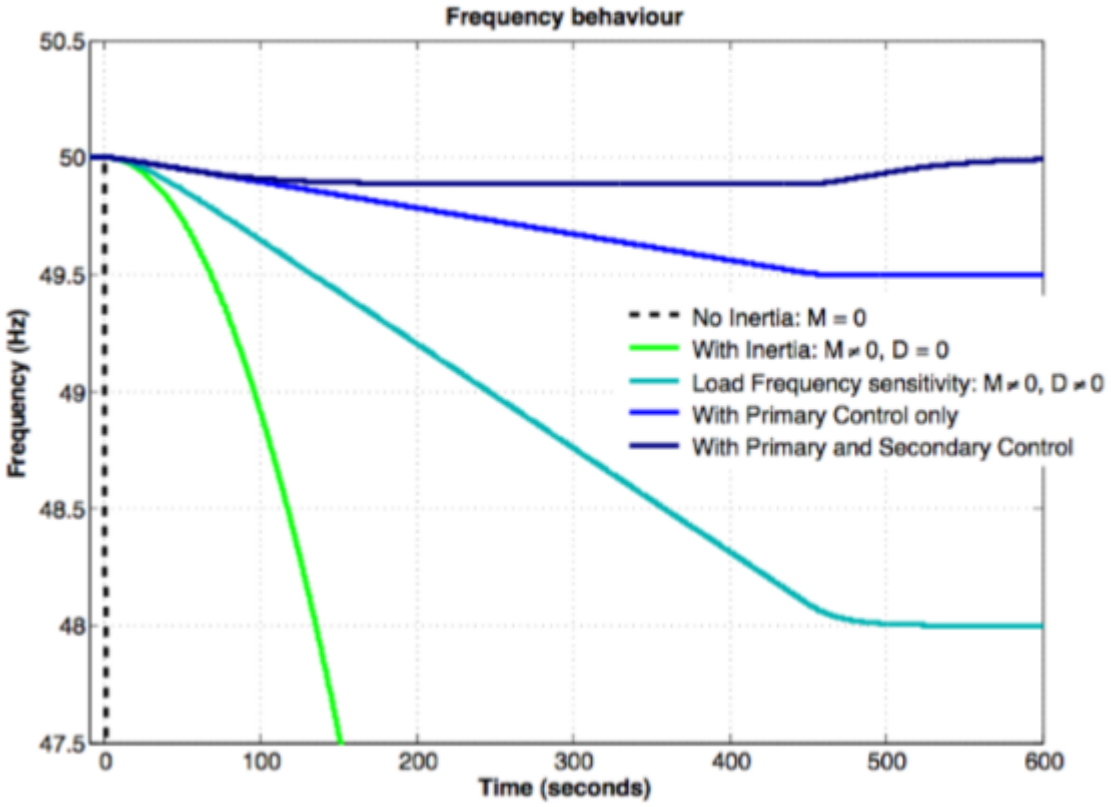

Figure 3-8: Frequency response during ramp imbalance (Diouf, 2013)

3.10.5.3. Tertiary Control

The tertiary control is also known as manual control. It is implemented as the last option in the frequency control spectrum. It is used to maintain and ensure the availability of primary control and secondary control reserves at all times. This is used to regulate final congestions in the system and it is normally the only control that triggers the reserve by considering existing economic condition at that moment (Diouf, 2013).

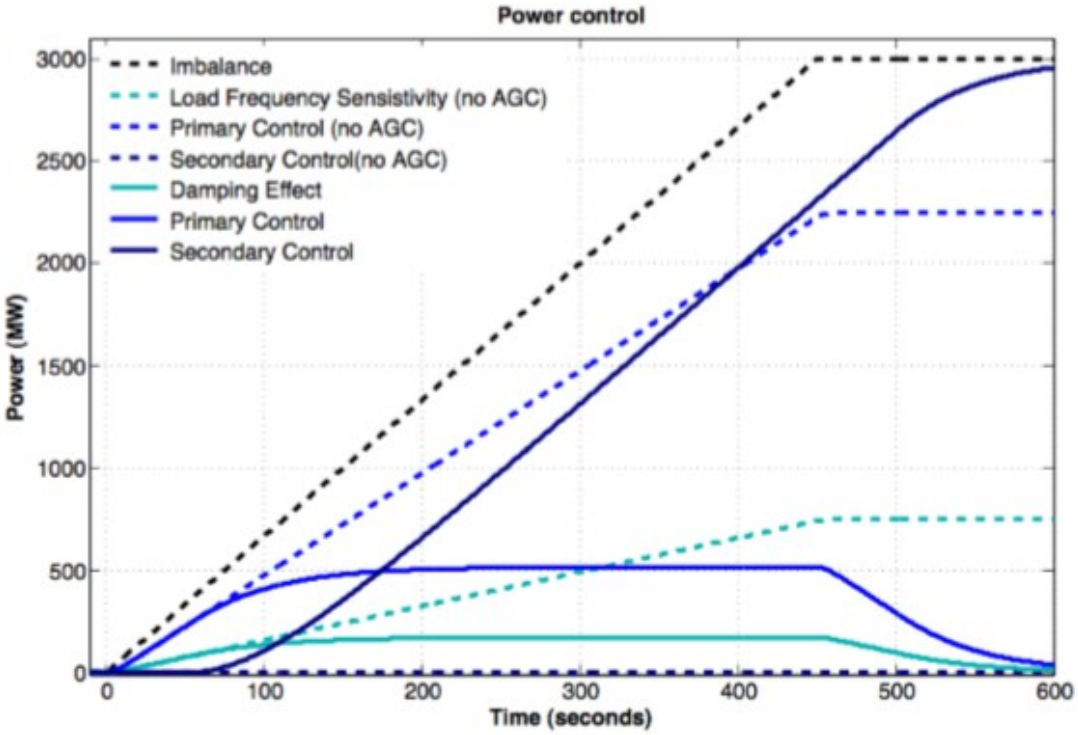

Figure 3-9: Contributions to maintain the frequency during an imbalance, from Figure 3.8 (Diouf, 2013)

3.11. Practical implications of frequency regulation

The major practical implication of frequency control is the need to use conventional units to carry out frequency regulation in power systems. Hence, conventional units were considered the major and only methods capable of providing frequency regulation in large interconnected power systems (Ela et al., 2014).

Automatic generation control (AGC) have been researched and implemented extensively over the years. But, battery energy storage system is barely new with a lot of research taking place at the moment with the sole aim of improving the technology and making it available to power utility companies world over. This is informed by the fact that most utility companies are integrating variable renewable energy sources into the power grid. However, the capacity to provide primary control and secondary control has always been an integral part of the requirements for grid integration of both conventional generation units and renewable energy resources. Due to economic constraints, all the units capable of providing frequency regulation/control do not provide on a regular basis and when required. In interconnected systems, only a small portion of the units connected to the grid practically provide frequency regulation. Thus, with the opening of the electricity markets in most countries, and as long as frequency control units are started and stopped at any suitable time, the units that provide power and participate in the provision of frequency control can vary at different intervals not properly controlled (Diouf, 2013). These variance is unique to a specific utility which decides

on the time intervals. This is dictated to by the economic restrictions and the method of acquiring frequency regulation ancillary services. In addition, the units designed to provide frequency regulation do not exclusively respond in the same way and are expected to keep a portion of their capacity as reserve for frequency regulation. The portion kept as reserve aimed for frequency regulation incurs some cost (Rebours et al., 2007). Therefore, deregulation the electricity market, which is based on promoting competitive behaviour amongst producers has strengthened the fact that, reserves aimed at providing frequency regulation must be avoided if not given the necessary incentives or made compulsory. Because of the above concerns raised by producers, they are presently given some form of incentives or adequately remunerated.

3.11.1. Primary control with conventional units

Primary control is achieved only when certain amount of the electrical power generated is kept as primary reserve in some of the generators or energy storage systems that are connected to the grid and the units are able to respond instantaneously to offer primary frequency regulation. The active power generated by a generator is based on the mechanical power output of that particular generator such as wind turbine, steam turbine and hydropower system while for renewable energy resources, it depends on the power rating and the efficiency of the system. However, for primary regulation, a large number of generators have inbuilt additional control loop in order to adjust their electrical power output according to frequency changes and the rotational speed of the system (Ela et al., 2014). The control loop is generally known as the governor control. For any system that provides primary control, the performance of such system must be assessed using the following parameters:

- The insensitivity band
- The droop
- The response time or lag time

3.11.1.1. The insensitivity band

The insensitivity band also referred to as the dead band, is the range in the spectrum where frequency deviations does not affect the units. The insensitivity band can be either not possible to remove or necessary. According to (Rebours et al., 2007) “as the mechanical governor system gets older, the insensitivity band becomes impossible to remove. Actually, contact between the moving parts created insensitivity either necessary or not”. Alternatively, an insensitivity band can be necessary. In addition, an insensitivity band can be fundamentally the outcome of the resolution of frequency measurements.

3.11.1.2. The droop

A generator droop "S", is the sensitivity of a unit varying its output determined by the frequency variation. The unit droop is represented as:

$$S = \frac{\Delta f / f_0}{\Delta P_{unit} / P_0} \tag{3.14}$$

Where:

- *S = the generator droop*
- *Δf = system change in frequency (i.e. $\Delta f = f - f_0$)*
- *f_0 = Desired frequency value*
- *ΔP_{unit} = MW output change of the unit determined by change in system frequency*
- *P_0 = Full output power of the generation unit*

According to (Diouf, 2013), the drop of a unit is normally 4% to 5%. Smaller droops are more sensitive to frequency changes and the more it impacts the return of the balance between the electric power generated and the power consumed. Actually, the value of the droop determines the frequency reaction of individual unit.

$$K_{unit} = -\frac{\Delta P_{unit}}{\Delta f} = -\frac{1}{S}\frac{P_0}{f_0} \tag{3.15}$$

In a situation of power and frequency imbalance in a system, the frequency response K_{unit} of individual generators contributes to the restoration of system frequency. Actually, the level of the frequency response K_{unit}, permits the calculation of the level of frequency that will ensure stability. However, the frequency response K and D produced by the frequency variation (i.e. the influence of each generator offering primary control and value of load frequency sensitivity) is calculated using:

$$K = \sum_{All-units} K_{unit} = \frac{1}{f_0} \sum_{All-units} \frac{P_0}{S} \tag{3.16}$$

$$\Delta f = -\frac{\Delta P}{K + D} \tag{3.17}$$

The frequency deviation is inversely proportional to the frequency response. An increase in the frequency response of the system "K + D" will result to a smaller frequency deviation. The above point is what differentiates a small standalone system and a large interconnected system. Primarily, the level of the load is comparatively greater in large interconnected systems hence, the load frequency sensitivity D is greater. As a result of the magnitude of these individual systems, the number of generators that normally contribute in primary control is more

than in insulated systems (Rebours et al., 2007). Thus, the value of the frequency response K tends to be higher as a result. In conclusion, the operations, capacities and abilities of units that offer secondary control are functions of the following characteristics:

- The quantity of secondary reserve
- The delay (i.e. the time response of the unit)
- Limitations of the generation rate of the units that offer secondary control.

3.12. Resources that have the capacity to provide frequency regulation

Theoretically, it has been established that any resource that has the capacity to generate or produce active power in a power system can provide load frequency regulation. In addition, and as rightly stated that loads, electrical vehicles (EV), storage systems and wind generation sources are capable of providing frequency regulation. Hence, in some situations offer a better response time than conventional generation units (synchronous generators). However, in Europe, USA, South Africa and most countries, grid operators still use conventional generation units for frequency regulation because other resources are not commonly available. With each at different stages of development due to technology advancement and integration (Rebours et al., 2007).

The current deregulation of electricity market and the introduction of energy markets in some countries have forced Transmission System Operators (TSO's) to split power transmission and production activities. Hence, Transmission System Operators who do not possess their own frequency control resource purchase it from other producers. Ancillary service such as frequency regulation has taken a commercial shape and it has also raised misunderstanding between TSOs and providers because of the mutual economic benefits (Rebours et al., 2007). Because of the above economic and other technical conflicts, grid system all over the world are experiencing an increase in the penetration of renewable energy generations sources capable of improving frequency regulation and also reduce over reliance on conventional generation units for frequency regulation. Thus, the interest in using alternatives for frequency regulation is increasing speedily in recent times.

In Berlin (Germany), installed battery energy storage system is providing frequency regulation services and spinning reserve (IRENA, 2017). Also installed is 40 MW flywheels in Stephentown (New York USA) that provides frequency regulation. In addition, Puerto Rico has installed over 35 MW of battery energy storage system that provides regulation. Some of the other countries using battery energy storage system for frequency regulation are, West Virginia (USA) with total installed capacity of 45 MW and Atacama Desert (Chile) with over 20 MW of installed battery energy storage system. However, in the British grid system, loads are modelled to provide frequency regulation services via automatic disconnection. The response

time of this service is within 2 seconds of command and it is named “Frequency Control by Demand Management” (FCDM). This service provided by loads according to the British system is made up of automatically disconnecting certain amount of loads at specified grid frequency (Rebours et al., 2007).

Another promising resource that can provide frequency regulation is the use of electric appliances (Rahmann & Castillo, 2014). An algorithm on how to control these electric appliances have also been proposed. Although, due to security challenges that requires ensuring the appropriate amount of reserves required, it has not been implemented anywhere at the moment (Rebours et al., 2007). Basically, if electric appliances show significant reserve potential, lack of assurance in the response time offered and the lack of visibility in the power delivered in real time makes it complex for system operators. Hence, using these appliances for frequency regulation can be seen as developing the load frequency sensitivity while it is established that primary control is not measured regarding this characteristic. According to (Rahmann & Castillo, 2014), New Zealand and Finland have incorporated load as frequency regulation resource in their grid system. It also showed that wind generation resources can also provide frequency regulation. Though, it was considered as loss of production.

Lastly, conventional generation units are seen not to be the only appropriate resources that can offer frequency regulation ancillary services but the use of other resources are not common at the moment. This may be attributed to the fact that most of the other resources are not yet economically competitive. Although, battery energy storage system is becoming economically competitive and available as a result of technology improvement.

CHAPTER 4: SYSTEM MODELLING AND ANALYSIS

4.1. Objective

This chapter describes the steps used to model the entire system in MATLAB/Simulink. The modelling of an enhanced frequency regulation functionality of grid-connected PV system capable of frequency regulation using Matlab/Simulink software is presented. Modelling and selection of appropriate values for different components in the system is vital in order to determine the effectiveness and functionality of the entire system. However, in order to achieve the aforementioned objectives, Photovoltaic system, the DC-DC boost converter, the DC-AC inverter, with improved LC filter, DC-DC bi-directional converter, energy storage system (battery) and the grid (Synchronous Generator) with specific control systems are presented in this chapter. This chapter is structured as follows: The Photovoltaic system modelling is explained together with its specific control system, including the calculations and the power rating in section 4.2.

In section 4.3 is the design method for the DC-DC boost converter with formulas and calculations for all the components. This is to ensure that the 500 Vdc from the PV system is boosted to 1 kVdc. The DC-AC inverter is presented in section 4.4 with corresponding control system while the L-filter, LC filter and LCL filter is presented in section 4.5. Thereafter, is the grid in section 4.6, energy storage system (Battery) in 4.7, DC-DC bi-directional converter in section 4.8 and conclusion in section 4.9. In this chapter, modelling of individual components and the functionality of the entire system is presented.
This system is made up of the following individual components:

- Photovoltaic system
- DC – DC boost converter
- DC – AC inverter
- The Filter
- The Grid (A Synchronous Generator)
- Energy Storage System (Battery)
- DC – DC bi-directional converter

4.2. Modelling of Photovoltaic system in Simulink

Photovoltaic system is modelled to get a better understanding of the internal performance which is determined by the sun irradiance expressed in W/m^2 and the cell temperature in degree Celsius (℃). The choice of these two parameters determines the power output of the

photovoltaic system therefore must be chosen carefully. However, the PV is modelled to ensure that it operates at the maximum power point using the maximum power point tracker.

4.2.1. Ideal Photovoltaic module

The output characteristic of an ideal Photovoltaic array is determined by the cell ambient temperature, output voltage of the array and available solar irradiance. Hence, these parameters must be selected carefully to ensure maximum power from the PV. For example, high solar irradiance increases the open circuit voltage whereas the short circuit current is linearly dependent on the ambient radiation.

In MATLAB/Simulink environment, the PV array block is a combination of arranged photovoltaic (PV) modules. The array of PV modules is assembled in series but connected in parallel with each having modules connected in series. However, the PV array block is a five parameter model that comprises a diode, shunt resistance (R_{sh}), current source IL (light-generated current), and series resistance (R_s) used to characterise the solar irradiance and temperature dependent I-V characteristics of the modules as presented in Figure 4.1.

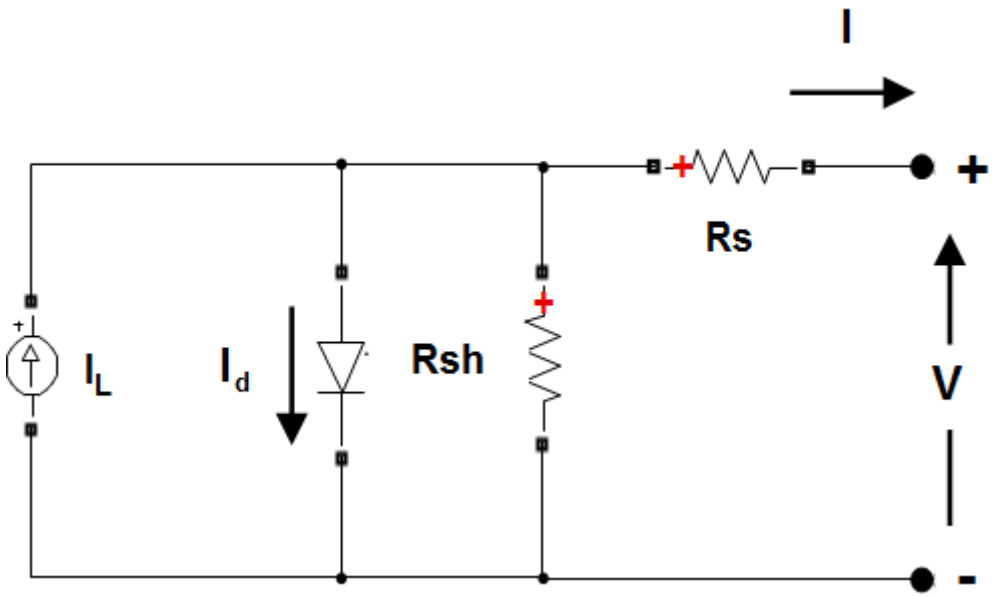

Figure 4-1: Equivalent circuit model of PV cell

An increase in the cell temperature increases the short circuit current but decreases the open circuit voltage. Thus, the cell efficiency reduces with increased temperature. The corresponding electrical circuit of a solar cell is represented with a photocurrent defined by a constant current source in parallel to a diode and to a shunt resistor signifying the leakage current and connected to series resistance which indicates the internal resistance to the current flow as shown in Figure 4.1.

The voltage-current characteristics equation of the solar cell from Figure 4.1 is represented in equation 4.1:

$$I = I_{ph} - I_s\left(exp\frac{e(V+IR_S)}{mKT_c}\right) - \frac{(V+IR_S)}{Rsh} \quad (4.1)$$

The photocurrent I_{ph} reasonably relies on the operating temperature of the solar cells and solar radiation as indicated in equation 4.2.

$$I_{ph} = \frac{\left(I_{SC}+Ki(T_c-T_{Ref})\right)\lambda}{1000} \quad (4.2)$$

The cell saturation current is temperature dependent as shown earlier hence it is expressed in equation 4.3 as:

$$I_S = I_{RS}\left(\frac{T_C}{T_{Ref}}\right)exp\left(\frac{qE\left(\frac{1}{T_{Ref}}-\frac{1}{T_c}\right)}{KA}\right) \quad (4.3)$$

$$I = I_{ph} - ID \quad (4.4)$$

The PV system shown in Figure 4.1 has components such as the shunt resistance which is connected in parallel with the diode but inversely proportional to the shunt leakage current. Although, the change in this resistance does not influence the PV array hence its corresponding leakage resistance is taken to soar to infinity without the leakage current to the ground. But a small change in the series resistance will affect the output power of the PV array significantly.

The appropriate model of a solar PV cell with necessary complexity is shown in equation 4.5 as:

$$I = I_{ph} - I_O\left(exp\frac{q(V+IR_S)}{mKT_C} - 1\right) \quad (4.5)$$

The solar cell is characterised by the following parameters:

- Open circuit voltage, V_{oc}: this is the maximum voltage available from a solar cell where, $I_D = I_{ph}$ while the generalised current is always taken as zero.
- Short circuit current: this is the highest current generated by a cell during the period when V = 0.
- The cell voltage without light is expressed mathematically as:

$$V_{oc} = \frac{mKT_C}{e} ln\left(\frac{I_{ph}}{I_O}\right) = V_t ln\left(\frac{I_{ph}}{I_o}\right) \quad (4.6)$$

Where: T_c = absolute cell temperature

$V_t = \frac{mkT_c}{e}$ = thermal voltage

- Maximum power point (MPP): the point on a power (I-V) curve where the product of the voltage and current is highest, i.e., the point that indicates highest value of power in the curve.
- Maximum efficiency: is the ratio of maximum power to the incident light power

$$Efficiency\ (\eta) = \frac{P_{max}}{P_{in}} = \frac{I_{max}V_{max}}{AG_a} \quad (4.7)$$

Where: G_a = is the ambient radiation

A = is the cell area

4.2.2. Photovoltaic system design

There are different solar panels available in Matlab/Simulink, each with unique specifications of power rating, maximum voltage and maximum current. The solar radiation and temperature must be selected to reflect the actual weather condition of that specific geographical location. This research used the incremental conductance method for maximum point tracking. The details of the PV system used in this research is presented in Figure 4.2 while additional details are shown in appendix 1. However, the solar irradiance and temperature is shown in Figure 4.3.

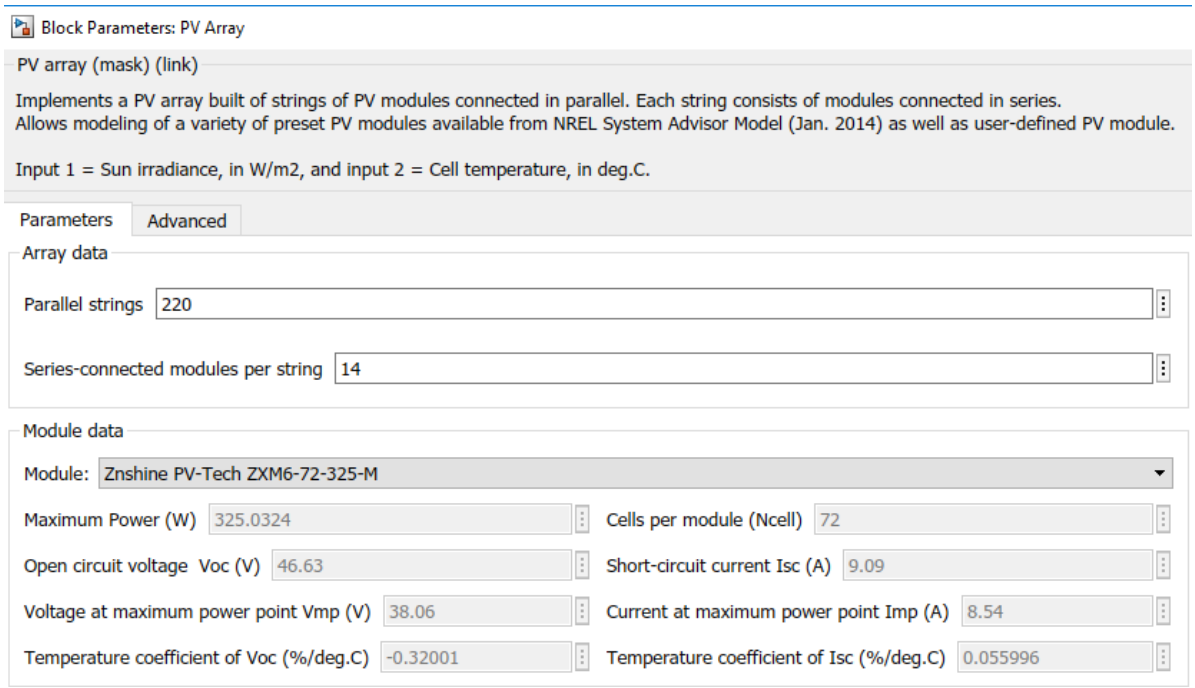

Figure 4-2: MW PV array Simulated values

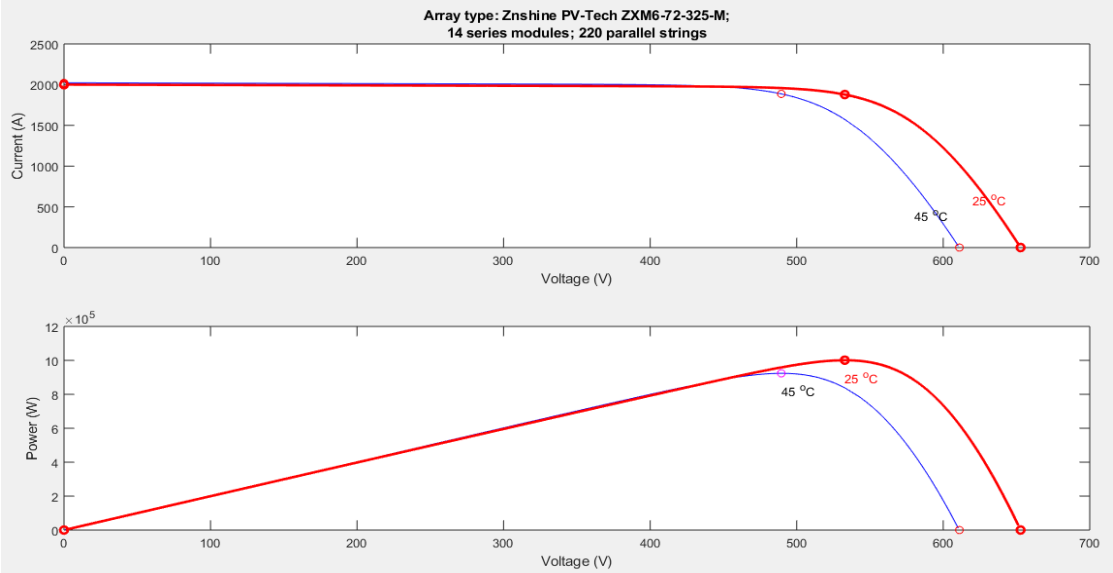

Figure 4-3: 1 MW PV Array at an irradiance of 1000 W/M^2 , temperatures at 25℃ and 45℃ respectively

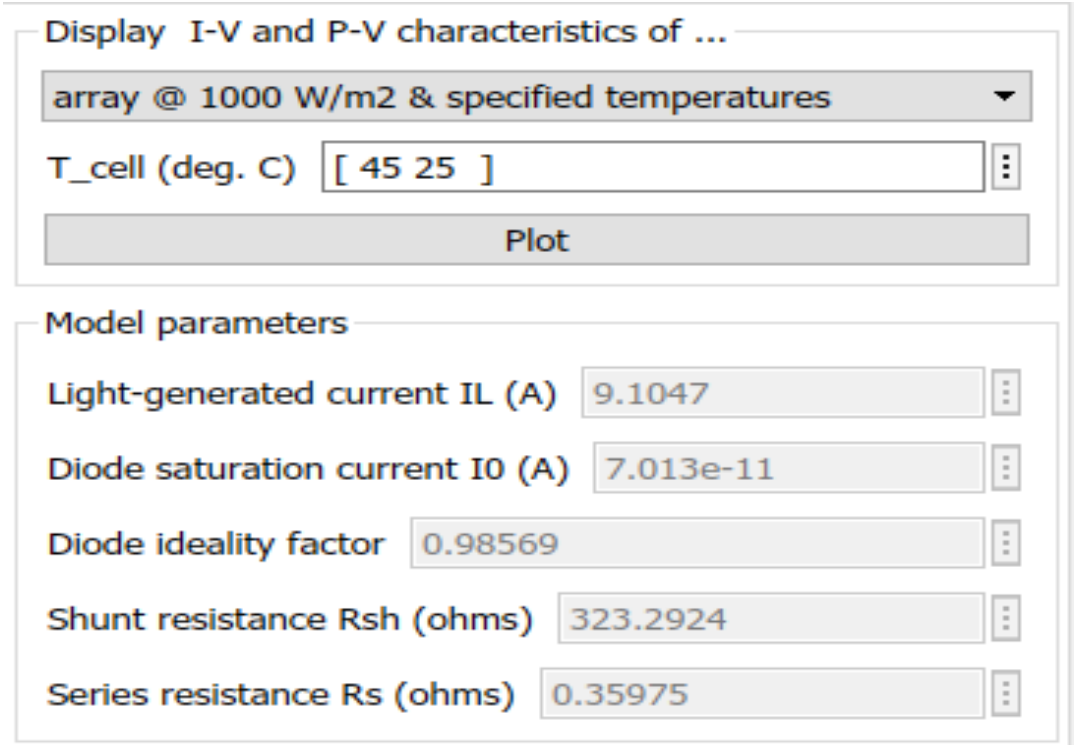

Figure 4-4: Specific values for each module

The system is designed for 1 MWp PV system delivering at 500 V_{dc}. The minimum DC voltage to be supplied to the inverter is 1 kV_{dc} with a modulation index, m_a of 0.87. To achieve the required 1 MW output from the PV system, ten 100 kW PV systems each connected in parallel are designed

then multiplied by ten. Because they are connected in parallel, the same amount of voltage is measured across individual PV system. Parameters for each module and PV array is shown in Figure 4.4 and 4.5 respectively.

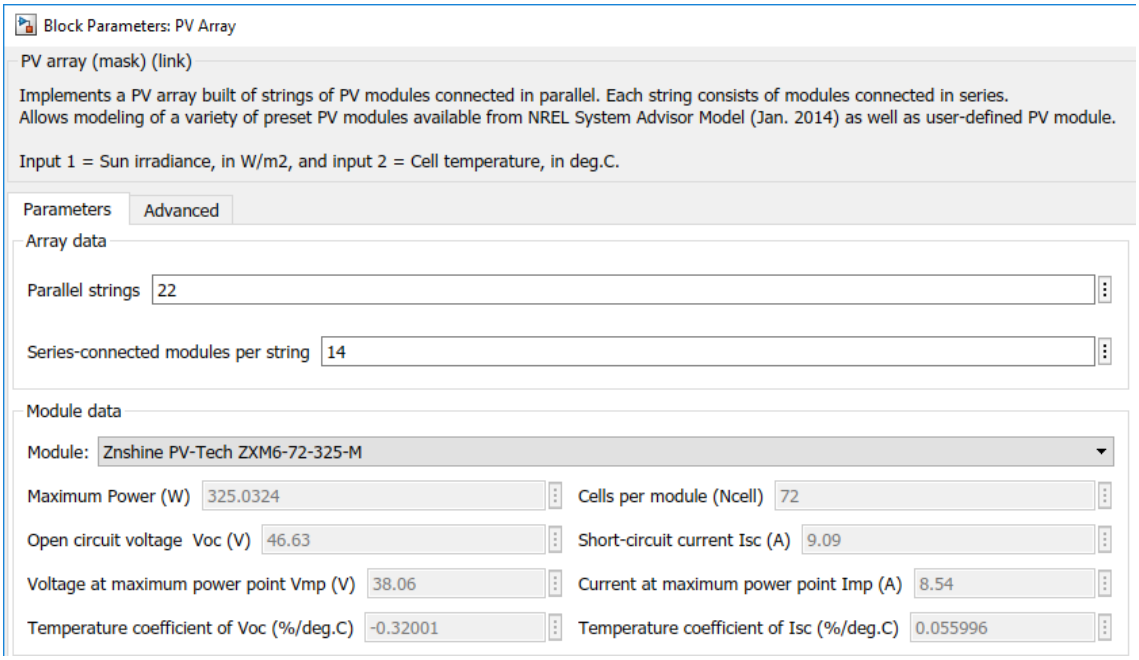

Figure 4-5: Simulated values of 100 KW PV array

Calculation used to achieve the number of modules needed to generate the required power output of 1 MWp.

Number of panels needed in series = $\frac{V_{dcmax}}{V_{mp}} = \frac{500}{38.06} = 13.137$

Because it is not feasible to have a fractional panel of 0.137, hence the number of panels required is rounded up to ≅ 14 panels.

Therefore, the actual output from the PV system: $14 * 38.06$ = 532.84 V_{dc}

The output current from the PV system: $I_{out} = \frac{P_{out}}{V_{out}} = \frac{100\ KW}{532.84\ V} = 187.67\ A$

The number of panels in parallel = $\frac{I_{pv}}{I_{mp}} = \frac{187.67}{8.54} = 21.975$

Because it is impossible to have a fractional panel of 0.975. hence, the number of panels in parallel is rounded up to 22 panels.

The real power is calculated as:

Actual power = (No. of panels in parallel $* I_{mp}$) $*$ (No. of panels in series $* V_{mp}$)

Therefore, actual power = (22 $*$ 8.54) (14 $*$ 38.06)

= 100.1099792 kW

By connecting 10 PV systems of 100.1099 kW each in parallel, the total PV system power output is: 1.001099792 MWp

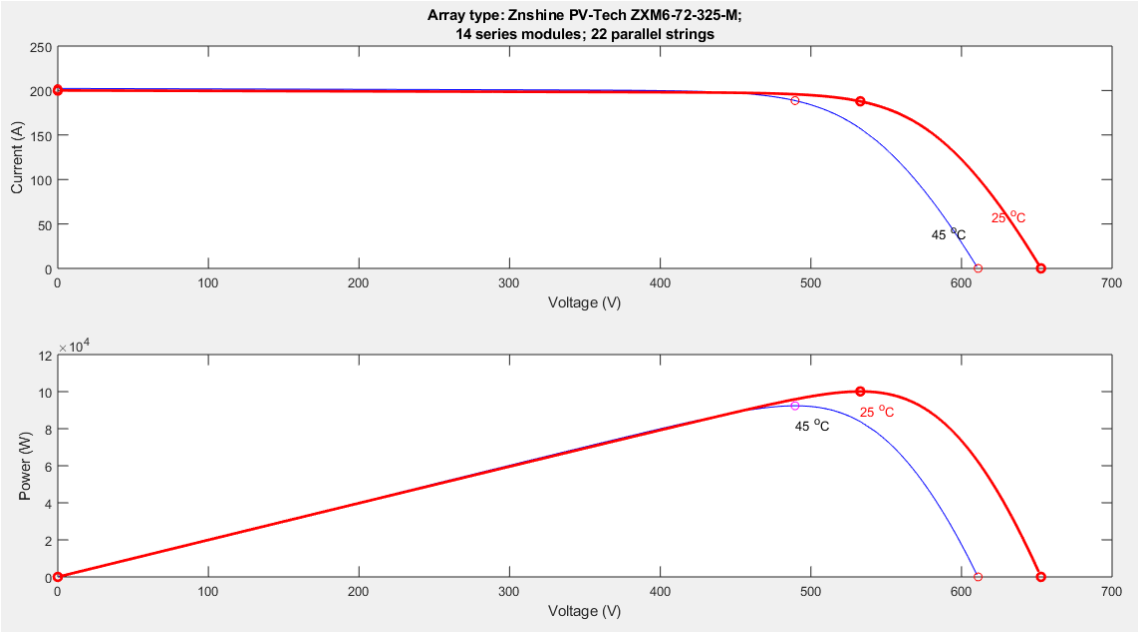

Figure 4-6: 100 kW PV Array at an irradiance of 1000 W/M^2 at 25℃ and 45℃ respectively

Figure 4.6 shows the 100 kW PV array at a solar irradiance of 1000 W/M^2 at 25℃ and 45℃ respectively. The solar irradiance has a significant impact on the output power of the solar PV system.

4.3. DC–DC Boost Converter design

To amplify the input voltage, a DC-DC boost converter is used to step-up the voltage in order to produce an output voltage greater than the voltage from the photovoltaic system. The DC-DC boost converter consists of a semi-conductor switch, an inductor, a diode and a pulse width modulator.

In this study, a two stage topology is selected for the photovoltaic system. The choice of this particular topology was based on the obvious reason that two stage topology allows for further expansion. It makes the system customizable, i.e., it can be converted to multi-string system to intensify the capability of the system in the future, with individual string having a specific MPPT and DC-DC converter. A solar cell is a current source therefore; a capacitor must be

connected in parallel across the PV output so that it appears as a voltage source to the DC-DC boost converter.

The PV capacitor (C_{pv}) is expressed as:

$$C_{PV} = \frac{DV_{PV}}{4\Delta V_{PV} f_s^2 L_{boost}} = \frac{0.467 \times 532.84}{4 \times 43 \times 10000^2 \times 441.98 \times 10^{-6}} = 32.73\mu F \quad (4.8)$$

The values used in equation 4.8 are presented below.

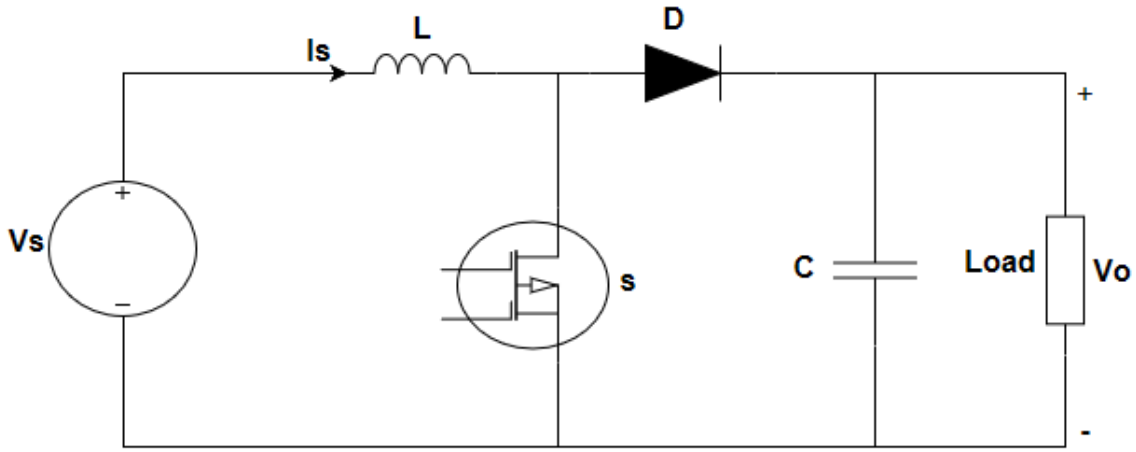

Figure 4-7: A boost converter circuit with diode and MOSFET

The volt-second balance method and capacitor charge balance method were used in the design of the boost converter for the PV system. In addition, a small ripple approximation technique was also used to determine the appropriate voltage and current of the boost converter respectively. The abovementioned methods were used to determine the value of all the components mentioned above. However, in modelling the boost converter, certain required assumptions were made.

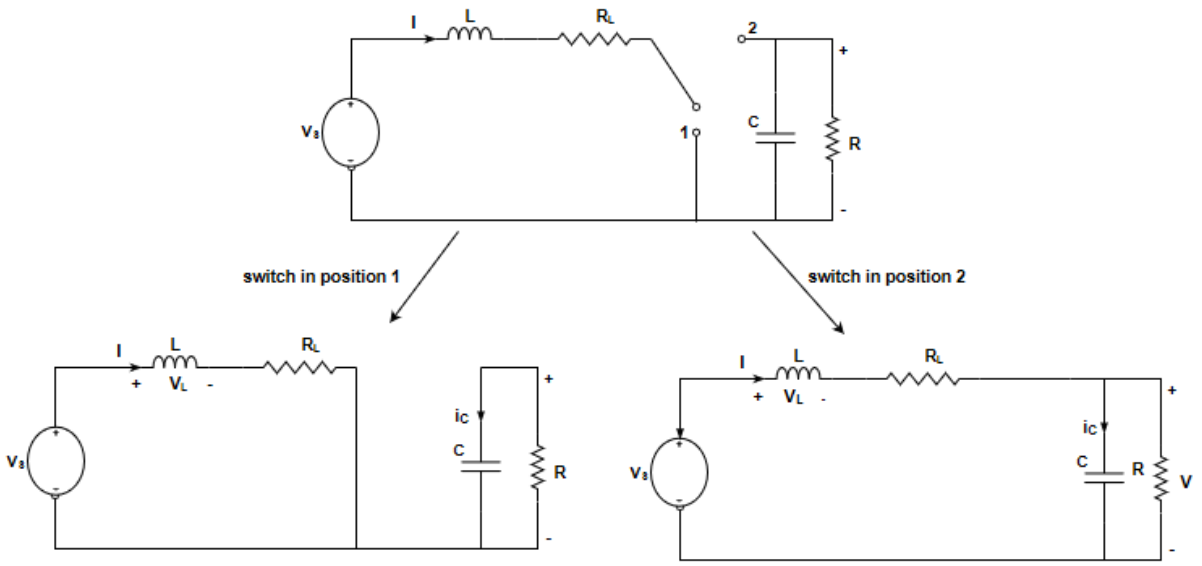

Figure 4-8: Ideal boost converter circuit with switch at position 1 and 2 respectively

An ideal boost converter is presented in Figure 4.7 and further divided into two switching positions 1 and 2 in Figure 4.8. When the switch is in position 1 then it is in the "ON" time of the duty cycle (DT) and "OFF" time of the duty cycle when the switch is in position 2 as indicated above. Practically, the switch is replaced by a power transistor and a diode, while the pulse width modulator (PWM) determines the either positions by sensing high or low voltage. The MOSFET power transistor will position the switch at position 1 whenever the gate circuit voltage is high and turns "OFF" the gate when it senses low voltage hence places the switch at position 2.

Once the MOSFET is on the "OFF" position, the inductor current will forward bias the diode while on the "ON" position, the switch will be in position 2.

To ensure that it is turned "ON" automatically, a diode is included in the circuit rather than a conventional mechanical switch. However, the voltage drop across the inductor is given by:

$$v_L = \frac{Ldi}{dt} \qquad (4.9)$$

If the MOSFET all of a sudden turn "OFF", then the inductor current will definitely be interrupted. Hence, the positive inductor current will be forced by the MOSFET in the "OFF" position to move towards zero. While the value of $\boldsymbol{Ldi/dt}$ is negative and big when the MOSFET is to be switched off. The voltage incline towards infinity when $\boldsymbol{Ldi/dt}$ is largely negative hence making the value of V_L huge and negative. Therefore, the negative voltage value connected will move towards infinity and become positive. This value however, will forward bias the diode before it reaches it. The inductor on the other hand discharges energy in a manner that the polarity of the inductor voltage is connected to the diode becomes positive

with reference to the other terminal connected to the source. Which means that the capacitor voltage must be greater than the source voltage hence, a boost converter.

4.3.1. Capacitor current and Inductor voltage during first phase

When the switch is in position 1 (closed) as indicated in Figure 4.8, the voltage across the inductor will be equal to the source voltage applied:

$$V_L = V_{in} \tag{4.10}$$

$$i_c = -\frac{v}{R} \tag{4.11}$$

Including the small ripple approximation therefore:

$$V_L = V_{in} \tag{4.12}$$

$$i_c = -\frac{V_{out}}{R} \tag{4.13}$$

Where:

$$V_{in} = input\ voltage, V_L = inductor\ voltage, i_c = capacitor\ current, V_{out} = output\ voltage, R = resistor$$

4.3.2. Capacitor current and Inductor voltage during the second phase

During the second phase when the switch is in position 2 as also indicated in Figure 4.8, ensuring that the source voltage is less than the output voltage, then the voltage across the inductor becomes negative and expressed as:

$$v_L = V_{in} - v \tag{4.14}$$

$$v_L = i_L - \frac{v}{R} \tag{4.15}$$

Including the small ripple approximation therefore:

$$v_L = V_{in} - V_{out} \tag{4.16}$$

$$i_c = I - \frac{V_{out}}{R} \tag{4.17}$$

4.3.3. DC-DC boost converter conversion ratio (D')

A graph showing the conversation ratio (D') of DC-DC boost converter is represented in Figure 4.9:

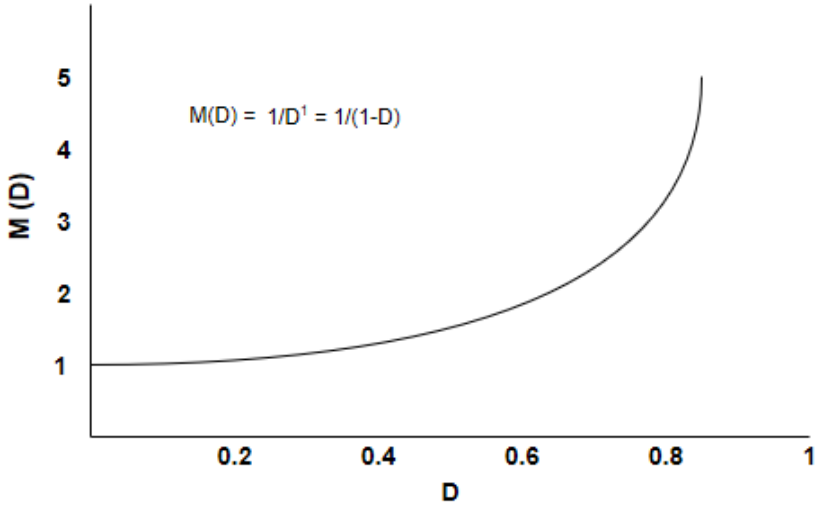

Figure 4-9: DC-DC boost converter conversion ratio

The conversion ratio D′, is equal to 1 when D = 0 as shown in Figure 4.9. This is an indication that the input voltage is equal to the output voltage. Also, the output voltage increases to infinity in a perfect DC-DC boost converter when the value of D moves towards 1 but the function gets larger as the duty cycle time rises. Although, this is not true for ideal converters because the output voltage is restricted to the allowable maximum voltage and will not tend to infinity due to losses present.

The duty cycle of the boost converter using the boost converter conversion ratio is determined by:

$$M(D) = \frac{V_{out}}{V_{in}} = \frac{1}{D'} = \frac{1}{1-D} \qquad (4.18)$$

Therefore, the duty cycle of the boost converter is achieved using the formula:

$$D = 1 - \frac{V_{in}}{V_{out}} = \frac{V_{PV}}{V_{DClink}} \qquad (4.19)$$

The value of the duty cycle $\rightarrow D = 1 - \frac{532.84}{1000}$

$$D = 1 - 0.53284$$

$$= 0.46716$$

4.3.4. Calculating inductor value using appropriate ripple current

The inductor ripple current (Δi_L) as shown in Figure 4.10, is the DT multiplied by the slope during the first interval. Hence, it is expressed as the peak-to-peak ripple and linked to the inductor current waveform.

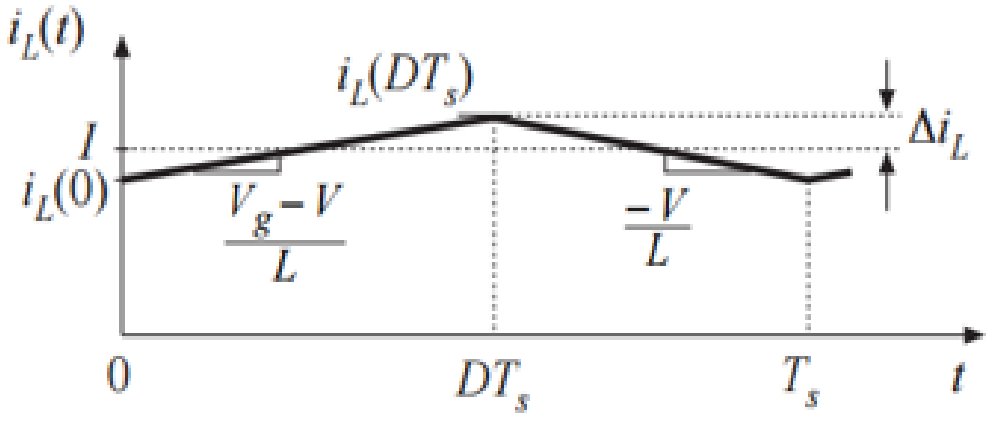

Figure 4-10: Inductor ripple current

Interval 1: The slope of inductor current

As shown in Figure 4.10, the input voltage V_g is applied through the inductor which further produces an inductor current that is a product of the input voltage and inductance. However, the level of increase of the inductor current remains in the positive domain and fixed as long as the inductor remains unsaturated if only the input voltage is kept unchanged. This is shown in equation 4.20.

$$\frac{d_{iL}(t)}{dt} = \frac{v_L(t)}{L} = \frac{V_{in}}{L} \tag{4.20}$$

Interval 2: The slope of inductor current

When the switch is in position 1 “OFF” as indicated in Figure 4.8 for a specific time interval that corresponds to (1-D) T = D’TS, then,

$$\frac{di_L(t)}{dt} = \frac{v_L(t)}{L} = \frac{V_{in} - V_{out}}{L} \tag{4.21}$$

Therefore, change in inductor current during interval 1 is:

$$2\Delta i_L = \frac{V_{in}}{L} * DT_s$$

Calculating for the peak inductor ripple current:

$$\Delta i_L = \frac{V_{in}}{2L} * DT_s \quad (4.22)$$

Equation 4.21 is used to calculate an appropriate value of an inductor if given the ripple current and the corresponding value of the peak current of the inductor. However, the value of the inductor L is calculated using equation 2.23:

$$L = \frac{V_{in} * D}{\Delta i_L * f_s} \quad (4.23)$$

Where: $i_L = \frac{P_{in}}{V_{in}} = \frac{100\ KW}{532.84\ V} = 187.67\ A$

Δi_L is assumed to be equal to 30% of i_L;

$$\therefore \Delta i_L = \frac{30}{100} * 187.67 = 56.3\ A$$

The Period T_s is : $\frac{1}{f} = \frac{1}{10000}$ s

Substituting the values using equation 2.23 therefore:

$$L = \frac{532.84 * 0.467}{56.3 * 10000} = 441.958 \text{ mH}$$

4.3.5. Capacitor value using appropriate capacitor ripple voltage

The output voltage of the boost converter is maintained by the capacitor when the switch is closed. Hence, the capacitor discharges a portion of the stored energy during this period and recharges when the switch is opened. Although, a fraction of the inductor current charges the capacitor when the switch is open, because the current is always greater than the current flowing through the load resistor. But, when it is periodic, the total change in capacitor voltage over a cycle is always zero for a capacitor.

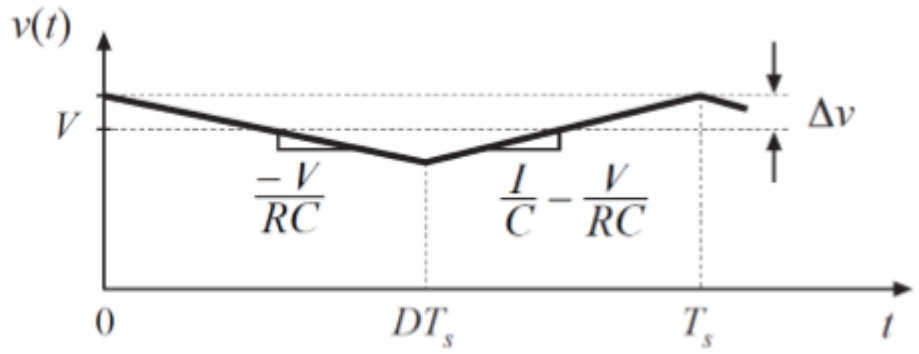

Figure 4-11: Capacitor ripple voltage

The ripple voltage can be obtained from the slope of the capacitor current as shown on the waveform in Figure 4.11. Focusing on interval 1 (ON time) of the capacitor current as indicated in Figure 4.11, the capacitor will be discharged by the load current and the capacitor voltage will reduce with a slope of –V/RC. Therefore, having the value of the interval and slope, ∆V then one can obtain the necessary value required to make the output of the ripple voltage enough to comply with the desired specification.

Interval 1: capacitor voltage:

$$\frac{dvC(t)}{dt} = \frac{i_c(t)}{C} = -\frac{V}{RC} \tag{4.24}$$

Interval 2: capacitor voltage:

$$\frac{dvC(t)}{dt} = \frac{ic(t)}{C} = i_L - \frac{V}{RC} \tag{4.25}$$

But change in capacitor voltage all through interval 2 = product of interval length and slope:

$$-2\Delta v = -\frac{V}{RC} * DTs$$

This implies that, the value of the capacitor is:

$$C = \frac{I_o * D}{f_S * \Delta V_C} \tag{4.26}$$

Where; $I_o = \frac{P_{out}}{V_{out}} = \frac{100000}{1000} = 100\ A$

The capacitor voltage is equal to the output voltage i.e., $V_{C=}\, V_O$

While, $\Delta \mathbf{V_C}$ is assumed to be 1 % of output voltage (V_{out})

$$\therefore \Delta V_C = \frac{1}{100} * 1000$$

$$= 10\ V$$

Therefore, substituting the values into equation 4.26:

$$C = \frac{100 * 0.467}{10000 * 10}$$

$$= 467\ \mu F$$

The load resistor (R_{load}) is calculated as follows:

$$R_{load} = \frac{V^2}{P} = \frac{1000^2}{100\ KW} = 10\Omega$$

4.4. The DC-AC Inverter

The function of the inverter is to convert the DC power from the solar PV through the DC-DC boost converter to a suitable AC power capable of grid integration at an acceptable power factor. It also converts the DC power from the storage system (battery) to a desired AC power for grid integration. This is controlled by the delta modulation index of the PWM as shown in Figure 4.12. However, the detailed voltage source control (VSC) is shown in Figure 4.13.

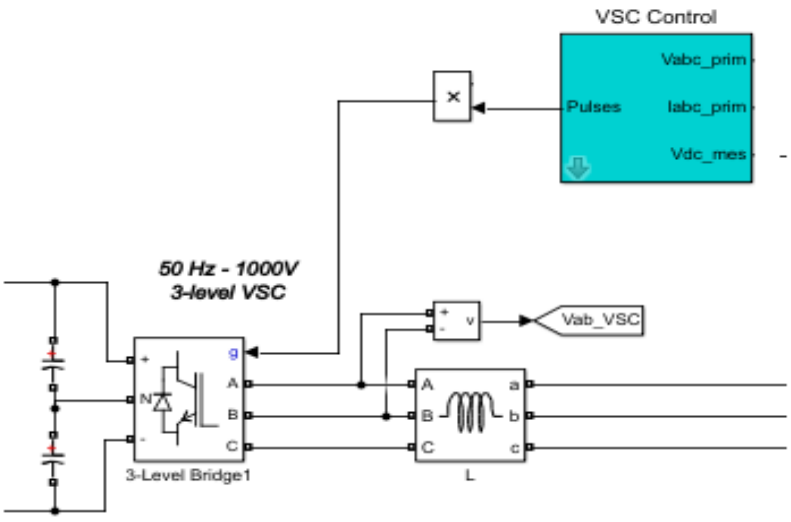

Figure 4-12: DC-AC Inverter with VSC control

It also regulates the voltage at the DC link by ensuring that the required reference AC currents at the output, the phase angle and magnitude are achieved according to the grid standard. To achieve this, a simple PI loop produces the magnitude of the current by equating the reference value to the DC link voltage, while the voltage phase angle details is provided by the phase locked loop (PLL). Hence, the PI controller is responsible for the dc bus voltage. The PI controller produces a negative reference current for a corresponding negative error and a positive reference current for a positive error. But, if the system experiences an increase in the dc bus voltage then the extra energy is transferred to the grid side because this is an indication that an additional energy is available at the dc bus. The power factor of the bridge is regulated by imposing added angle $\boldsymbol{\theta}$. The switching device is an IGBT with a low switching frequency as compared to MOSFET while the DC link capacitor functions as an input to the inverter. This study uses a three phase, two level inverter as shown in Figure 4.12. The PI controller produces a positive reference current and the bridge functions as an inverter. The reference current produced represents the sum of the three phase power represented as I_{ref}*sin($\boldsymbol{\omega}$t $\pm$ $\boldsymbol{\theta}$). To generate the three single phase currents, the total current is divided by three while the reference currents for the other two phases are achieved by separating them 120° apart. All the reference currents are equated to each real phase currents. Hence, the error present bars the flip-flop and moves the pulses to the distinct switches. A positive error is an indication that the current is less than the reference value and thus, the flip-flop moves the clock pulses to higher value and the IGBT is switched to “OFF” in an attempt to avoid short circuit. Because of a challenge to track the sinusoidal current, the switching frequency of the bridge is not fixed rather fluctuates. But in this study, the frequency is set at 20 kHz. The LC filter at the output and operational frequency however determines the active shape of the AC current. To achieve a more desired and accurate tracking, the switching frequency must be increased accordingly.

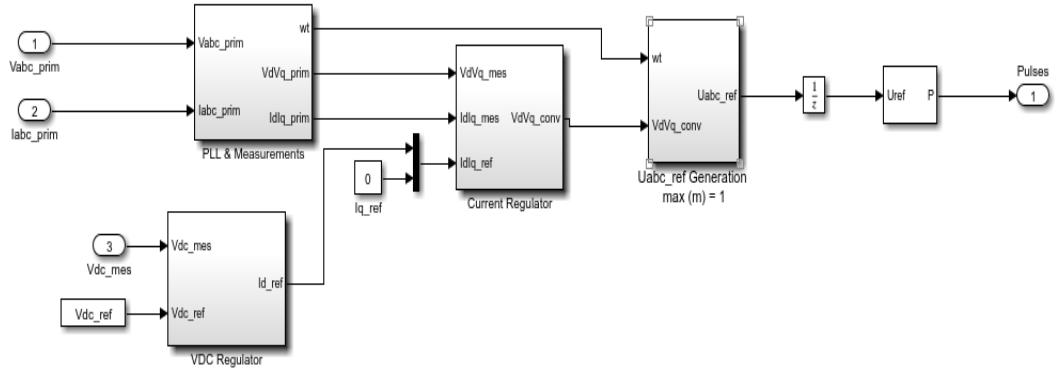

Figure 4-13: Inverter VSC control

4.5. Inverter Filter design

Power from solar PV system before injecting into the grid is normally implemented by means of a voltage source inverter (VSI) system as indicated earlier. However, the harmonic present in the output voltage from the inverter is controlled by introducing an appropriate filter between the voltage source inverter system and the grid in that way maintaining the power quality of the grid system. The most available filters are the L-filter, LC-filter and LCL-filter with each having specific advantages and disadvantages (Raji, 2012).

4.5.1. L - Filter

The level of harmonic content attenuation in a grid connected solar PV system depends on the effectiveness and the type of filter used. Of all the types of filters mentioned above, the first order filter which has an inductor connected in series with the mains is the most commonly used in recent times. This is due to its simplicity, affordability and none resonance complications associated with the second and third order filters. Although, this filter has a major disadvantage of the size of filter required to achieve reasonable attenuation of the harmonics. This type of filter is suitable for high frequency switching plan of the voltage source inverter system model. Hence, to achieve the required AC output voltage, the DC voltage is restricted to 1000 V_{DC}, a switching frequency of 10 KHz, maximum inductor ripple current of 20% of the peak-to-peak current and the ripple voltage is limited to 1% of the maximum peak-to-peak output voltage.

The filter parameter L_f can be determined if the inductor ripple current value is specified using equations 4.27.

$$L_f = \frac{V_{dc}}{4 f_s \Delta_i} \tag{4.27}$$

Where:

L_f = inductance of the inductor

V_{dc} = the DC bus voltage

f_s = the switching frequency

Δi = the inductor ripple current

Therefore, substituting the values:

$V_{dc} = 1000\, V_{dc}$

$f_s = 10\, KHz$

$\Delta_i = 20\%\ of\ the\ output\ current\ (I_o)$

$$I_o = \frac{P_o}{V_o} = \frac{1\ MW}{1\ kV}$$

$$= 1000\ A$$

$$\therefore\ \Delta_i = 20\ \%\ of\ 1000$$

$$= 200\ \text{A}$$

$$L_f = \frac{1000}{4 * 10000 * 200} = 125\ \mu H$$

4.5.2. LC Filter

The LC filter which is a second order filter is mostly used in VSI applications to reduce harmonic contents present at the output voltage of the inverter. Figure 4.14 shows an LC filter commonly used in grid connected and standalone Solar PV power system. One of the major disadvantage of this type of filter is that the resonance frequency of the filter differs with the inductance value of the grid (Heydari et al., 2019). Hence, the design of the output LC-filter is necessary to reduce the inverter output harmonics and also ensures that it provides clean power to the grid. In conditions were the LC filter is not possible then the third order filter (LCL) can be used to solve this problem if designed properly. Because of the design simplicity and high switching frequency, the LC filter was used in this study.

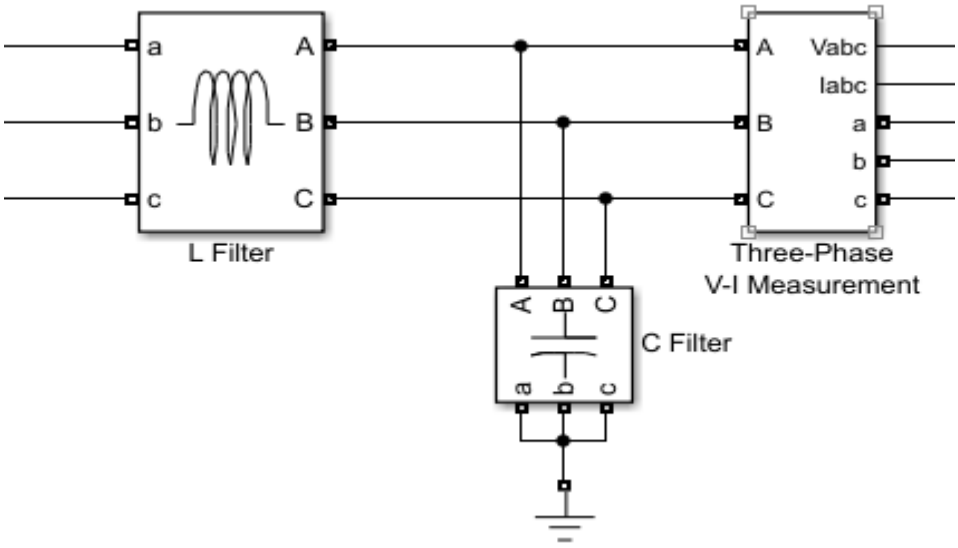

Figure 4-14: LC filter in MATLAB/Simulink

The filter parameters, L_f and C_f can be determined if the inductor ripple current and voltage values are specified using equations 4.27 and 4.28 respectively.

$$C_f = \frac{\Delta i}{8 f_s \Delta V_o} \tag{4.28}$$

Where:

C_f = the capacitance of the capacitor

ΔV_o = the allowable output ripple voltage (1% of V_o)

$V_o = 1000\, V_{dc}$

$\therefore\ \Delta V_o = \frac{1}{100} \times 1000$

= 10 V

$f_s = 10\ kHz$

$\therefore C_f = \frac{200}{8 \times 10 \times 10^3 \times 10}$

$= 250 \mu H$

4.5.3. LCL Filter

The third order filter which is made up of two inductors and a capacitor mitigates the challenges associated with attenuation of harmonics in the system. But the design of this type of filter is complex and costly compared to the first and second order filters. The dynamic regulation of the third order filter is more difficult because of the introduction of additional poles and additional zeros compared to normal first order filter. Therefore, without the introduction of proper damping, the addition of more poles and zeros can make the system unstable. The filter topology for LCL filter is shown in Figure 4.15.

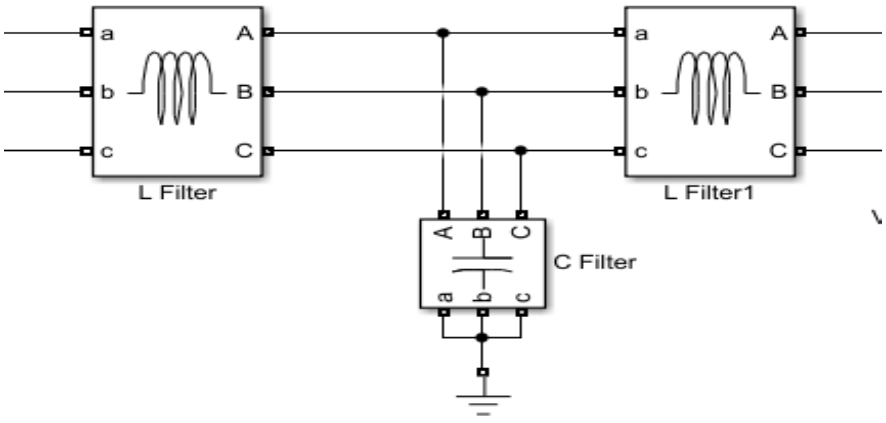

Figure 4-15: LCL filter in MATLAB/Simulink

The LCL filter has an attenuation of 60 Db/decade for frequencies that are above the normal resonant frequency which makes it suitable for lower switching frequencies. It is also best suitable for decoupling between the grid impedance, the filter and lower current ripple over the grid inductor. This filter is appropriate for current ripple attenuation even with little inductance, but when not properly designed it can create resonance and unstable states in the system. Therefore, proper damping must be added to mitigate the difficulties highlighted above. In addition, the cut-off frequency of this type of filter must be at least one half of the entire switching frequency of the inverter in order to allow correct attenuation in the inverter's entire switching frequency spectrum.

4.6. The Grid (Synchronous Generator)

The grid is an interconnected network of power generation and utilization units designed to move power from the generation point to where it would be consumed. The grid is designed to ensure the balance of power production and consumption, generation and load, or supply and demand while maintaining active and reactive power flow. As a matter of importance, the frequency of the system must be maintained at, or very close to its nominal frequency of 50 Hz at all times in the case of South Africa. This value however, differs from grid to grid as some countries are operating at 60 Hz. Any noticeable change from the nominal frequency value demands an urgent response by the system operator. There must be load shedding or power generation must be increased whenever the frequency drops lower than the nominal frequency because it indicates that there is too much load in the system. While load must be increased or generation reduced whenever the frequency is higher than the nominal frequency. This shows that the power generated is more than the load at that material time. Hence, the power generated and consumed must be maintained in order to keep the frequency stable at the nominal frequency. The grid is modelled as a synchronous generator operating a three-phase voltage source with a Line to Line RMS voltage of 11 kV and 4 MW. A 4.1 MW load is

connected to the grid as shown in Figure 4.16. The synchronous generator parameters are expressed in per/unit (pu) as shown in Figure 4.17.

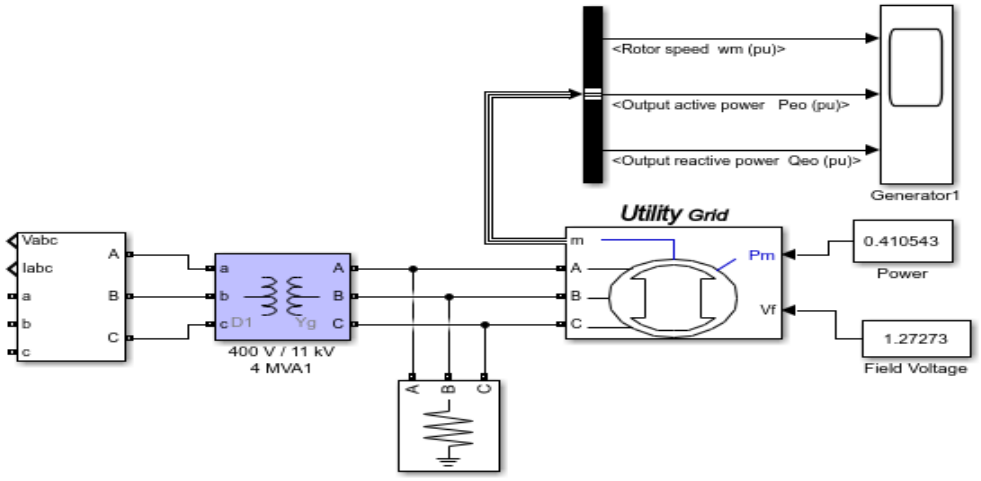

Figure 4-16: Grid (synchronous generator) model of 3.1 MW at 11 KV

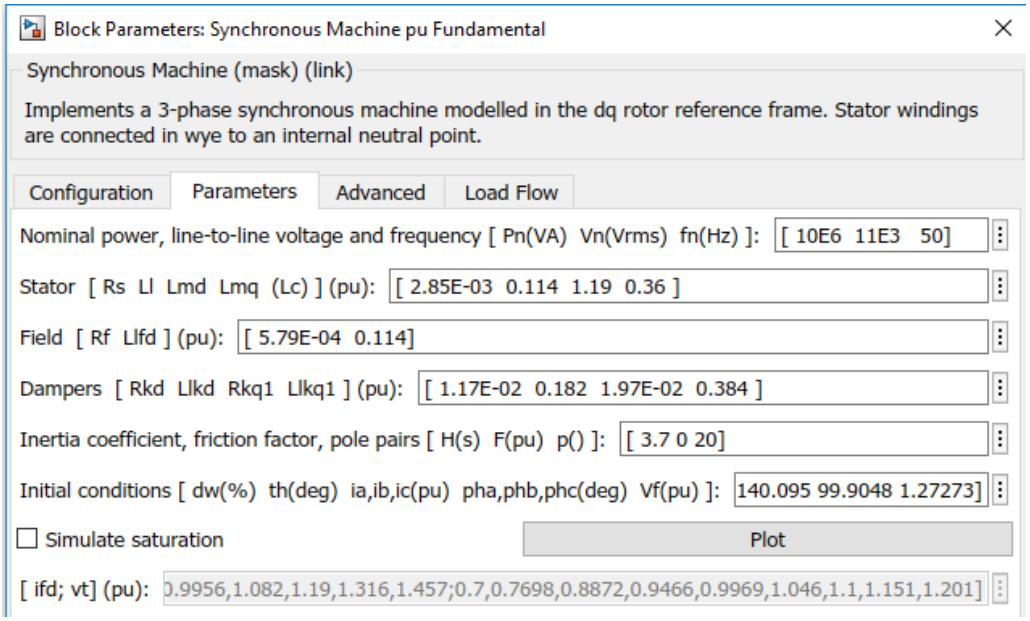

Figure 4-17: Synchronous Generator values expressed in p.u

4.7. Battery modelling and sizing

Battery is used as a storage device then connected to the output of the DC-DC boost converter through a DC-DC bidirectional converter to either supply or consume active power. It is modelled to operate as a boost or buck converter with the assistance of controllers provided to the converter switches. When the battery is injecting power to the grid it will function as a boost converter and when consuming power from the grid, it would operate as a buck converter. Hence, the battery current is negative when charging and positive when discharging. The PV is connected to the grid through a DC-DC boost converter then a DC-AC

inverter and coupled through an L-filter. The coupling L-filter helps to filter out the ripples present in the PV output. A capacitor is further connected to the DC link of the inverter to ensure stability, constant power supply to the grid and to ensure proper elimination of ripples.

In conducting this research, the battery model was selected from the MATLAB/SIMULINK SimPowerSystems library considering factors such as the battery lifespan, capacity, charge and discharge rate, V-f and P-Q regulations, etc. The detailed explanation of the battery model is shown in (Tremblay & Dessaint, 2009). Because of the fluctuation and unstable power output from the PV system together with the significant unstable load consumption, the Lithium-Ion battery are the most common type of battery storage in grid-connected PV system applications. This is to ensure that the battery maximum capacity is harnessed. Therefore, the modelled battery of choice for this research is the "Lithium-Ion" battery with correct choice of parameters for this specific application. The Lithium-Ion battery is modelled to be discharged up to SOC of 20% for both suggested control techniques, and modelled to charge up to SOC of 80%. According to (Tremblay & Dessaint, 2009), the battery model is an analytical model having two distinct but related equations expressing the battery charge and discharge models. The Lithium-Ion battery discharge and charge model is shown in Equations (4.29) and (4.30) respectively. In addition, to better understand the modelling of battery in grid-connected PV system and to get the details of the battery model view appendix 2.

Discharge Model ($i^* > 0$)

$$f_1(it, i^*, i) = E_0 - K.\frac{Q}{Q - it}.i^* - K.\frac{Q}{Q - it}.it + A.exp(-BA.it) \quad (4.29)$$

Charge Model ($i^* < 0$)

$$f_2(it, i^*, i) = E_0 - K.\frac{Q}{it + 0.1.Q}.i^* - K.\frac{Q}{Q - it}.it + A.\exp(-B.it) \quad (4.30)$$

Where:

E_0	=	*the constant voltage, in V*
K	=	*the polarisation constant, in* Ah^{-1}
Q	=	*maximum battery capacity, in Ah*
i	=	*battery current, in A*
it	=	*extracted capacity, in Ah*
*i**	=	*low frequency current dynamics, in A*
exp	=	*exponential zone dynamics, in V*
A	=	*exponential voltage, in V*
B	=	*exponential capacity, in* Ah^{-1}

The battery size and capacity is selected to offer maximum support power to ameliorate the power output from the PV system during little or no power generation from the PV system. For this research, the MPPT connected to the PV system is modelled to produce 1 MW at STC. Thus, the battery is selected to offer 1 MW of power for a period of 1 hour in the event that the PV is not generating any power due to lack of irradiance. Hence, the battery is modelled as a backup to provide frequency regulation. So, an hour is considered suitable because it is for short timeframe applications to offer frequency regulation and supply power to the grid in case of over loading or the PV not generating enough power to meet the load.
The Lithium-Ion battery parameters modelled for the purpose of V-f and P-Q control hence frequency regulation is shown in Figure 4.18 and Figure 4.19 respectively.

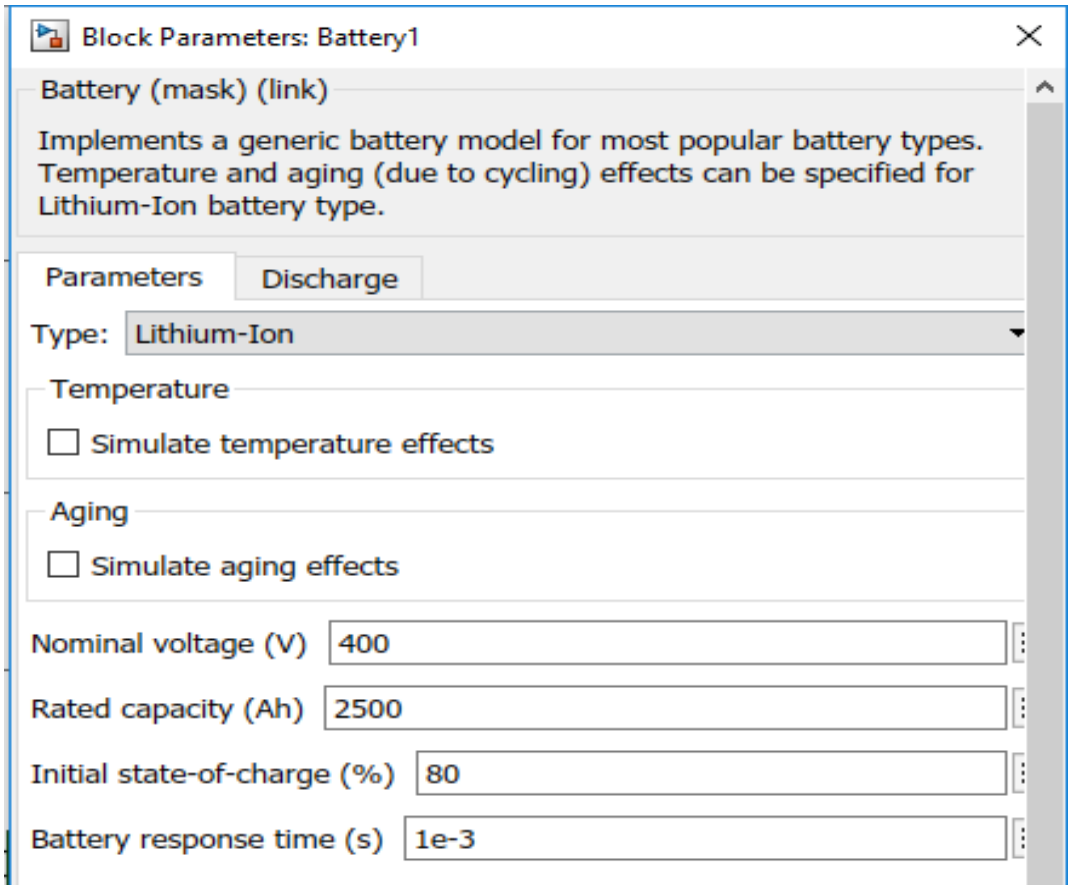

Figure 4-18: Nominal voltage and rated capacity (Ah) of Battery

The discharge characteristics of the battery used for this research is shown in Figure 4.21. Where Figure 4.21a shows the different nominal and exponential zones of the curve using the nominal current of 13 A to plot the values. While the discharge curves for various values of discharge currents is shown in Figure 4.21b respectively. But it is obvious that an increase in the discharge current led to a significant decrease in the discharge time. Hence, the nominal current of 13 A, the storage system (battery) can make power available for just slightly more

than 3 hours. Although, operating at the maximum current of 32.5 A, it can only provide active power for just a little more than 1 hour before it is completed emptied (discharged).

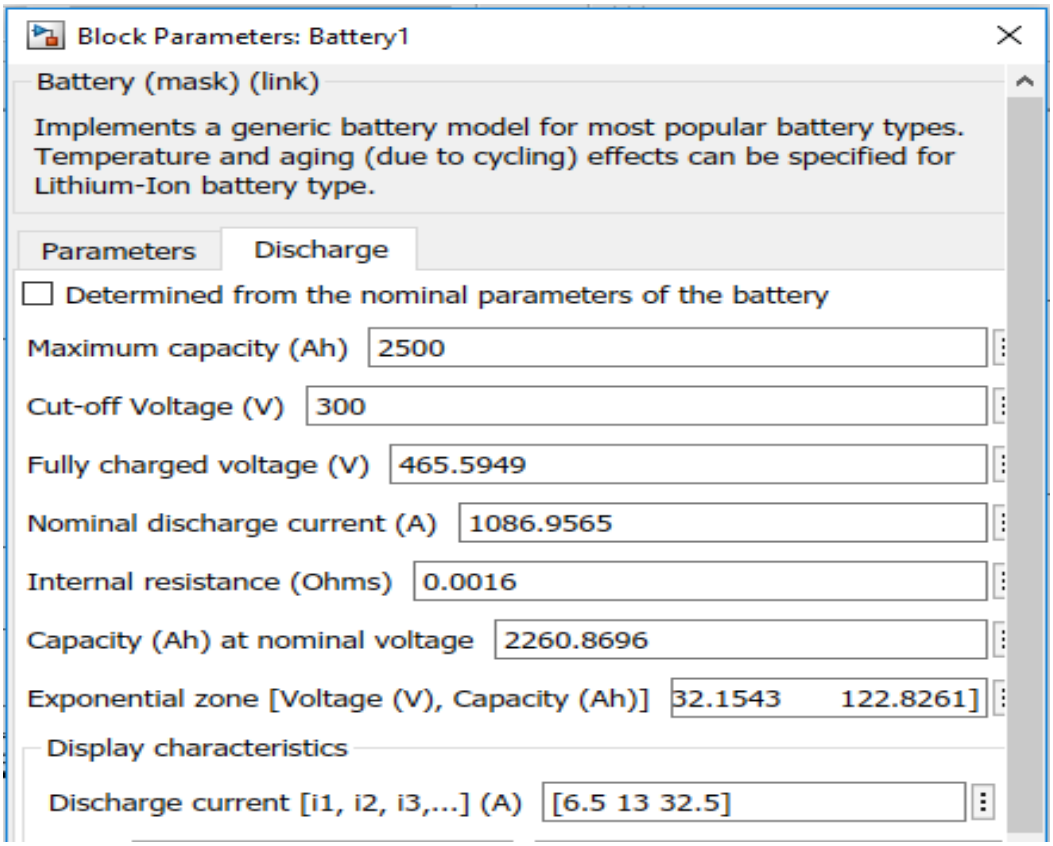

Figure 4-19: Simulated values of the Battery system

Battery parameters can be adjusted within the battery model block as shown in Figure 4.18. Nominal voltage is set to 400 V DC and this voltage level is boosted to 1000 VDC through the DC-DC bidirectional converter. Battery capacity is modifiable through a capacity setting. The SOC setting of the battery demonstrates the setting to the original state of charge of the battery when the model is started.

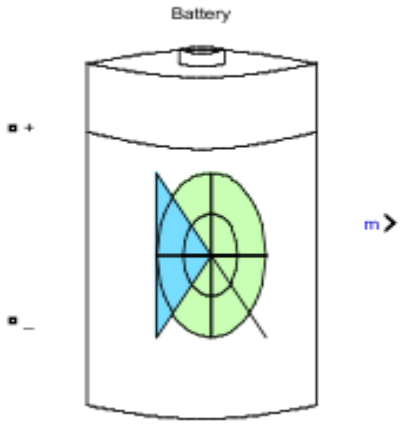

Figure 4-20: Battery block

Figure 4.20 shows the battery block which can be accessed through the electrical elements subdivision under the SimPowerSystems group inside MATLAB software. The battery model block has three terminals that has two physical terminals, while the third terminal has three inner status signals. Terminal “m” has three signals namely: SOC, voltage and current while the positive and negative poles are linked to the output of the DC-DC boost converter (DC bus). Figure 4.22 shows the battery discharge characteristics represented in Ampere-hour.

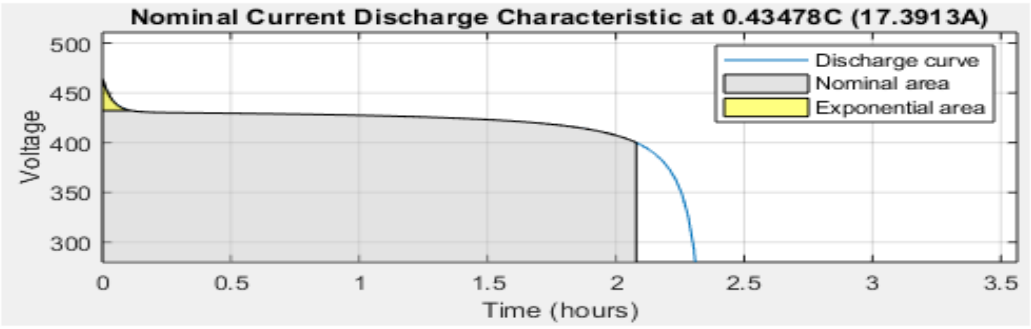

(a)

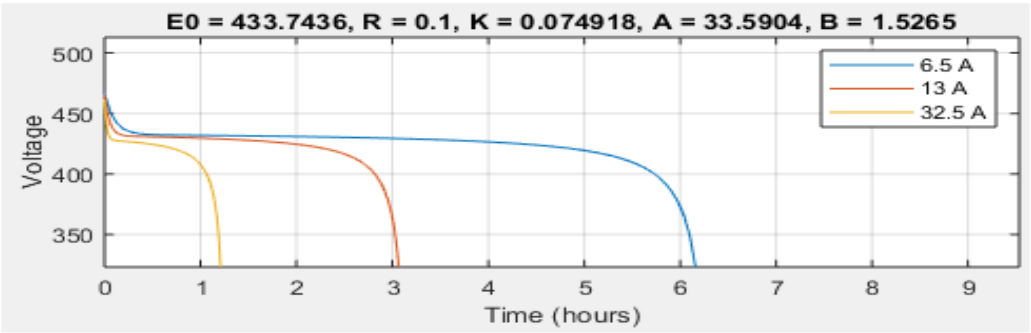

(b)

Figure 4-21: Battery discharge characteristics a) Nominal discharge current (13 A); b) variable discharge currents.

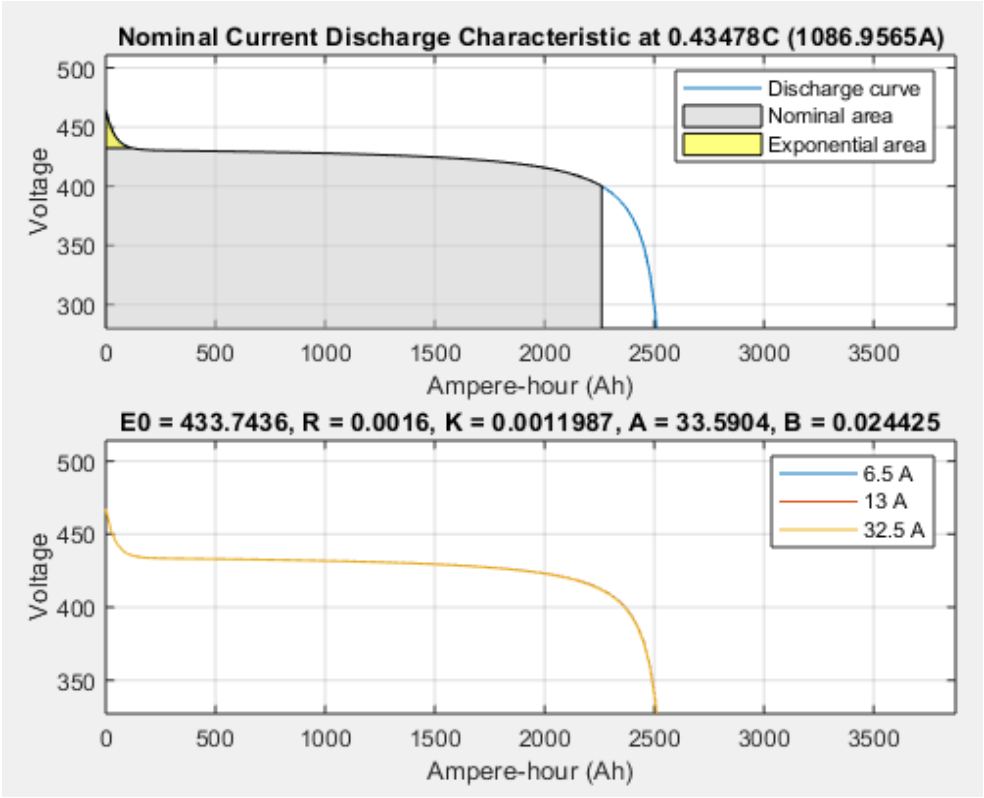

Figure 4-22: Battery discharge represented in ampere-hour

4.8. DC-DC Bi-directional Converter

The DC-DC bidirectional converter allows bi-directional current flow, simple in using minimal storage components and controls battery charging and discharging of current. Some conventional and normally used non-isolated topologies of DC-DC bi-directional converters are shown in Figure 4.23. They are broadly classified into fundamental topologies such as Cúk converter, SEPIC converter, Half-bridge converter and later derived topologies such as interleaved half-bridge converter and cascaded half-bridge converter as shown in Figure 4.24.

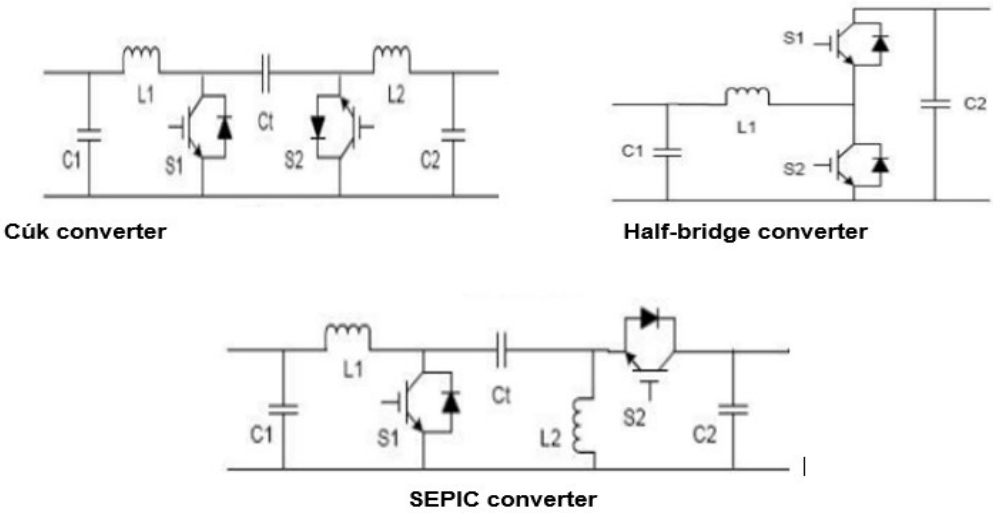

Figure 4-23: Fundamental non-isolated DC-DC converter topologies

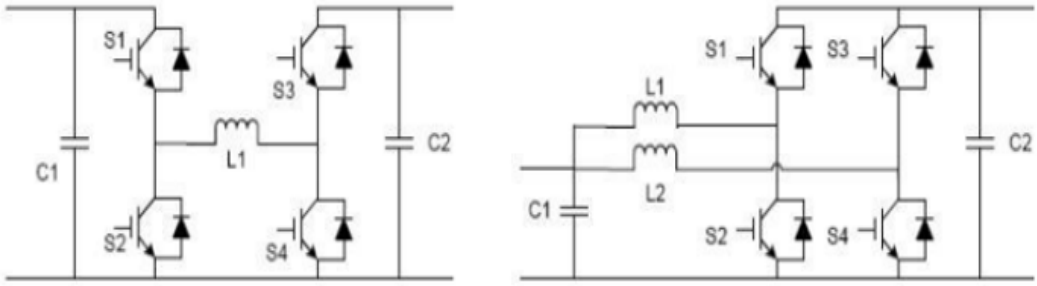

Figure 4-24: Derived non-isolated DC-DC converter topologies

The Cúk and SEPIC converters converts power bi-directionally using two main switches. Although, the half-bridge converter is the most commonly used DC-DC bi-directional converter due to its simplicity and straightforward application, hence, it is used in this study. The interleaved and cascaded half-bridge converters are derived from the fundamental half-bridge hence, their characteristics can be assessed according to the characteristics of the fundamental half-bridge converter.

The main disadvantage of using the half-bridge converter is that the capacity of the output capacitor and the discontinuous output current is significantly affected when operating in the boost mode, while the main advantage is that the topology uses only two switches and small storage components. This is because it has less inductor conduction and lower switching and conduction losses on active elements. Hence, making it more cost effective and can handle higher efficiencies more than Cúk and SEPIC converters. The derived interleaved half-bridge converter would have been the best choice for this study because of reduced stresses and increased efficiencies. But the half-bridge converter was chosen due to light weight, design simplicity and desire to reduce cost.

The half-bridge non-isolated DC-DC bi-directional converter used in this study is shown in Figure 4.25. The battery is connected on the low voltage (400 Vdc) side while the high voltage (1000 V) is connected just after the DC-DC boost converter. This topology can operate as buck or boost depending on the prevailing load demand hence the grid frequency and the battery state of charge (SOC).

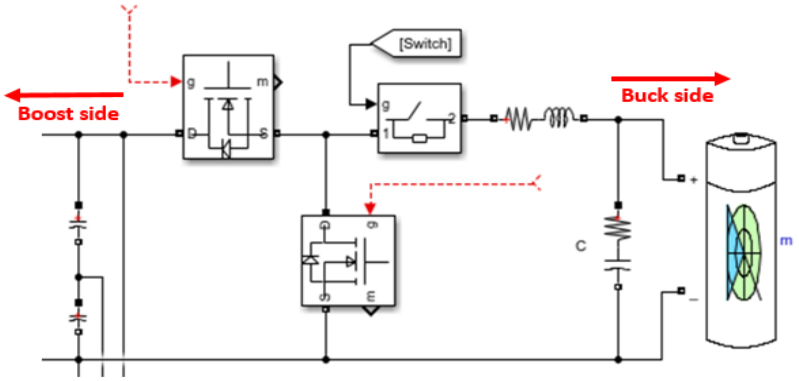

Figure 4-25: DC-DC Bi-directional converter in MATLAB/Simulink

The inductor value of the DC-DC bi-directional converter can be calculated using equation 4.31

$$L_{min} = \frac{(1-D)^2 V H^2}{2PCf} \tag{4.31}$$

Where:

L_{min} = minimum inductor value

D = Duty cycle (0.467)

V_H = High voltage (1000 Vdc)

P_C = Critical light-load power (500 kW)

f = switching frequency (100 kHz)

$$\therefore L_{min} = \frac{0.467(1-0.467)^2 \times 1000^2}{2 \times 500 \times 10^3 \times 100 \times 10^3} = 1.327 \times 10^{-6} H, \text{let the inductor } \approx 3\mu\text{H}$$

The capacitor can be calculated using equation (4.32)

$$C_H = C_L = \frac{D}{R_{Hf}(\Delta V_H / V_H)} \tag{4.32}$$

Where:

$$R_H = \frac{L_{min} 2f}{D(1-D)^2}$$

$$L_{min} = 1.327\mu H$$

$$f = 100\ kHz$$

$$D = 0.467$$

$$V_L = 400\ Vdc$$

$$\therefore R_H = \frac{1.327 \times 10^{-6} \times 2 \times 100 \times 10^3}{0.467(1-0.467)^2}$$

$$= 1.066\ \Omega$$

$$\Delta V_H = \frac{V_H D}{R_H C_H f}$$

Where:

$$V_H = 1000\ Vdc$$

$$C_H = 4.67\ mF$$

$$\therefore \Delta V_H = \frac{1000 \times 0.467}{1.066 \times 4.67 \times 10^{-3} \times 100 \times 10^3}$$

$$= 0.938$$

$$\therefore C_H = \frac{D}{R_H f(\Delta V_H / V_H)}$$

$$= \frac{0.467}{1.066 \times 100 \times 10^3 (0.938/1000)}$$

$$= 4.67\ mF$$

The DC-DC Bi-directional converter connects the modelled Lithium Ion battery to the boost converter through a DC link as shown in Figure 4.25. This particular converter is modelled to control the charging and discharging of the battery. However, the DC-DC converter operates in the buck mode when charging the battery hence, ensuring that the battery current becomes negative. But when the battery is supplying power to the grid, the converter operates in the boost mode and the battery current becomes positive.

The system uses Equation 4.33 and 4.34 to manage the charge and discharge of the battery considering the prevailing load demand hence the grid frequency and the battery state of charge (SOC) at that specific moment.

$$P_{grid} + P_{pv} > Load_{grid} = Charge\ battery \quad (4.33)$$

$$P_{grid} + P_{pv} < Load_{grid} = Discharge\ battery \quad (4.34)$$

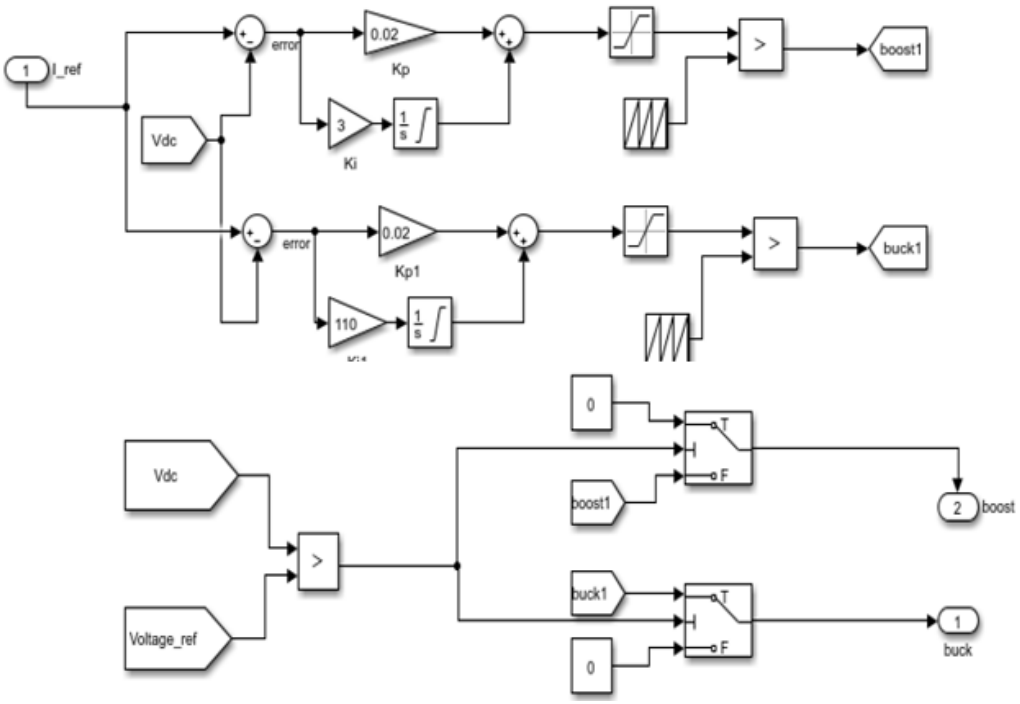

Figure 4-26: Bi-directional converter controller executed in MATLAB/Simulink

The control is modelled to operate independently not considering the power dynamics in the system hence, generates both buck and boost signals as shown in Figure 4.26. It's mode of operation is selected intelligently based on the available battery power and the pulses are passed to either of the semiconductor switch. The ultimate decision to either buck or boost is dependent on the type of signal received from the grid. However, if the control does not receive any signal from the grid, then, the battery SOC of charge will be used as the deciding factor to either operate in buck or boost mode. Subsequently, if the measured grid frequency is equal to the nominal frequency then, the battery will be disconnected temporarily.

The flowchart in Figure 4.27 is used to implement the energy management in the system. The values of nominal frequency and battery SOC is entered using MATLABfunction (fcn) block in the MATLAB/Simulink environment. These two values are then used to determine the grid frequency and the battery SOC at that specific moment. The grid frequency is however, determined by the power availability and the load demand. If the power from both the grid and the PV system is less than the load, then the frequency would be less than the nominal frequency and if the battery SOC is greater than 20% then, the bidirectional converter would be set into the boost. Which means, the battery would supply power to the system in order to stabilize the frequency.

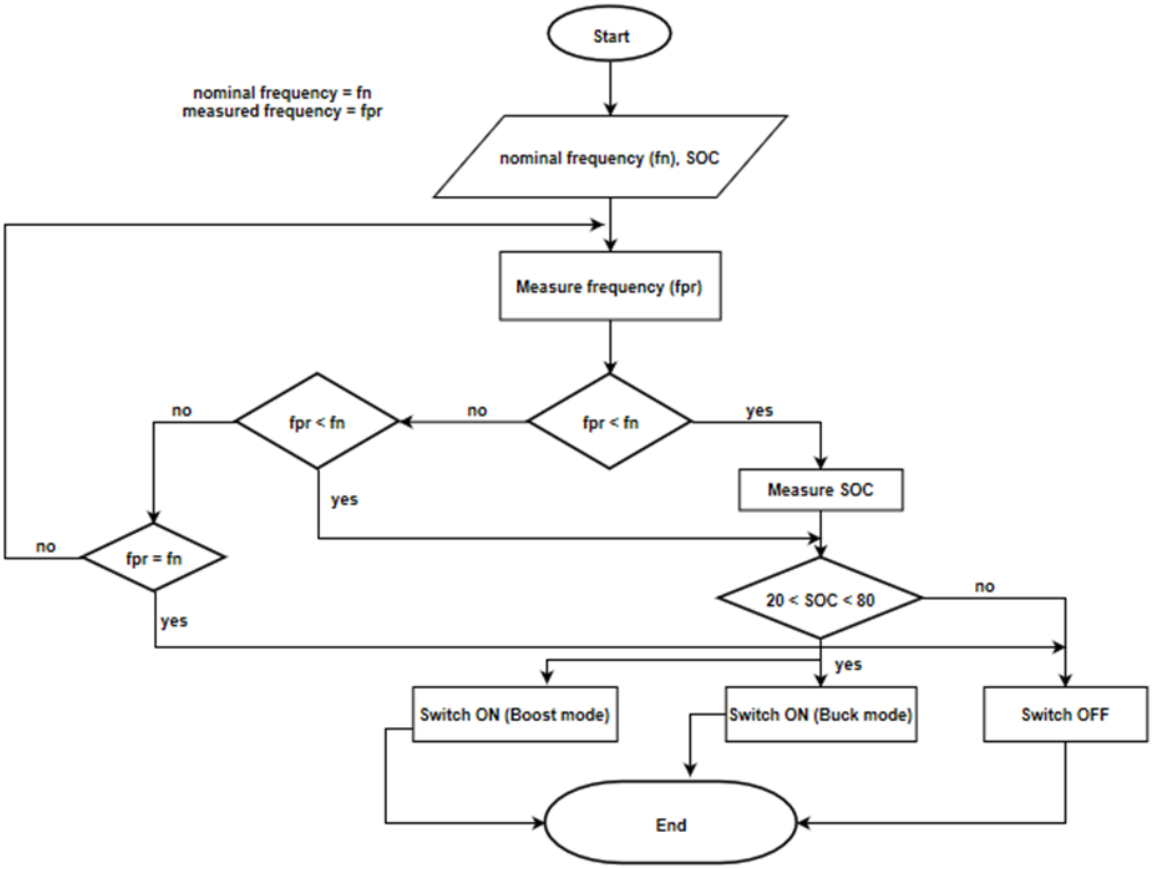

Figure 4-27: Flowchart for grid frequency stability

CHAPTER 5: SIMULATION RESULTS AND DISCUSSION

5.1. Introduction

This chapter focuses mainly on the simulation results and discussion of the results. A grid connected PV system capable of frequency regulation is modelled and simulated in the MATLAB/Simulink environment. This is to ensure frequency regulation using energy storage system, (battery) in this instance.

The remaining sections of this chapter shows the simulation results of the PV system and discusses the output obtained in section 5.2. In section 5.3, the modelling and simulation results of the DC-DC boost converter are discussed accordingly. Section 5.4 shows the simulation results of the inverter indicating the output voltage immediately after the inverter but before the LC filter and the output voltage after the LC filter. In addition, the grid frequency for three different cases are presented. The first case is when the measured frequency (fpr) is equal to nominal frequency (fn) and battery SOC is equal to 80%. Hence, the switch is in the "OFF" position. The second case is when the measured frequency is less than the nominal frequency and battery SOC is greater than 20% (boost mode). The third case is when measured frequency is greater than the nominal frequency and the battery SOC is less than 80% (buck mode). All three cases are presented and discussed in section 5.5.

5.2. Simulation of PV array model

The PV system was designed and simulated using MATLAB/Simulink software. The system was modelled in SIMULINK environment using electronic components such as diodes, resistor and a current source that is comparable to a solar cell as presented in Figure 5.1 and Figure 5.2 respectively. Furthermore, more solar cells were then connected in series and parallel to create a PV array with a power generation capacity of 1 MW. The solar irradiance is varied between 900 W/m^2 and 1000 W/m^2 during the simulation to properly understand the behaviour of the system and power output of a PV system with regards to changes in solar irradiance.

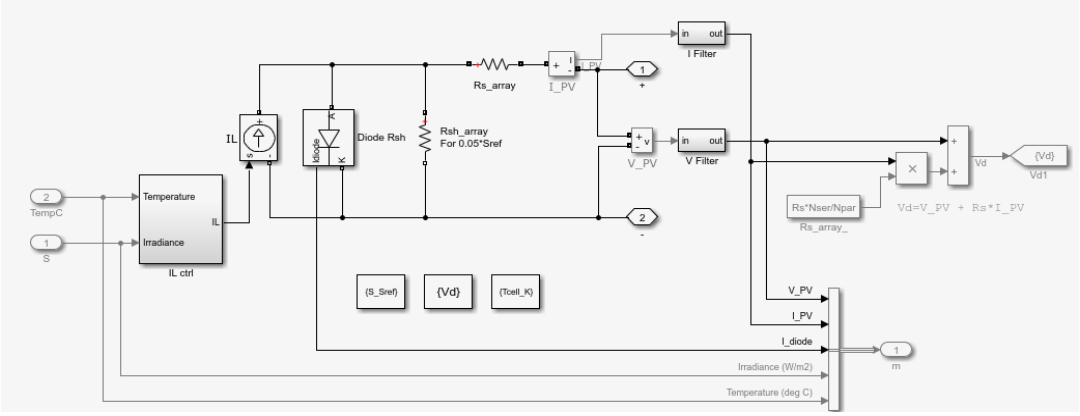

Figure 5-1: Illustration of a diode characteristic in MATLAB/Simulink

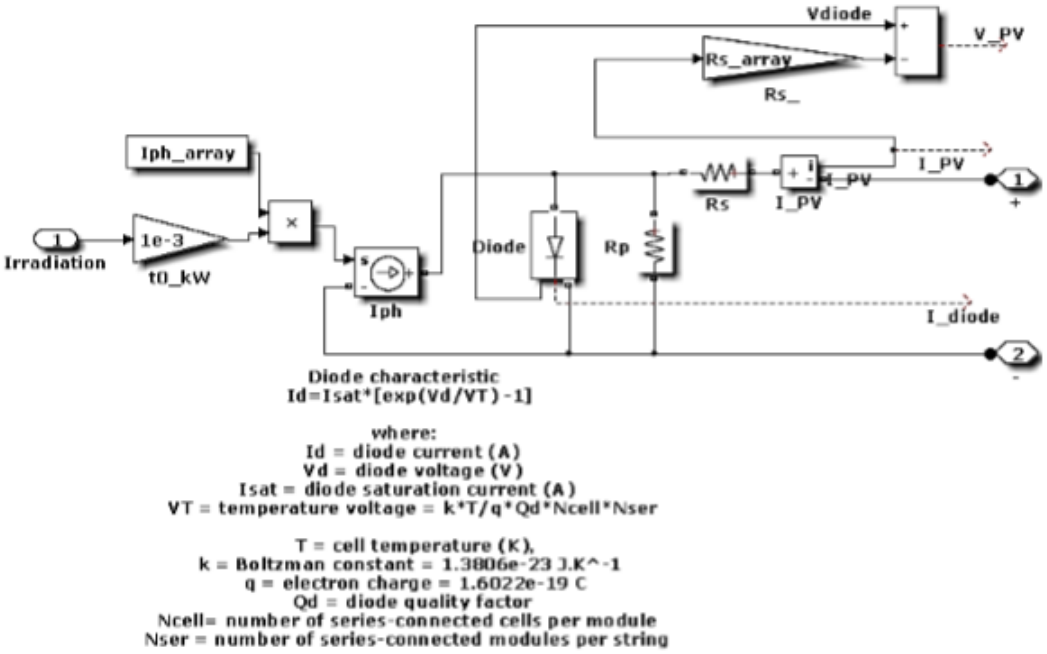

Figure 5-2: MATLAB/SIMULINK equivalent circuit of a solar cell

In order to step up or boost the output voltage of the PV system, it is fed directly to a DC-DC boost converter. The output voltage from the PV system is 532 V_{dc} and boosted to 1000 V_{dc} with a duty cycle of 0.467. The duty cycle is controlled and executed to ensure the output voltage is kept at 1000 V_{dc} using Equation 5.1 because the output from the PV system is not stable. As the input voltage changes, the duty cycle also varies but ensures a constant DC-link voltage.

$$D = 1 - \frac{V_{in}}{1000} \tag{5.1}$$

This makes it possible for the inverter to produce a constant phase-to-phase Vrms of 1000 V and a peak output voltage of 240 VAC at the output terminal of the inverter. In order to eliminate the ripples present, a three-phase LC filter is added hence, it will deal with the harmonic contents by levelling out the output voltage accordingly. The LC filter is a second-order filter that comprises a conductor and capacitor connected in parallel across the load at the inverter output. This type of filter can be used both in stand-alone mode and grid-connected system for voltage control. In this study, the load was varied between 1 MW to 4.1 MW to properly understand the Load-frequency relationship in power system. A grid-connected PV system with energy storage system (battery) connected using a DC-DC bidirectional converter is shown in Figure 5.3.

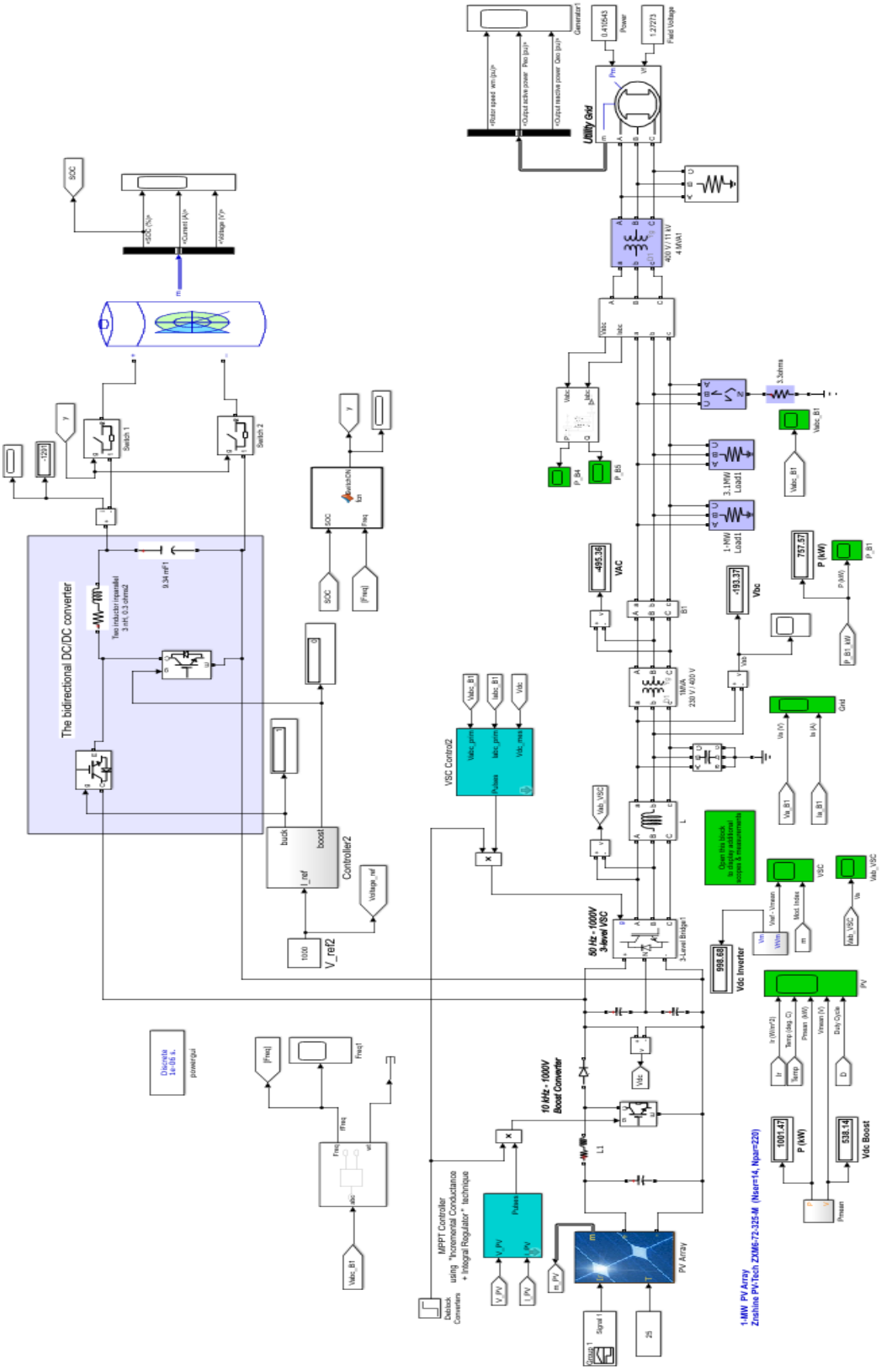

Figure 5-3: Grid-Connected PV system with battery storage

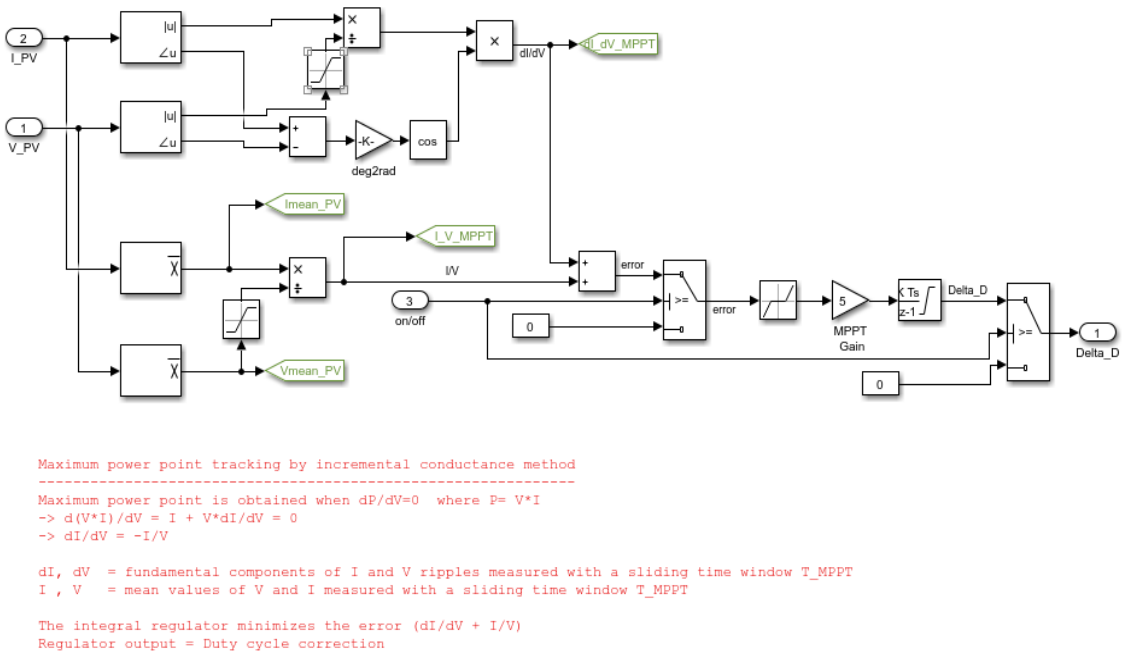

Figure 5-4: Maximum power point tracking by Incremental Conductance Method

Solar technology has experienced technological advancement in recent years. This has led to the integration of various methods that will freely track the peak power point of the PV module during operation. Some of such algorithm are the Incremental conductance, parasitic capacitance, current-based peak power tracking and perturbation and observation methods. This study used the incremental conductance method as presented in Figure 5-4. Essentially, incremental conductance algorithm is used to obtain and compare the incremental conductance and conductance. Both are achieved by calculating the product of current and voltage. One significant advantage of this algorithm (incremental conductance) is the capacity to track maximum power with less complications regarding the control in MATLAB/Simulink environment.

5.2.1. Simulation results

The type of PV system selected and modelled was simulated to ascertain the correctness of the design and also provides an opportunity to analyse and evaluate its performance. Hence, two PV system with different power ratings were simulated. The first PV system was modelled and simulated with a power capacity of 100.109 kW, output current of 187.67 A and an output voltage of 532.84 V_{dc}. While the other PV system has 10 (ten) parallel but the same characteristics PV arrays, with each having the same characteristics as the first PV system. I.e., 10 PV system with the same characteristics as the first PV system are connected in parallel having a combined total power capacity of 1.001099 MW, total output current of 1876.74 A and a voltage of 532.84 Vdc.

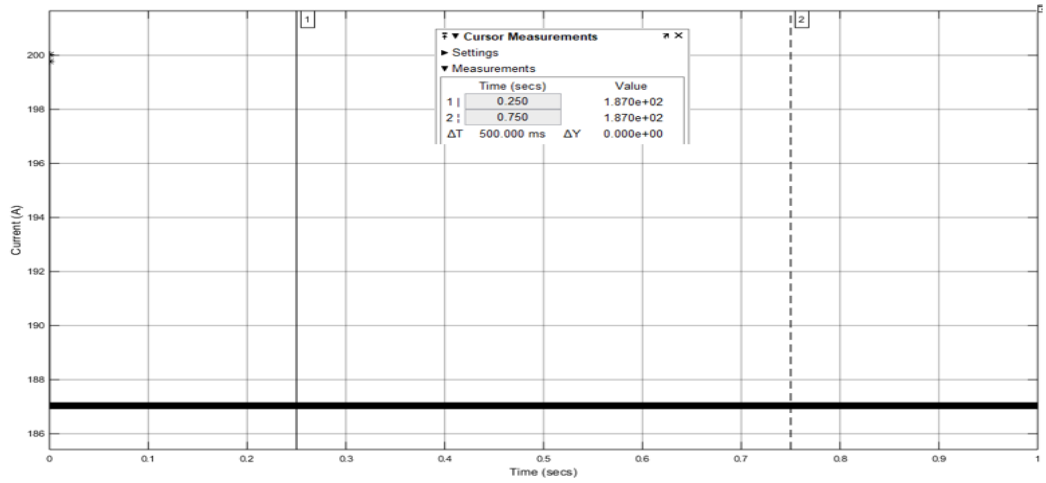

Figure 5-5: The output current of 100 kW PV system

Figure 5.5 shows the output current of the 100 kW PV system at a constant solar irradiance of 1000 W/m^2. The calculated value of the output current is 187.67 A as shown in section 4.2.2 while the simulated value is 187 A at 250 ms and 750 ms respectively. By comparison, the simulated value is 0.67 V different from the calculated value. This is an indication of the accuracy of the simulation results.

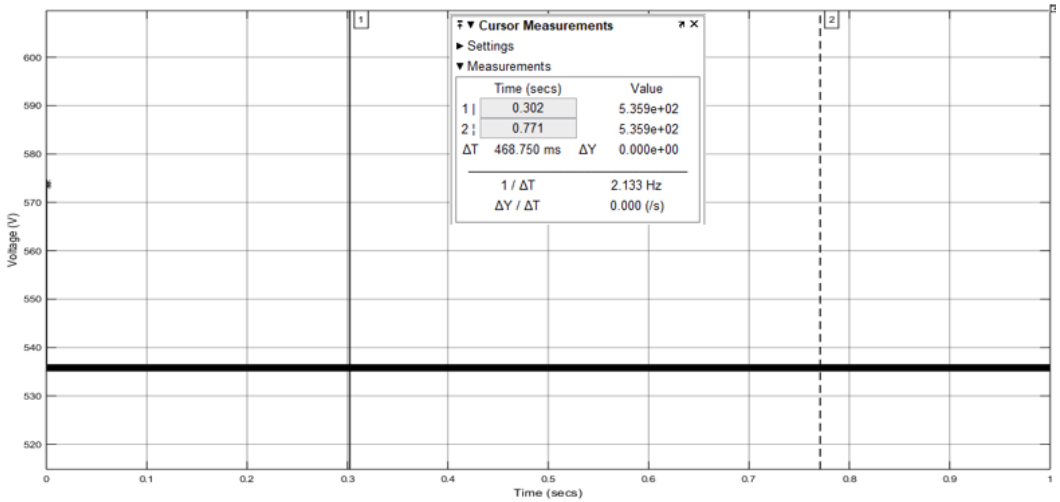

Figure 5-6: The output voltage of 100 kW PV system

The output voltage from the 100 kW PV system is shown in Figure 5.6. It serves as the input to the DC-DC boost converter. The calculated value of the output voltage is 532.84 Vdc as presented in section 4.2.2 while the simulated value is 535.9 Vdc. However, comparing the simulated value with the calculated value, there is a slight difference of 0.57% or 3.06 Vdc which is still within an acceptable range.

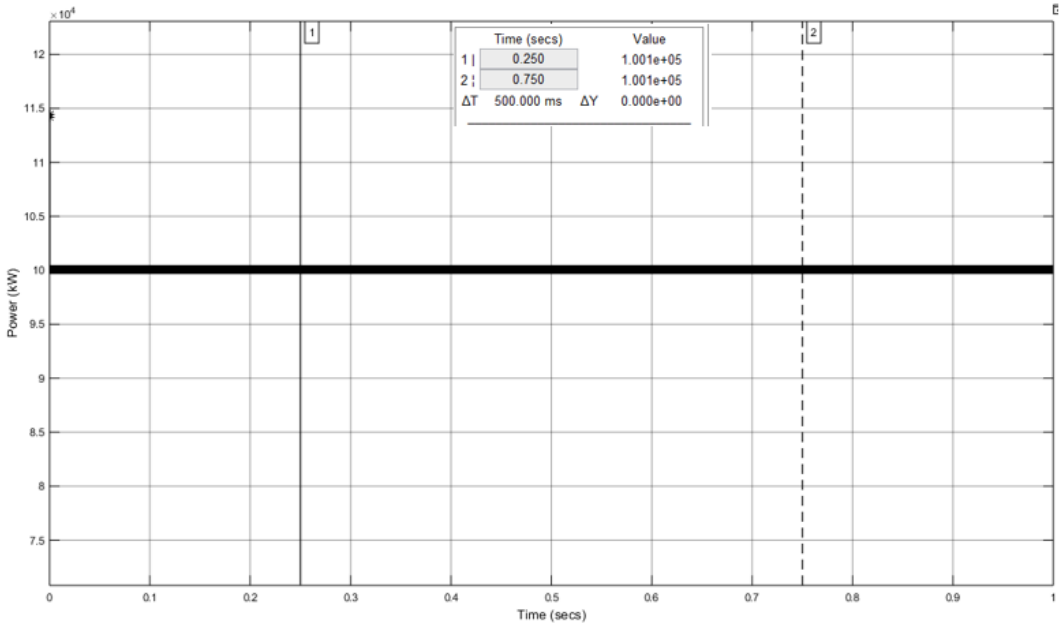

Figure 5-7: The output Power of 100 kW PV system

Figure 5.7 shows the simulated output power generated by the 100 kW PV system which is dependent on simulation time. However, in this instance the power shows to be stable throughout the simulation period. The power generated at this stable state is 1.001 kW compared to the calculated value of 100.11 kW. This shows an accurate modelling, simulation and design because the difference between the simulation value and calculated value is very little.

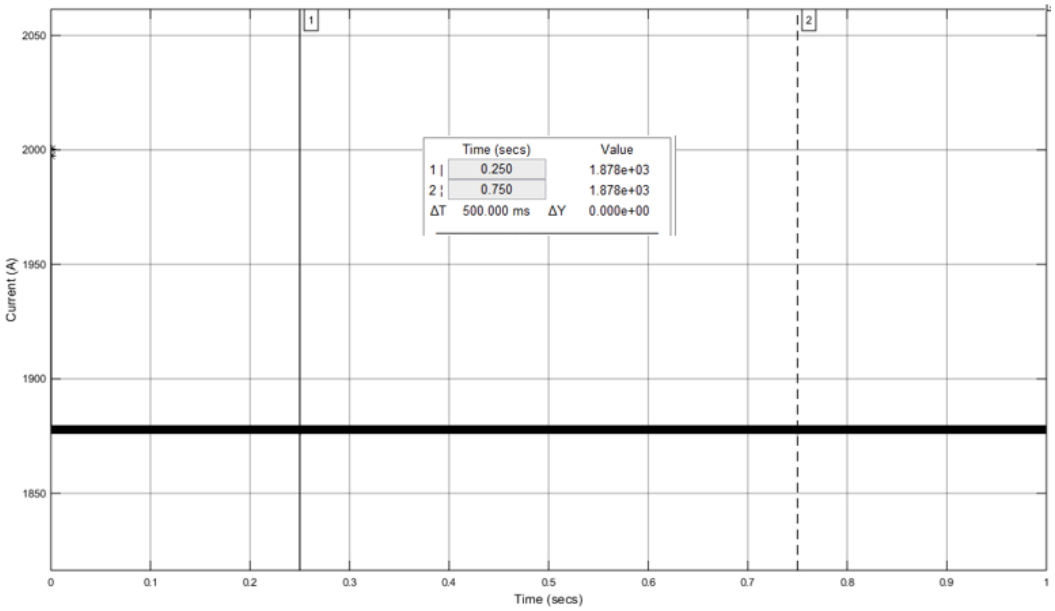

Figure 5-8: The output current of the 1 MW PV system

Figure 5.8 shows the output current of the 1 MW PV system at a constant solar irradiance of 1000 W/m^2. The calculated value of the output current is 1876.74 A as presented in section 4.2.2 while the simulated value is 1878 A at 250 ms and 750 ms respectively. By comparison, the simulated value is slightly different from the calculated value. The difference is 0.067% which is within an acceptable range. Hence, it indicates an accurate simulation results.

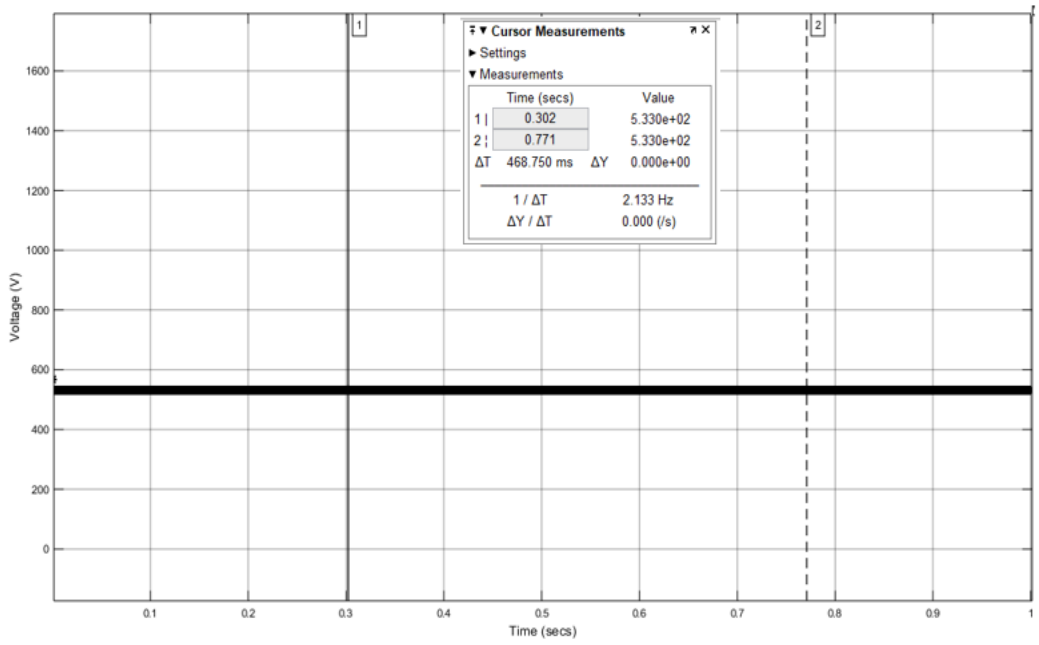

Figure 5-9: The output voltage of the 1 MW PV system

The output voltage from the 1 MW PV system is shown in Figure 5.9. It serves as the input to the DC-DC boost converter. The calculated value of the output voltage is 532.84 Vdc as presented in section 4.2.2 while the simulated value is 533 Vdc. However, there is a slight variance of 0.03 % (0.16 Vdc) when comparing the simulated value with the calculated value but the difference is within acceptable range.

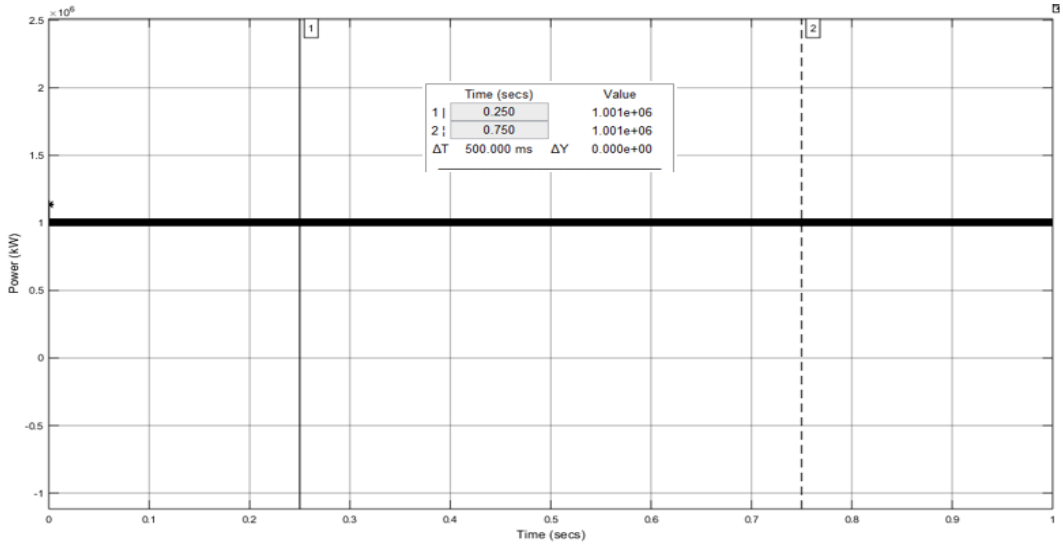

Figure 5-10: The output Power of the 1 MW PV system

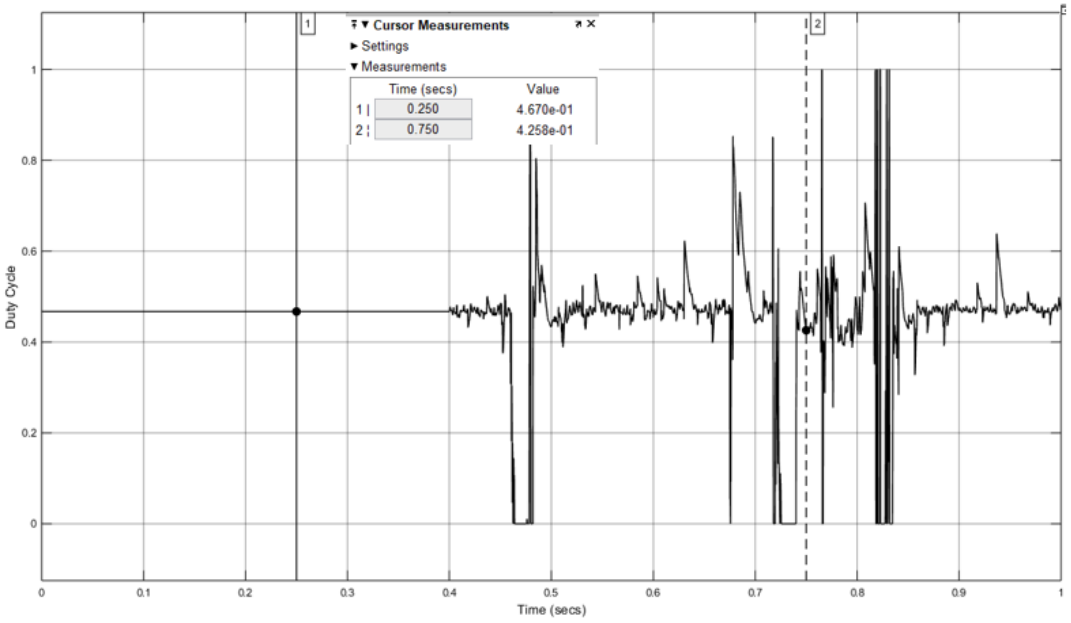

Figure 5-11: Fluctuations in the duty cycle of the 1 MW PV system

Figure 5.10 shows the simulated output power generated by the 1 MW PV system which is dependent on simulation time. However, in this instance the result showed a constant power output throughout the simulation period. The power produced according to the simulation is stable at 1.001 MW compared to the calculated value of 1.0011 MW in section 4.2.2. This shows an accurate simulation and design because the difference between the simulation value and calculated value is 0.01%. This is the output power from the PV system connected to the grid when producing at maximum point. The voltage from Figure 5.9 is further boosted to the required output voltage of 1000 Vdc by an equivalent duty cycle of the DC-DC converter; this

duty cycle is shown in Figure 5.11. However, the duty cycle is shown to be stable at 0.426 from the beginning but started experiencing instability at 400 ms due to the input voltage at the transitory period. The power measurement block used in MATLAB/Simulink environment is on appendix 3 for further clarity and understanding.

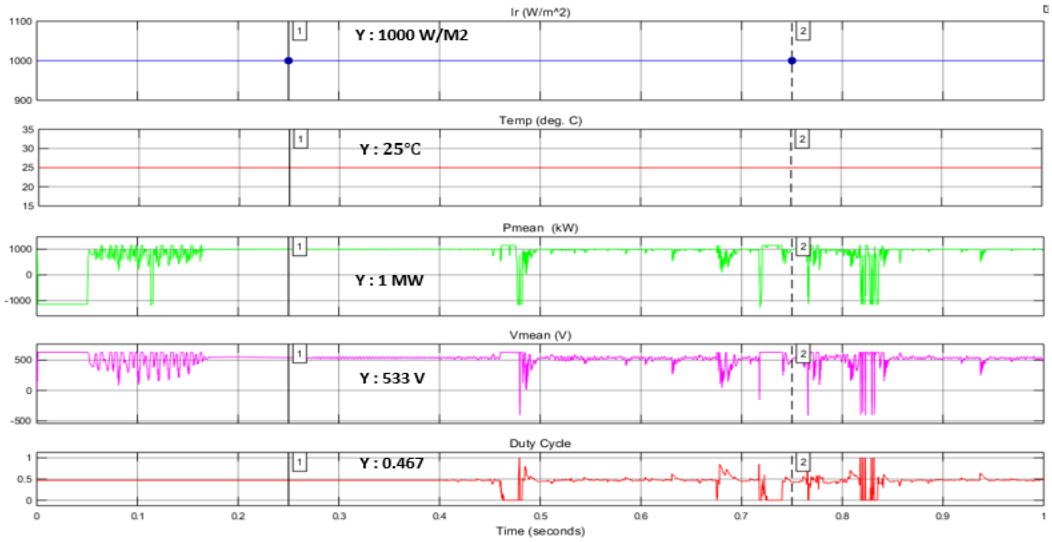

Figure 5-12: PV system simulated output values

A summary of the simulated values of the 1 MW PV system is presented in Figure 5.12. The values correspond to the calculated values in chapter 4 which is an indication that the simulation values are accurate. Although, any change in the solar irradiance has shown to have a significant impact on the output power of the PV system as the same is applicable to the temperature. An increase in the temperature will led to a decrease in the power output on the PV system while an increase in the solar irradiance leads to improved output power from the PV system.

5.3. Simulation result of DC-DC boost converter

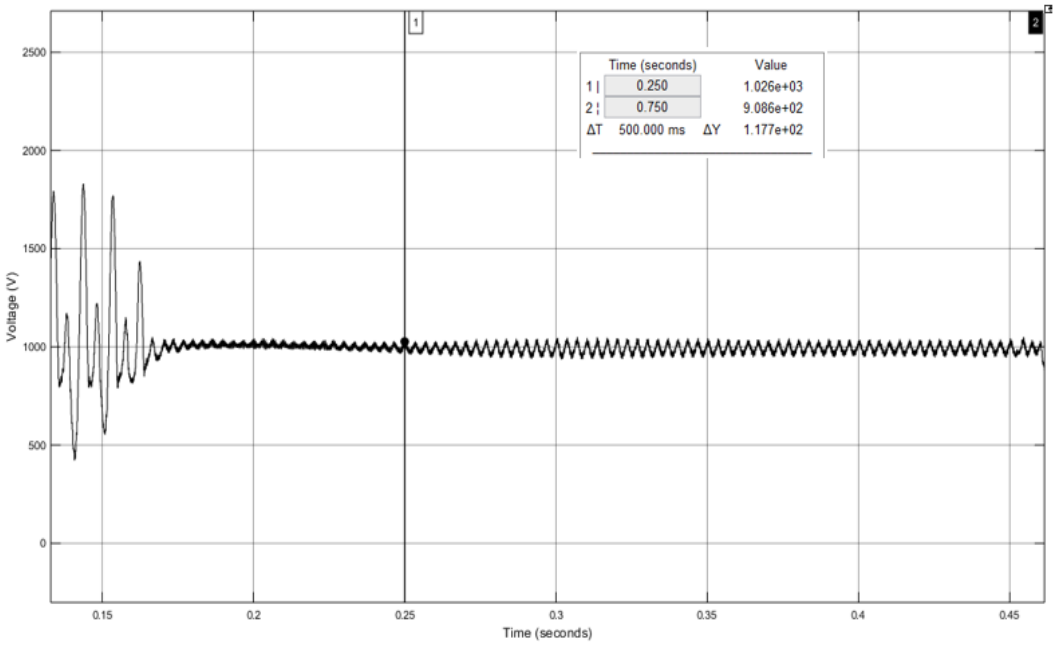

Figure 5-13: Output voltage of the DC-DC boost converter

The output voltage of the DC-DC boost converter in relation to simulation time is presented in Figure 5.13. It showed that the output voltage surged to 1600 V_{dc} during the transition period and become stable at about 160 ms. Subsequently, the output voltage remained at 1000 Vdc with little ripples between 160 ms and 250 ms. Thereafter, the voltage dropped to 908.6 Vdc at 450 ms. Although, the model and design accommodated 1% deviation from the stable state, the output voltage matched the anticipated voltage calculated in chapter 4 and the simulation result close to the calculated value of the PV system output voltage as shown in Figure 5.13.

5.4. Simulation results of the inverter

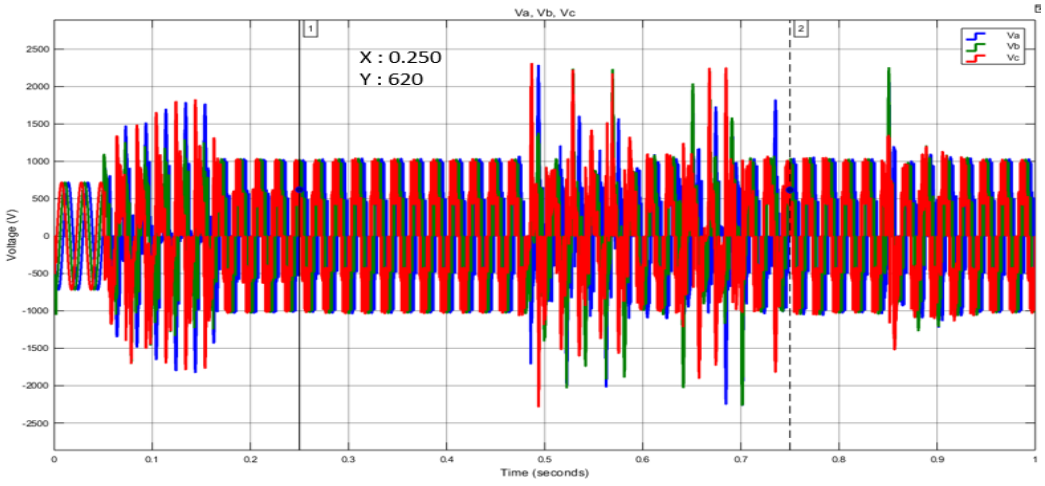

Figure 5-14: The output voltage of the 1 MW PV system inverter before the LC-filter

To achieve the AC component, an inverter was used to convert the DC to AC using the method in chapter four. The inverter output voltage waveforms are presented and labelled as $V_{abc,}$ where; V_a is represented by the blue waveform, V_b is represented by the green waveform and V_c is represented by the red waveform respectively as shown in Figure 5.14. The output of the phase voltages at the output terminal of the inverter in Figure 5.14 are measured immediately before the LC filter. These voltages indicated that the output voltage waveforms contained lower and higher harmonic components. However, the harmonic content present is as a result of the switching effect of the inverter switches. These voltages are known to be 120 degrees out of phase to each other and each phase swings between 0 V and 620 V respectively. The switching transition is further represented in Figure 5.15 using only the V_a.

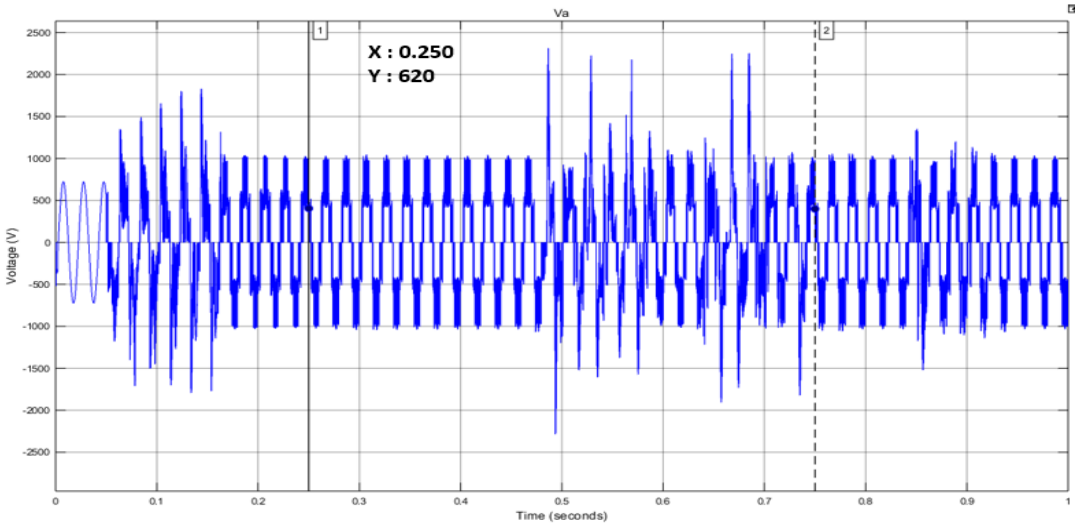

Figure 5-15: V_a phase to illustrate the switching transition

The inverter voltage showing clearly the switching transition period is presented in Figure 5.15 for only phase a. It is seen that between 100 ms and 150 ms, the voltage (Va) increased to double the voltage due to switching effect of the inverter. In addition, the voltage returned to normal voltage of 620 V as presented. This voltage contains some ripples that is eliminated by the LC filter.

5.4.1. Simulation results of the inverter after the LC-filter

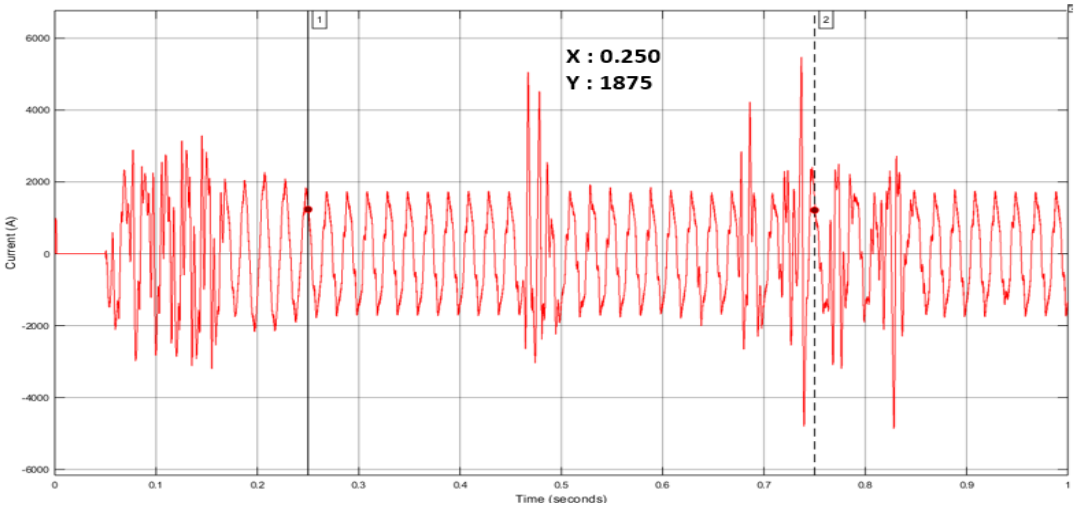

Figure 5-16: The output current after the L filter (Phase a)

The simulated output current of the three-phase inverter is 1875 A at 250 ms as shown in Figure 5.16. However, the calculated output current is 1876.74 A as presented in chapter 4. This represents an accurate simulation value with just a 0.093% difference as compared to the calculated value.

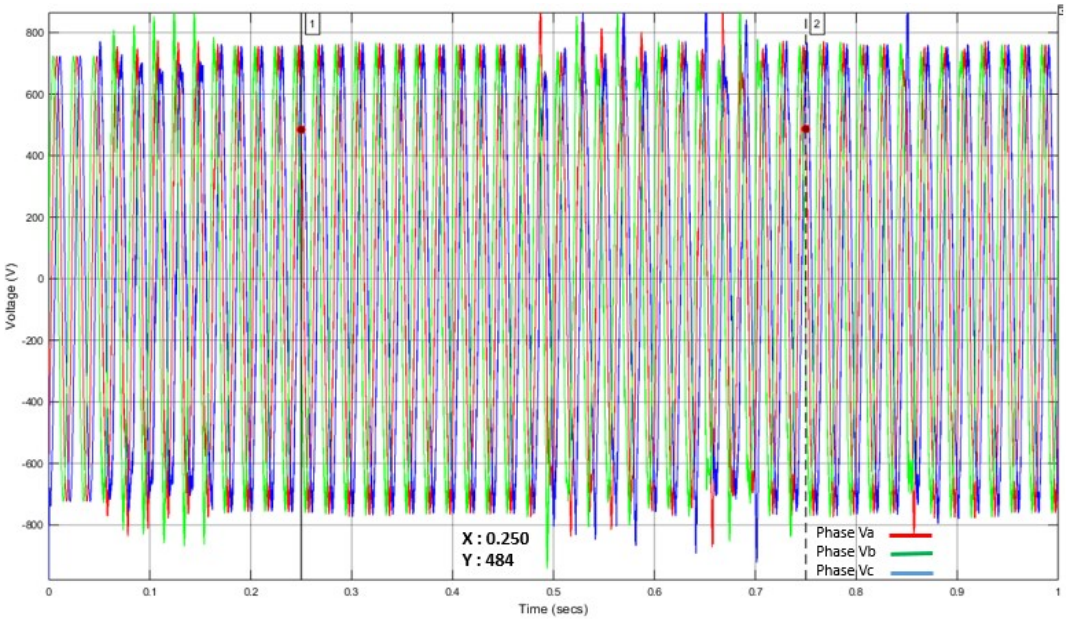

Figure 5-17: Filtered output voltage of the three-phase inverter

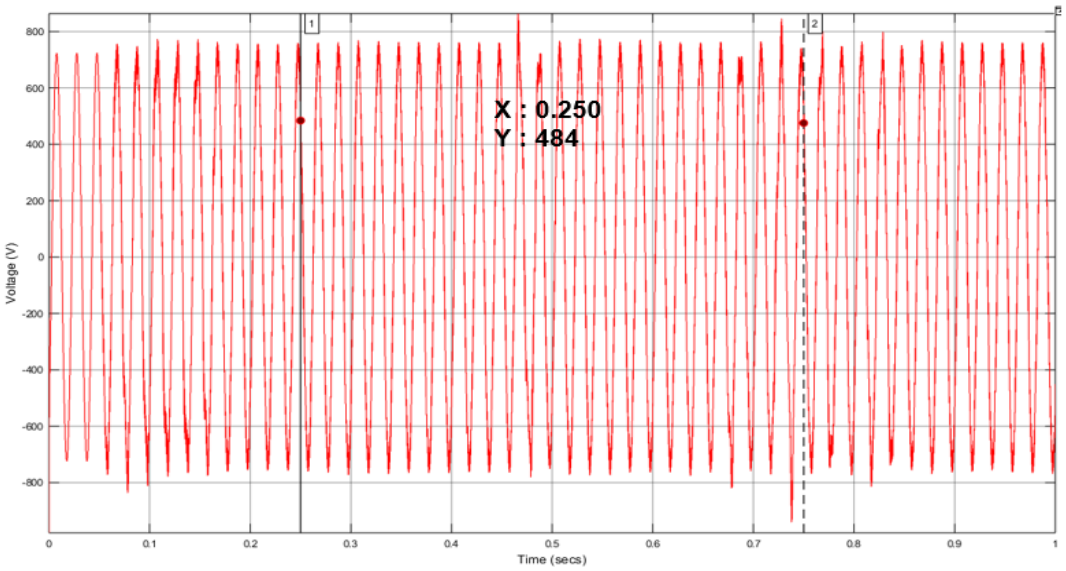

Figure 5-18: Filtered output voltage of the three-phase inverter showing only phase a

The LC filter after the inverter has decreased and eliminated the higher order harmonic components that are meant to introduce ripples on the output voltage. Hence, the remaining comprises of only basic and fundamental lower-order harmonics. The line-to-line output voltage waveforms V_{ab} from Figure 5.15 is shown as 620 Vac while the line-to-line rms voltage is 484 V at a corresponding nominal frequency of 50 Hz as shown in Figure 5.17. These values correspond to the anticipated values of the output voltage considering the amplitude modulation index, ma and the inverter input voltage as shown in Figure 5.18. Each phase changes between 0V and +/620 V with the individual phases being out of phase to each other by 120 degrees. Figure 5.18 presents only Va phase to demonstrate the switching transition.

5.5. Grid Frequency Results

Three case studies based on the load conditions, power supplied by the grid (synchronous generator), PV system, power dynamics, solar irradiance and battery SOC were used to evaluate the grid frequency and the battery storage system ability to inject power to the system to stabilize the grid frequency.

5.5.1. Case study 1

This scenario considers a constant AC load of 4.1 MW, solar irradiance varied between 900 W/m^2 to 1000 W/m^2, the power supplied by the PV system is 1 MW, power generated by the grid (synchronous generator) is 3.1 MW.

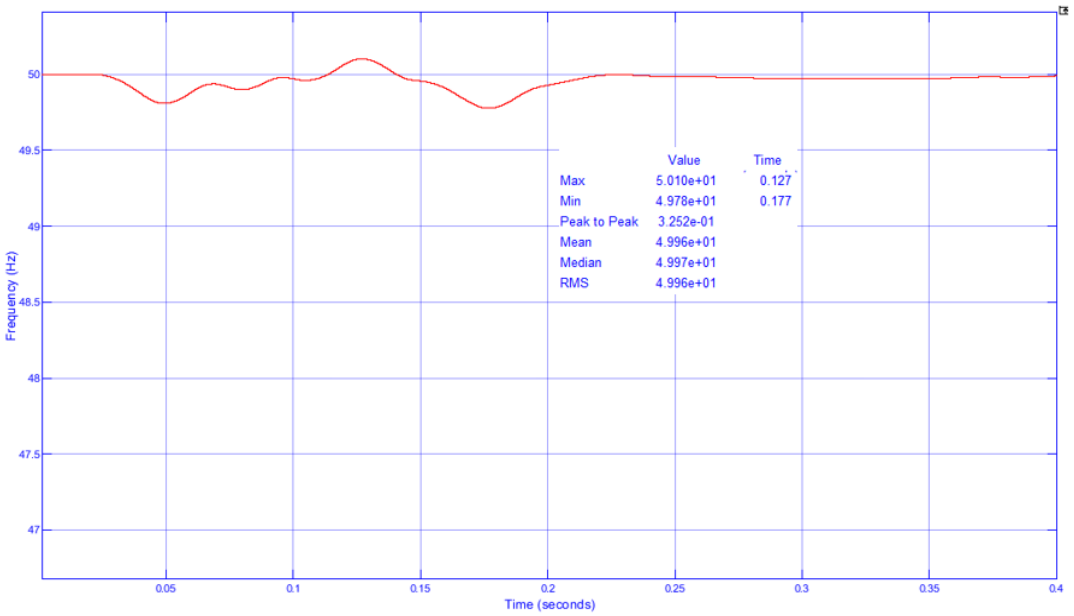

Figure 5-19: Grid frequency for case study 1

The result from Figure 5.19 presented shows that the power generated by the grid (synchronous generator) together with the power from the PV system was equal to the AC load. Hence, the grid frequency was stable at 49.96 Hz which is almost equal to the nominal frequency of 50 Hz. The dip in the frequency in Figure 5.19 at 50 ms and 170 ms was due to the variance in the solar irradiance from 1000 M/m^2 to 900 W/m^2.

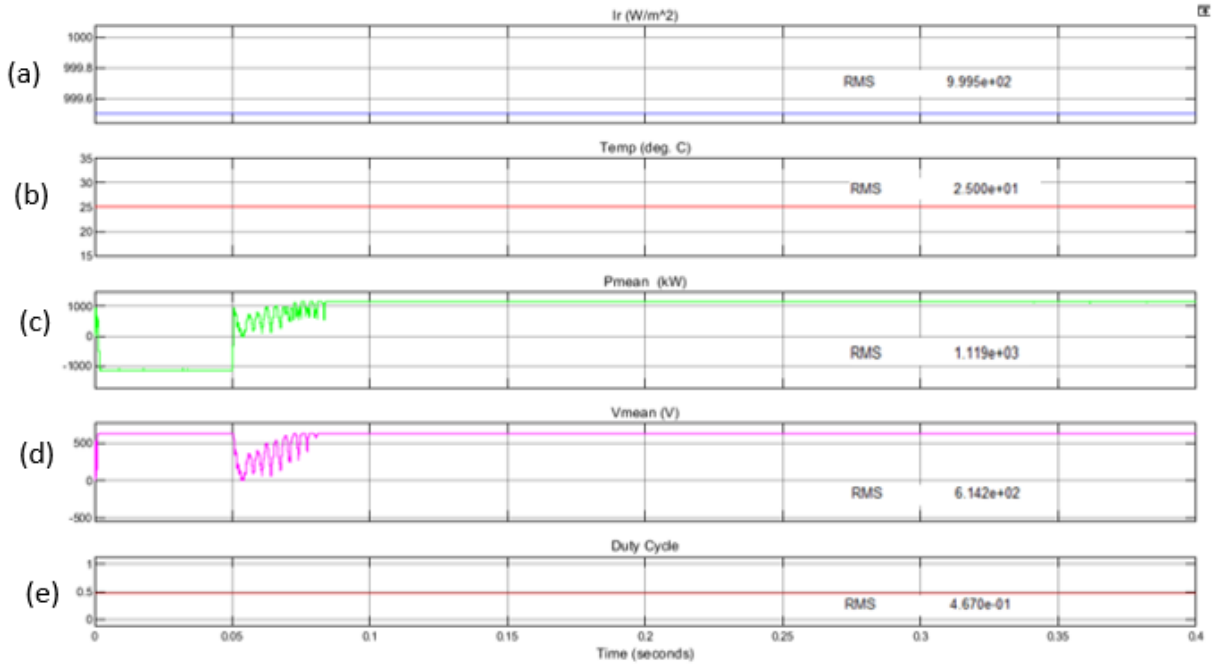

Figure 5-20: PV system simulated values

The result in Figure 5.20 also showed that the PV system was properly modelled. The values for the solar irradiance, temperature, power output, voltage (Vdc) and the duty cycle are very close to the calculated values. However, there are small variance which can be attributed to the losses in the system as shown in Figure 5.20.

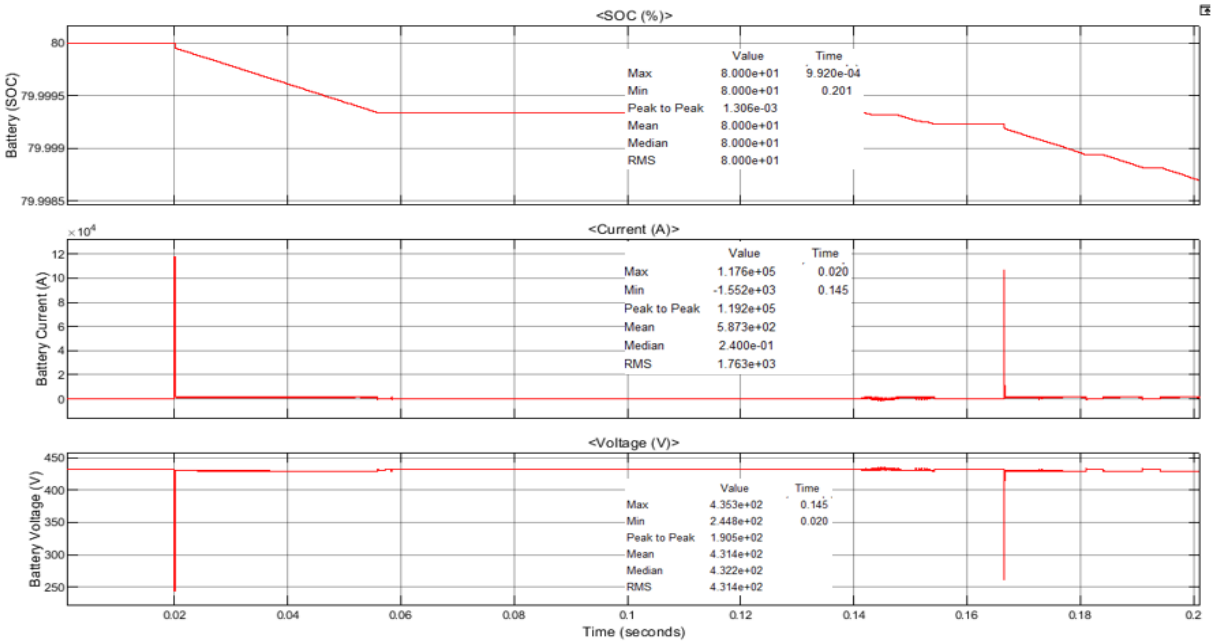

Figure 5-21: Battery simulated values

According to Figure 5-21, the battery SOC appeared exactly the same with the modelled value but the current is 2400 A as against the 2500 A computed in the model which can be attributed to the losses in the system. Also evident is a little change in the battery voltage of about 7 %. This voltage is the nominal voltage of the battery as shown in Figure 5.21.

5.5.2. Case study 2

This scenario considers a constant AC load of 10 MW, solar irradiance varied between 900 W/m^2 to 1000 W/m^2, the power supplied by the PV system is 1 MW, power generated by the grid (synchronous generator) is kept constant at 3.1 MW. The result showed that the power generated by the grid (synchronous generator) together with the power from the PV system was less than the AC load demand. Hence, the grid frequency dropped to 48.18 Hz which is less than the nominal frequency of 50 Hz as shown in Figure 5-22. This is because the load is inversely proportional to the frequency. An increase in the load will lead to a decrease in the frequency.

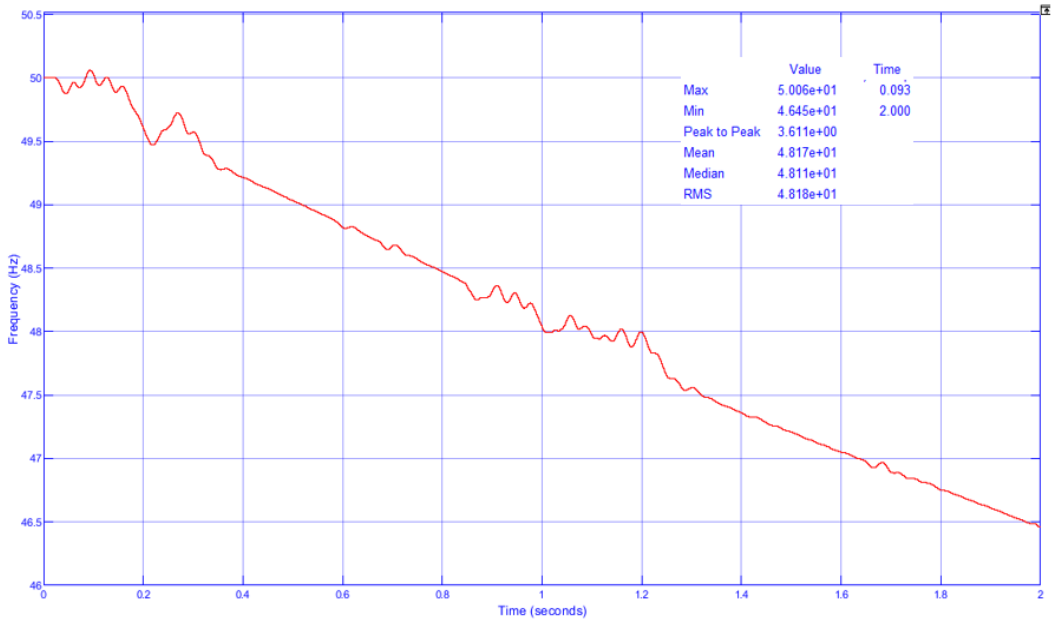

Figure 5-22: Grid frequency for case study 2

During the second case scenario, the grid frequency dropped to 48 .18 Hz as shown in Figure 2.22. This is because the output power from the PV system plus the output power from the synchronous generator is less than the AC load. Furthermore, the battery SOC is less than 20% hence, the battery could not supply power to the grid.

5.5.3. Case study 3

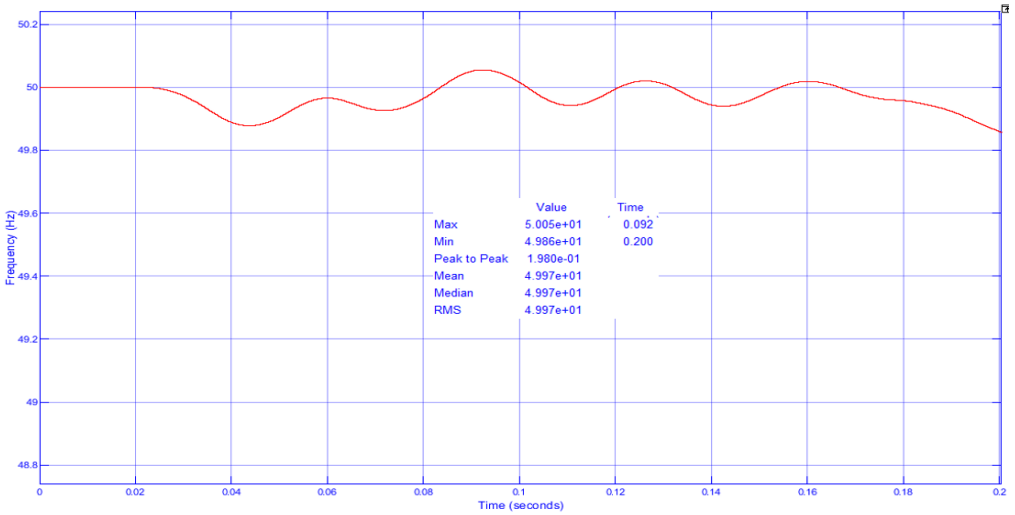

Figure 5-23: Grid frequency for case study 3

This scenario considers a constant AC load of 10 MW, solar irradiance varied between 900 W/m^2 to 1000 W/m^2, the power supplied by the PV system is 1 MW, power generated by the grid (synchronous generator) is kept constant at 3.1 MW. This case added the battery storage

system to support the grid frequency and stabilize it. The result showed that the power generated by the grid (synchronous generator) together with the power from the PV system was less than the AC load demand. But with the addition of the battery system, the grid frequency was stabilised at 49.97 Hz in 20 ms as presented in Figure 5-23. However, it is not exactly 50 Hz but close to the nominal frequency.

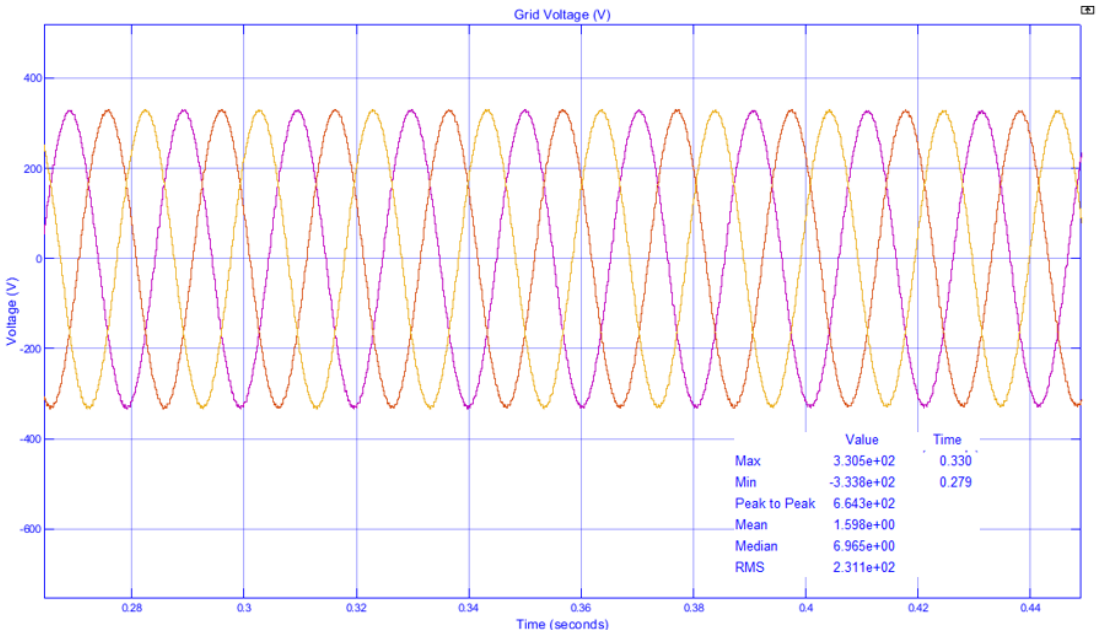

Figure 5-24: Voltage before the LC Filter

Figure 5.24 presents the voltage before the LC filter with the battery storage system connected to the grid-connected PV system through a DC-DC bidirectional converter. The calculated value is 240 V as shown in chapter 4 while the simulated value is 231 V. This is a pure sinusoidal AC voltage. The voltage difference is caused by the switching effect of the inverter.

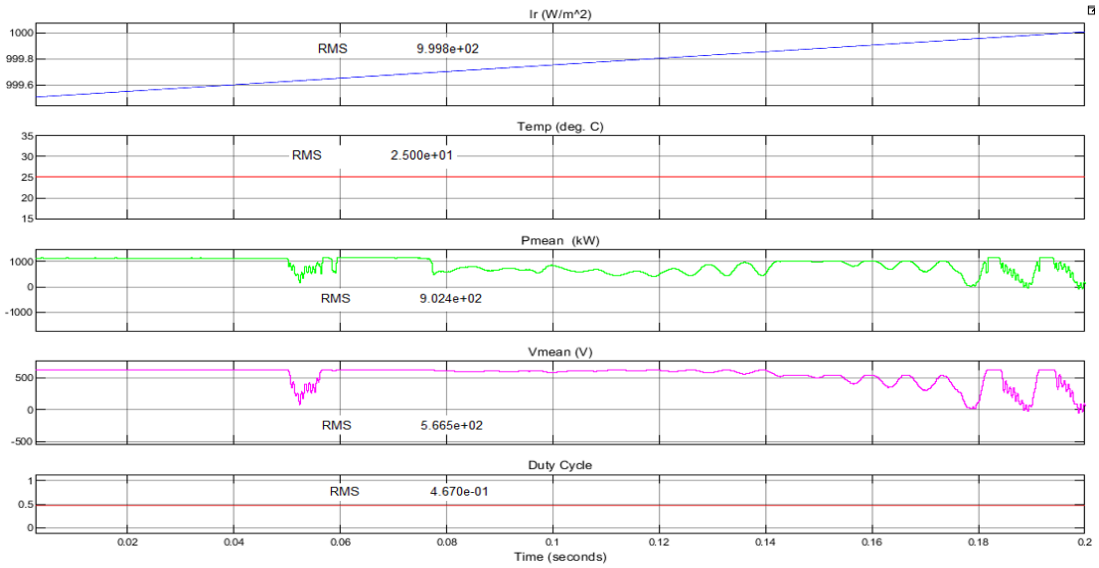

Figure 5-25: Simulated PV values for case study 3

The result in Figure 5.25 also showed that the PV system was properly modelled. The values for the solar irradiance, temperature, power output, voltage (Vdc) and the duty cycle are very close to the calculated values. However, there are small variance which can be attributed to the losses in the system.

CHAPTER 6: CONCLUSION AND FUTURE WORK

6.1. Conclusion

A flowchart to support and enhance grid frequency stability in a grid-connected PV system is presented. This is part of the smart grid environment drive that is incorporated into current power systems. The method employed provides adequate regulation of active and reactive power available in the system hence for grid frequency regulation. The system was modelled and simulated in the MATLAB/Simulink environment comprising a 1 MW PV array, a DC-DC boost converter, 1 MW Lithium-ion battery, a DC-DC bidirectional converter, three-phase inverter and the grid (Synchronous Generator). This system was modelled only as an element that is part of a wider scope where individual components in the system can be scaled to meet the user's requirement and to respond to other grid demands. A bidirectional communication between the grid and the battery was included to ensure regular update regarding the availability of active and reactive powers in the system. The received update will inform the control to set the DC-DC bidirectional converter to either operate in the buck or boost modes. The results obtained showed that according to the commanded signals and the prevailing power availability and load demands, the battery system can respond instantaneously and participate in grid frequency regulation. The system used independent, easy to implement and not complex control techniques. To test the system's ability, three different scenarios were simulated and verified. In the first scenario, the grid frequency (f_{nom}) was equal to the measured frequency (f_{pr}) at 50 Hz and the battery SOC is greater or equal to 80% hence, there was no need for frequency regulation and the battery was disconnected. In the second scenario, the measured frequency was less than the grid frequency and the battery SOC is between 20% and 80% hence, the DC-DC bidirectional converter operates in the boost mode. The battery is triggered into the discharge mode in this case. The third scenario is when the measured frequency is greater than the grid frequency and the battery SOC is less than 80% hence, the DC-DC bidirectional converter operates in the buck mode. The excess available power in the system in this case is used to charge the battery. The control method used can be implemented with other renewable energy sources and the system can be either down sized or up scaled depending on what the research is set to achieve. The choice of Lithium-ion battery showed a major advantage in power management structure because the battery current can be regulated by offering flexibility to the user according to battery internal formation and demands. In addition, the system can be resized according to any set requirements which makes it a very important factor to consider in power management. The result showed that it is practical to use battery storage system for frequency regulation in a grid-connected PV system.

6.2. Recommendations and future work

The practicability of implementing the modelled system considering all the control and other factors should be carried out. The choice and size of the battery technology has a substantial impact on the response time and the amount of power it can discharge, hence, other battery technology should be studied. This is because of the different life span, self-discharge rate, cost of installation and the weight. Therefore, a study is required to ascertain the most affordable battery technology that can be implemented for this purpose. In addition, a study should also be conducted to have detailed understanding of the criteria to be used in selecting the appropriate inverter size for such purpose. This is necessary because the inverter handles both active and reactive power flow in the system.

REFERENCES

Adhikari, S. 2013. *Control of Solar Photovoltaic (PhV) Power Generation in Grid-Connected and Islanded Microgrids*. University of Tennessee, Knoxville.

Aghamohammadi, M.R. & Abdolahinia, H. 2014. A new approach for optimal sizing of battery energy storage system for primary frequency control of islanded Microgrid. *International Journal of Electrical Power and Energy Systems*, 54: 325–333. http://dx.doi.org/10.1016/j.ijepes.2013.07.005.

Alam, M.S. & Alouani, A.T. 2010. Dynamic modeling of photovoltaic module for real-time maximum power tracking. *Journal of Renewable and Sustainable Energy*, 2(4): 2–17.

Alepuz, S., Busquets-Monge, S., Bordonau, J., Gago, J., González, D. & Balcells, J. 2006. Interfacing renewable energy sources to the utility grid using a three-level inverter. *IEEE Transactions on Industrial Electronics*, 53(5): 1504–1511.

Alrahim Shannan, N.M.A., Yahaya, N.Z. & Singh, B. Single-diode model and two-diode model of PV modules: A comparison. In *Proceedings - 2013 IEEE International Conference on Control System, Computing and Engineering, ICCSCE 2013*. Penang, Malaysia: IEEE: 210–214.

Alvarez, R.A., Pacala, S.W., Winebrake, J.J., Chameides, W.L. & Hamburg, S.P. 2012. Greater focus needed on methane leakage from natural gas infrastructure. In *Proceedings of the National Academy of Sciences of the United States of America*. Newyork: 6435–6440.

Ari, G.K. & Baghzouz, Y. 2011. Impact of High PV Penetration on Voltage Regulation in Electrical Distribution Systems. In *3rd International Conference on Clean Electrical Power: Renewable Energy Resources Impact*. Las Vegas: IEEE: 744–748.

Ataei, A., Nedaei, M., Rashidi, R. & Yoo, C. 2015. Optimum design of an off-grid hybrid renewable energy system for an office building. *Journal of Renewable and Sustainable Energy*, 7(5): 2–25. http://dx.doi.org/10.1063/1.4934659.

Awad, B., Wu, J. & Jenkins, N. 2008. Control of Distributed Generation. *Elektrotechnik und Informationstechnik*, 125(12): 409–414.

Ballance, J.W., Bhargava, B. & Rodriguez, G.D. 2003. Monitoring Power System Dynamics Using Phasor Measurement Technology for Power System Dynamic Security Assessment. In *2003 IEEE Bologna PowerTech - Conference Proceedings*. IEEE: 2–8.

Bertani, R. 2015. Geothermal power generation in the world 2010–2014 update report. Geothermics, 60, 31-43. In *World Geothermal Congress*. Melbourne, Australia: 1–19.

Bevrani, H. & Shokoohi, S. 2013. An intelligent droop control for simultaneous voltage and frequency regulation in Islanded microgrids. *IEEE Transactions on Smart Grid*, 4(3): 1505–1513.

Bhatt, R. & Chowdhury, B. 2011. Grid frequency and voltage support using PV systems with energy storage. *NAPS 2011 - 43rd North American Power Symposium*: 1–6.

Bird, L., Milligan, M. & Lew, D. 2013. *Integrating Variable Renewable Energy: Challenges and Solutions*.

Bjørk, R. & Nielsen, K.K. 2015. The Performance of a Combined Solar Photovoltaic (PV) and Thermoelectric Generator (TEG) System. *Solar Energy*, 120: 187–194.

Bracale, A., Carpinelli, G., De Falco, P., Rizzo, R. & Russo, A. 2016. New advanced method and cost-based indices applied to probabilistic forecasting of photovoltaic generation. *Journal of Renewable and Sustainable Energy*, 8(2). http://dx.doi.org/10.1063/1.4946798.

Canova, A., Giaccone, L., Spertino, F. & Tartaglia, M. 2009. Electrical Impact of Photovoltaic Plant in Distributed Network. *IEEE Transactions on Industry Applications*, 45(1): 341–347.

Chao, K.-H., Tseng, M.-C., Huang, C.-H., Liu, Y.-G. & Huang, L.-C. 2013. Design and Implementation of a Bidirectional DC-DC Converter for Stand-Alone Photovoltaic Systems. *International Journal of Computer, Consumer and Control (IJ3C)*, 2(3): 44–55. https://pdfs.semanticscholar.org/c8ce/2e345a70c23cd722770bb182cb49cc886b4f.pdf.

Delghavi, M.B. & Yazdani, A. 2009. A Control Strategy for Islanded Operation of a Distributed Resource (DR) unit. In *2009 IEEE Power and Energy Society General Meeting*. IEEE: 1–8.

Department of Mineral Resources, S.A. *South Africa's Mineral Industry*.

Diouf, E. 2013. *Frequency Control Ancillary Services in Large Interconnected Systems*. University of Manchester.

Doukas, H., Patlitzianas, K.D., Kagiannas, A.G. & Psarras, J. 2005. Renewable energy sources and rationale use of energy development in the countries of GCC: Myth or reality? *Renewable Energy*, 31(6): 755–770.

Durić, M.B., Terzija, V. V. & Škokljev, I.A. 1994. Power System Frequency Estimation Utilizing the Newton-Raphson Method. *Archiv für Elektrotechnik*, 77(3): 221–226.

Ela, E., Gevorgian, V., Tuohy, A., Kirby, B., Milligan, M. & O'Malley, M. 2014. Market Designs for the Primary Frequency Response Ancillary Service-Part I: Motivation and Design. *IEEE Transactions on Power Systems*, 29(1): 421–431.

Elbatran, A.H., Abdel-Hamed, M.W., Yaakob, O.B., Ahmed, Y.M. & Arif Ismail, M. 2015. Hydro power and turbine systems reviews. *Jurnal Teknologi*, 74(5): 83–90.

Eltawil, M.A. & Zhao, Z. 2010. Grid-connected photovoltaic power systems: Technical and potential problems-A review. *Renewable and Sustainable Energy Reviews*, 14(1): 112–129.

Enslin, J.H.R. & Heskes, P.J.M. 2004. Harmonic-interaction Between a Large Number of Distributed Power Inverters and the Distribution Network. *IEEE Transactions on Power Electronics*, 19(6): 1586–1593.

Esram, T. & Chapman, P.L. 2007. Comparison of Photovoltaic Array Maximum Power Point Tracking Techniques. *IEEE Transactions on Energy Conversion*, 22(2): 439–449.

Farmer, W.J. 2018. *Optimising Power System Frequency Stability using Virtual Inertia from Inverter-based Renewable Energy Generation*. University of Stellenbosch.

Freitas, S., Reinhart, C. & Brito, M.C. 2018. Minimizing Storage Needs for Large Scale Photovoltaics in the Urban Environment. *Solar Energy*, 159(September 2017): 375–389. https://doi.org/10.1016/j.solener.2017.11.011.

Fried, L. 2011. *Global Wind Statistics*. Brussels.

Gerdi, B., Dijkshoorn, L. & Ramsak, P. 2013. *Geothermal Energy Status and Policy Review*

Geothermal Energy Status and Policy Review.

Golpîra, H. & Bevrani, H. 2019. Microgrids Impact on Power System Frequency Response. *Energy Procedia*, 156(September 2018): 417–424. https://doi.org/10.1016/j.egypro.2018.11.097.

Govender, P. & Sivakumar, V. 2019. Investigating Diffuse Irradiance Variation Under Different Cloud Conditions in Durban, Using k-means Clustering. *Journal of Energy in Southern Africa*, 30(3): 22–32.

Gul, M., Kotak, Y. & Muneer, T. 2016. Review on Recent Trend of Solar Photovoltaic Technology. *Energy Exploration and Exploitation*, 34(4): 485–526.

Heydari, R., Khayat, Y., Naderi, M., Anvari-Moghaddam, A., Dragicevic, T. & Blaabjerg, F. 2019. A Decentralized Adaptive Control Method for Frequency Regulation and Power Sharing in Autonomous Microgrids. *Research gate*, (June): 2427–2432.

Ibrahim, H. & Anani, N. 2017. Variations of PV Module Parameters with Irradiance and Temperature. *Energy Procedia*, 134: 276–285. https://doi.org/10.1016/j.egypro.2017.09.617.

Ibrahim, O. & Raji, A.. 2015. *Design and Development of a Smart Inverter System*. Cape Peninsula University of Technology.

IEA. 2019. *End-of-Term Report and End-of-Term Report and Strategic Plan*.

IEEE. 2011. *Technical specifications for solar PV installations*. Ethekweni.

IRENA. 2017. *Electricity Storage and Renewables: Costs and Markets to 2030*. http://irena.org/publications/2017/Oct/Electricity-storage-and-renewables-costs-and-markets.

Jain, A., Behl, M. & Mangharam, R. 2017. Data Predictive Control for Building Energy Management. In *American Control Conference*. IEEE: 1–10. http://repository.upenn.edu/mlab_papershttp://repository.upenn.edu/mlab_papers/96.

Jaramillo-Lopez, F., Kenne, G., Damm, G. & Lamnabhi-Lagarrigue, F. 2013. Adaptive Control Scheme for Grid-Connected Photovoltaic Systems with Unknown Bounds. In *IFAC Proceedings Volumes (IFAC-PapersOnline)*. Caen, France: IFAC: 671–676. http://dx.doi.org/10.3182/20130703-3-FR-4038.00055.

Johnstone, N., Haščič, I. & Popp, D. 2010. Renewable Energy Policies and Technological Innovation: Evidence Based on Patent Counts. *Environmental and Resource Economics*, 45(1): 133–155.

Joseph, B., Kulkarni, A. & Prabhu, S. 2017. Modeling of Solar Photovoltaic Standalone and Grid Connected System for Power System Load Flow Studies. *International Journal of Emerging Research in Management &Technology*, 9359(2): 59–67.

Kim, S., Seo, Y. & Singh, V.P. 2016. Estimating Global Solar Irradiance for Optimal Photovoltaic System. *Procedia Engineering*, 154: 1237–1242. http://dx.doi.org/10.1016/j.proeng.2016.07.446.

Kofi-opata, E. & Kofi-opata, E. 2013. *Alternative energy and the developmental state in Ghana by*. University of Toledo.

Kotsopoulos, A., Heskes, P.J.M. & Jansen, M.J. 2005. Zero-crossing Distortion in Grid-Connected PV Inverters. *IEEE Transactions on Industrial Electronics*, 52(2): 558–565.

Kroposki, B., Pink, C., Deblasio, R., Thomas, H., Simoes, M. & Sen, P.K. 2010. Benefits of Power Electronic Interfaces for. *IEEE Transactions on Energy Conversion*, (March 2015): 901–908.

Kumar, V., Pandey, A.S. & Sinha, S.K. 2016. Grid integration and power quality issues of wind and solar energy system: A review. In *International Conference on Emerging Trends in Electrical, Electronics and Sustainable Energy Systems, ICETEESES 2016*. IEEE: 2–10.

Laaksonen, H., Saari, P. & Komulainen, R. 2005. Voltage and Frequency Control of Inverter. In *2005 International Conference on Future Power Systems*. IEEE: 2–6.

Li, B., Wang, J., Bao, H. & Zhang, H. 2014. Islanding Detection for Microgrid Based on Frequency Tracking Using Extended Kalman Filter Algorithm. *Journal of Applied Mathematics*, 2014: 1–12.

Lopes, J.A.P., Moreira, C.L. & Madureira, A.G. 2006. Defining Control Strategies for Microgrids Islanded Operation. *IEEE Transactions on Power Systems*, 21(2): 916–924.

Magdy, G., Shabib, G., Elbaset, A.A., Kerdphol, T., Qudaih, Y. & Mitani, Y. 2017. A New Coordinated Fuzzy-PID Controller for Power System Considering Electric Vehicles. *Energy and Power Engineering*, 09(04): 425–435.

Mai, R.K., He, Z.Y., Fu, L., He, W. & Bo, Z.Q. 2010. Dynamic Phasor and Frequency Estimator for Phasor Measurement Units. *IET Generation, Transmission and Distribution*, 4(1): 73–83.

Majumder, R., Bag, G. & Chakrabarti, S. 2011. Performance of Power Electronic Interfaced DERs Integrated with Communication Network. In *IEEE Power and Energy Society General Meeting*. IEEE: 1–7.

Mandadapu, U., Vedanayakam, V. & Thyagarajan, K. 2017. Effect of Temperature and Irradiance on the Electrical Performance of a Pv Module. *International Journal of Advanced Research*, 5(3): 2018–2027.

Mansouri, S.A. 2011. *Tudy of a*. Ohio State University.

Marafia, A.H. 2001. Feasibility study of photovoltaic technology in Qatar. *Renewable Energy*, 24(3–4): 565–567.

Masters, G.M. 2005. *Renewable and efficient electric power systems*. Canada: Wiley Interscience.

Mathema, P. 2008. *Optimization Of Integrated Renewable Energy System – Micro Grid*. Tribhuvan University.

Mazibuko, N. 2015. *Interconnection of Solar Power to the Grid Through the Power Plant Auxiliary System*. University of KwaZulu-Natal.

Messenger, R.A. & Ventre, J. 2018. *Photovoltaic Systems Engineering*. Second. Florida: Taylor & Francis.

Misak, S. & Prokop, L. 2017. *Operation Characteristics of Renewable Energy Sources*. Ostrava, Poruba: Springer Nature. http://link.springer.com/10.1007/978-3-319-43412-4.

Moreno, R.M., Pomilio, J.A., Pereira Da Silva, L.C. & Pimentel, S.P. 2009. Mitigation of Harmonic Distortion by Power Electronic Interface Connecting Distributed Generation Sources to a Weak Grid. In *Brazilian Power Electronics Conference, COBEP2009*.

IEEE: 41–48.

El Moursi, M.S., Zeineldin, H.H., Kirtley, J.L. & Alobeidli, K. 2014. A dynamic master/slave reactive power-management scheme for smart grids with distributed generation. *IEEE Transactions on Power Delivery*, 29(3): 1157–1167.

Nelson, J. 2010. 2132-2 Winter College on Optics and Energy Physics of Solar Cells (I). , (February): 1–62.

Oliva, A.R. & Balda, J.C. 2003. A PV Dispersed Generator: A Power Quality Analysis Within the IEEE 519. *IEEE Transactions on Power Delivery*, 18(2): 525–530.

Omran, W. 2010. *Performance Analysis of Grid-Connected Photovoltaic Systems*. University of Waterloo, Canada.

Paatero, J. V. & Lund, P.D. 2007. Effects of Large-Scale Photovoltaic Power Integration on Electricity Distribution Networks. *Renewable Energy*, 32(2): 216–234.

Pan, C.T., Cheng, M.C. & Lai, C.M. 2012. A Novel Integrated DC/AC Converter with High Voltage Gain Capability for Distributed Energy Resource Systems. *IEEE Transactions on Power Electronics*, 27(5): 2385–2395.

Pappu, V.A.K. 2010. *Implementing frequency regulation capability in a solar photovoltaic power plant*. Missouri University of Science and Technology.

Pegels, A. 2010. Renewable Energy in South Africa: Potentials, Barriers and Options for Support. *Energy Policy*, 38(9): 4945–4954. http://dx.doi.org/10.1016/j.enpol.2010.03.077.

Del Pero, C., Butera, F.M., Piegari, L., Faifer, M., Buffoli, M. & Monzani, P. 2016. Characterization and Monitoring of a Self-Constructible Photovoltaic-Based Refrigerator. *Energies*, 9(9): 2–15.

Petinrin, J.O. & Shaaban, M. 2015. Renewable Energy for Continuous Energy Sustainability in Malaysia. *Renewable and Sustainable Energy Reviews*, 50(October 2015): 967–981. http://dx.doi.org/10.1016/j.rser.2015.04.146.

Du Plooy, H. 2016. *Comparative Strategies for Efficient Control and Storage of Renewable Energy in a Microgrid*. Cape Peninsula University of Technology.

Quaschning, V. 2005. *Understanding Renewable Energy Systems - (Malestrom).pdf*. London: Earthscan.

Rahim, A.H.A., Tijani, A.S., Fadhlullah, M., Hanapi, S. & Sainan, K.I. 2015. Optimization of Direct Coupling Solar PV Panel and Advanced Alkaline Electrolyzer System. *Energy Procedia*, 79: 204–211. http://dx.doi.org/10.1016/j.egypro.2015.11.464.

Rahman, H.A., Nor, K.M., Hassan, M.Y., Thanakodi, S., Majid, M.S. & Hussin, F. 2010. Modeling and Simulation of Grid Connected Photovoltaic System for Malaysian Climate Using Matlab/Simulink. In *PECon2010 - 2010 IEEE International Conference on Power and Energy*. Kuala Lumpur: IEEE: 935–940.

Rahman, J. 2017. *Frequency control in the presence of renewable energy sources in the power network*. ÉCOLE DE TECHNOLOGIE SUPÉRIEURE ÉCOLE DE TECHNOLOGIE SUPÉRIEURE.

Rahmann, C. & Castillo, A. 2014. Fast frequency response capability of photovoltaic power plants: The necessity of new grid requirements and definitions. *Energies*, 7(10): 6306–

6322.

Raji, A.K. 2012. *Performance Evaluation and Improvement of Grid-Connected Technology*. Cape Peninsula University of Technology.

Rastegarnia, A., Khalili, A., Vahidpour, V. & Islam, K. 2015. Frequency Estimation of Unbalanced Three-Phase Power Systems Using the Modified Adaptive Filtering. *American Journal of Signal Processing*, 5: 16–25.

Rebours, Y.G., Kirschen, D.S., Trotignon, M. & Rossignol, S. 2007. A survey of Frequency and Voltage Control Ancillary Services - Part II: Economic Features. *IEEE Transactions on Power Systems*, 22(1): 358–366.

REN21. 2017. *Renewables 2017 Global Status Report*. www.ren21.net/gsr.

REN21 Steering committee. 2011. *Renewables 2011 Global Status Report*.

Richardson, D.B. & Richardson, D.B. 2016. *Modeling , optimization and large-scale grid integration of solar photovoltaic energy in Ontario ' s electricity system by photovoltaic energy in Ontario ' s electricity system*. University of Toronto.

Samrat, N.H., Ahmad, N. Bin, Choudhury, I.A. & Taha, Z. Bin. 2014. Modeling, Control, and Simulation of Battery Storage Photovoltaic-wave Energy Hybrid Renewable Power Generation Systems for Island Electrification in Malaysia. *Scientific World Journal*, 2014: 1–22.

Savaghebi, M., Jalilian, A., Vasquez, J.C. & Guerrero, J.M. 2011. Selective Compensation of Voltage Harmonics in an Islanded Microgrid. In *2nd Power Electronics, Drive Systems and Technologies Conference, PEDSTC*. IEEE: 279–285.

Şerban, I., Ion, C.P., Marinescu, C. & Georgescu, M. 2007. Frequency Control and Unbalances Compensation in Autonomous Micro-Grids Supplied by RES. In *Proceedings of IEEE International Electric Machines and Drives Conference*. IEEE: 1–6.

Shadmand, M.B. & Balog, R.S. 2013. Design Considerations for Long-Term Remote Photovoltaic-Based Power Supply Using Non-planar Photovoltaic Surfaces. In *EEE International Conference on Technologies for Homeland Security*. IEEE: 2–8.

Shah, R., Mithulananthan, N., Bansal, R.C. & Ramachandaramurthy, V.K. 2015. A review of key power system stability challenges for large-scale PV integration. *Renewable and Sustainable Energy Reviews*, 41: 1423–1436. http://dx.doi.org/10.1016/j.rser.2014.09.027.

Shamsipour, R. & Shamsipour Dehkordi, R. 2015. Review on Sustainable Energy Potential. *IOSR Journal of Environmental Science Ver. II*, 9(11): 2319–2399. www.iosrjournals.org.

Sidhu, T.S. 1999. Accurate measurement of power system frequency using a digital signal processing technique. *IEEE Transactions on Instrumentation and Measurement*, 48(1): 75–81.

Sigfússon, B. & Uihlein, A. 2015. *2015 JRC Geothermal Energy Status Report. European Commission - Joint Research Centre*. http://publications.jrc.ec.europa.eu/repository/handle/JRC99264.

Soultanis, N.L. & Hatziargyriou, N.D. 2007. Control issues of inverters in the formation of L.V. micro-grids. In *IEEE Power Engineering Society General Meeting, PES*. IEEE: 1–7.

Tan, L., Date, A., Fernandes, G., Singh, B. & Ganguly, S. 2017. Efficiency Gains of Photovoltaic System Using Latent Heat Thermal Energy Storage. *Energy Procedia*, 110(December 2016): 83–88. http://dx.doi.org/10.1016/j.egypro.2017.03.110.

Tan, Y.T. 2004. *Impact on the Power System of a Large Penetration of Photovoltaic Generation*. University of Manchester Institute of Science and Technology.

Tholomier, D., Kang, H. & Cvorovic, B. 2009. Phasor Measurement Units: Functionality and Applications. In *2009 Power Systems Conference: Advance Metering, Protection, Control, Communication, and Distributed Resources*. IEEE: 1–12.

Trabelsi, M. & Ben-Brahim, L. 2011. Development of a grid connected photovoltaic power conditioning system based on flying capacitors inverter. In *International Multi-Conference on Systems, Signals and Devices*. IEEE: 1–6.

Tremblay, O. & Dessaint, L.A. 2009. Experimental Validation of a Battery Dynamic Model for EV Applications. *World Electric Vehicle Journal*, 3(2): 289–298.

Tsai, S.J.S., Zhong, Z., Zuo, J. & Liu, Y. 2006. Analysis of Wide-Area Frequency Measurement of Bulk Power Systems. In *2006 IEEE Power Engineering Society General Meeting, PES*. IEEE: 1–8.

Vásquez, J.C., Guerrero, J.M., Gregorio, E. & Rodríguez, P. 2008. Vasquez et al. - 2008 - Adaptive droop control applied to distributed generation inverters connected to the grid.pdf. *IEEE International Symposium on Industrial Electronics*, (1): 2420–2425.

Verhoeven, B. 1998. *Utility Aspects of Grid-Connected Photovoltaic Power Systems*. http://www.hme.ca/gridconnect/IEA_PVPS_Task_5-01_Utility_aspects_of_PV_grid-connection.pdf.

Vijayapriya, T. & Kothari, D.P. 2011. Smart Grid: An Overview. *Smart Grid and Renewable Energy*, 02(04): 305–311.

Vokas, G.A. & Machias, A. V. 1995. Harmonic Voltages and Currents on Two Greek Islands with Photovoltaic stations: Study and Field Measurements. *IEEE Transaction on Energy Conversation*, 10(2): 302–306.

Weckend, S., Wade, A. & Heath, G. 2016. *End-of-Life Management Solar Photovoltaic Panels*.

Yang, Y. & Blaabjerg, F. 2015. Overview of Single-phase Grid-connected Photovoltaic Systems. *Electric Power Components and Systems*, 43(12): 1352–1363.

Yaramasu, V., Wu, B., Sen, P.C., Kouro, S. & Narimani, M. 2015. High-power wind energy conversion systems: State-of-the-art and emerging technologies. *Proceedings of the IEEE*, 103(5): 740–788.

Yari, V., Nourizadeh, S. & Ranjbar, A.M. 2010. Wide-Area Frequency Control During Power System Restoration. In *IEEE Electrical Power and Energy Conference*. IEEE: 1–4.

Zhong, Q.-C. 2017. Primary frequency control of future power systems. *IEEE Smart Grid Newsletter*, (August). http://smartgrid.ieee.org/newsletters/june-2017/primary-frequency-control-of-future-power-systems.

Zhou, X., Liu, S., Wang, M., Dai, Y. & Tang, Y. 2014. Parameter Identification of Interconnected Power System Frequency after Trip-out of High Voltage Transmission Line. *Frontiers in Energy*, 8(3): 386–393.

APPENDICES

Appendix 1 Maximum Power Point Tracking by Incremental Conductance Method

The maximum power point tracking is connected to ensure that the PV system delivers maximum power.

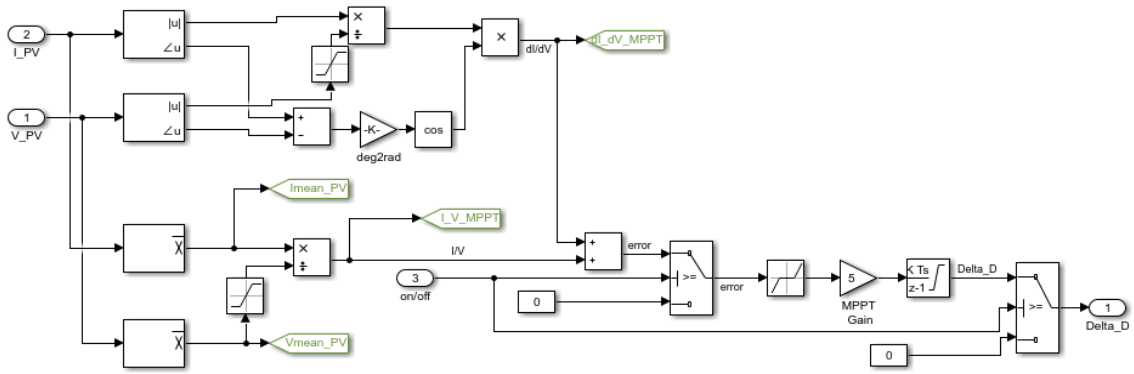


```
Maximum power point tracking by incremental conductance method
-----------------------------------------------------------------
Maximum power point is obtained when dP/dV=0  where P= V*I
-> d(V*I)/dV = I + V*dI/dV = 0
-> dI/dV = -I/V

dI, dV  = fundamental components of I and V ripples measured with a sliding time window T_MPPT
I , V   = mean values of V and I measured with a sliding time window T_MPPT

The integral regulator minimizes the error (dI/dV + I/V)
Regulator output = Duty cycle correction
```

Appendix 2 Battery model indicating the SOC and Current

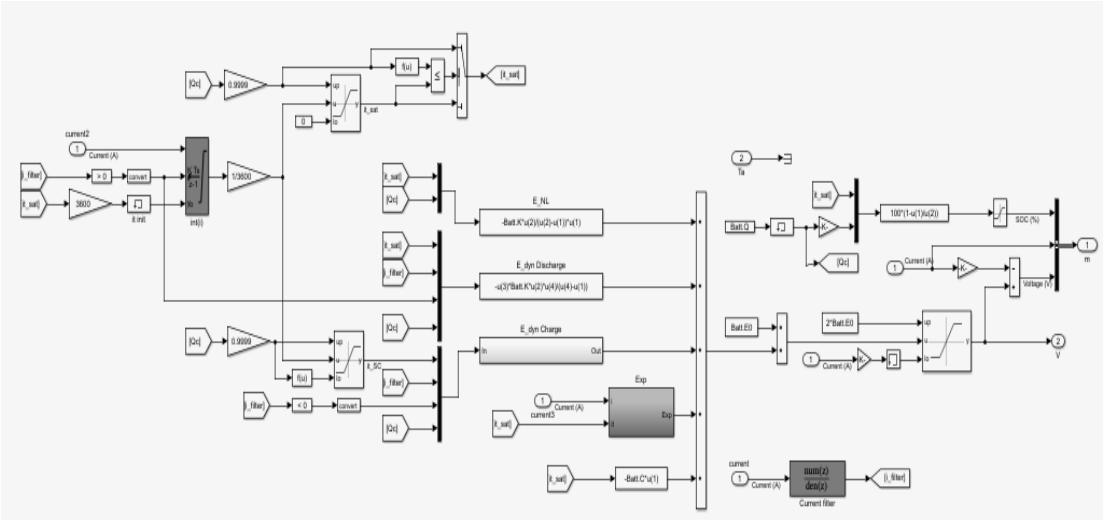

Appendix 3 Power measurement block

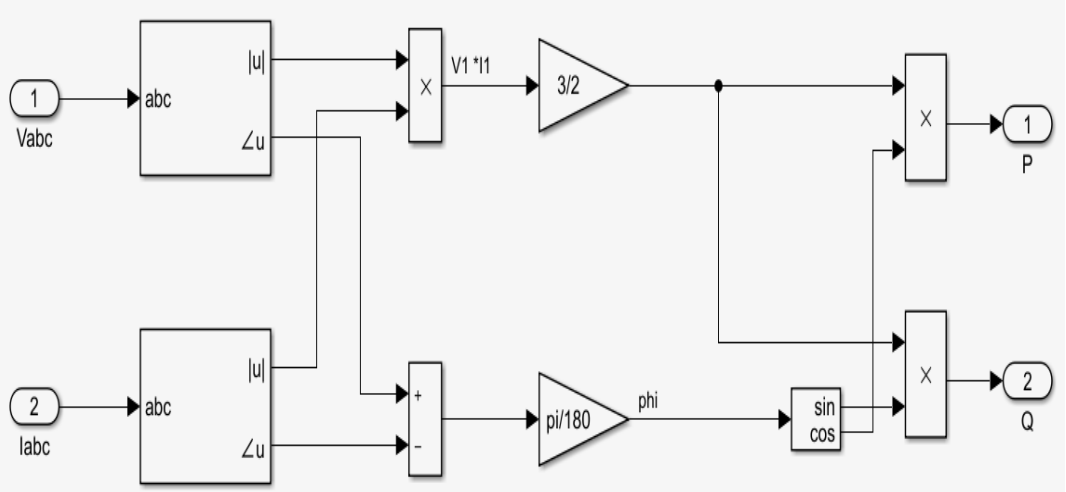

Appendix 4 Current Regulator (with feedforward)

Current Regulator (with feedforward)

harmonic filter neglected

Ltot = Lxfo + Lchoke
Rtot = Rxfo + Rchoke

Vd_mes + Id*R - Iq*L + deriv(Id)*L= Vd_conv
Vq_mes + Id*L + Iq*R + deriv(Iq)*L= Vq_conv

For Ltot >> Rtot :
(Vd_prim - Vd_conv) ~= + Iq * Ltot
(Vq_prim - Vq_conv) ~ = - Id * Ltot

Sign Convention: Current going out of the converter = positive current

Id positive --> The converter generates active power ("Inverter mode") = Active Power P positive

Iq positive --> The converter absorbs reactive power ("Inductive mode") = Reactive Power Q negative